The Radio Science Bulletin

ISSN 1024-4530

INTERNATIONAL
UNION OF
RADIO SCIENCE

UNION
RADIO-SCIENTIFIQUE
INTERNATIONALE

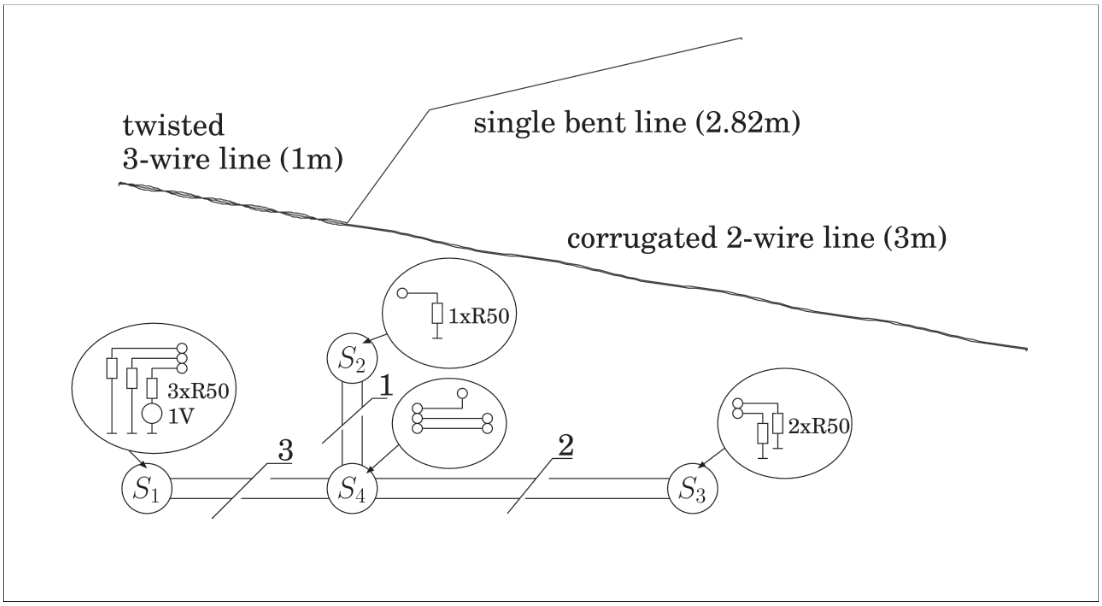

No 307
December 2003

Publié avec l'aide financière de l'ICSU
URSI, c/o Ghent University (INTEC)
St.-Pietersnieuwstraat 41, B-9000 Gent (Belgium)

Contents

Front cover: Figure 22 from "Transmission-Line Super Theory: A New Approach to an Effective Calculation of Electromagnetic Interactions (more on pp. 33-60)

For information, please contact :
The URSI Secretariat
c/o Ghent University (INTEC)
Sint-Pietersnieuwstraat 41, B-9000 Gent, Belgium
Tel.: (32) 9-264 33 20, Fax: (32) 9-264 42 88
E-mail: ursi@intec.rug.ac.be
http://www.ursi.org

The International Union of Radio Science (URSI) is a foundation Union (1919) of the International Council of Scientific Unions as direct and immediate successor of the Commission Internationale de Télégraphie Sans Fil which dates from 1913.

Editorial

Another Milestone

This issue marks another milestone for the *Radio Science Bulletin*. This issue contains the first two *Reviews of Radio Science* for this triennium. For the last four triennia, the *Reviews* have been collected at the time of the General Assembly and published as separate books (each totaling close to 1,000 pages). As decided by the URSI Council at the Maastricht General Assembly, for this triennium the *Reviews* will be published in the *Radio Science Bulletin*. The topics and authors of the *Reviews* are still invited by the URSI Commissions, and the peer reviews are carried out by the Commissions. This will continue to insure the quality, timeliness, and importance of the material. However, publishing them in the *Bulletin* throughout the triennium will make their delivery to the radio science community even more timely, and will allow them to be read and used as they become available.

The Senior Associate Editor in charge of the *Reviews of Radio Science* is Phil Wilkinson. It is because of his efforts, and the efforts of the Associate Editors for the Commissions (relevant to this issue, Flavio Canavero for Commission E and Frank Prato for Commission K), that we have the *Reviews* in this issue, and that we will continue to have *Reviews* in subsequent issues. Thank you!

We will of course continue to publish other quality papers of general interest to the radio science community, and I'm happy to report that we have a number of such papers currently under review. More are always welcome!

What's in this Issue

There was a time when the use of electromagnetic fields as a therapy for medical conditions was viewed with significant skepticism. However, there is now substantial evidence that pulsed electromagnetic fields – particularly those with frequencies from a few hertz up to about 500 Hz and having high rates of magnetic-field change (of the order of Teslas/second) – can have a variety of significant, positive biological effects. Naomi Shupak, Frank Prato, and Alex Thomas review the status of the research and practical use of such fields in therapeutic applications. These include a variety of applications in different types of bone repair; osteoporosis; joint diseases and other rheumatological disorders; spinal therapies; regeneration of soft tissues; therapy for nerve and neurological disorders, including multiple sclerosis and psychiatric disorders; and therapies for cancer, stroke, cardiac problems, and pain. Such therapies have been successful in many of these applications; in others, they have not. Part of the value of this review is that it reports and analyzes both the successes and failures in the field, and highlights where more research is needed. This is one of the Commission K *Reviews*, and I think you will find it both timely and fascinating.

Electromagnetic compatibility (EMC) is concerned with the interaction of electromagnetic fields and electronic equipment, and resultant effects. When interference from your computer's system unit affects the display on your monitor, or when the airplane crew asks that all electronic devices be shut off on takeoff or landing, you are being affected by EMC issues. Characterizing the interaction of electromagnetic fields with the often complex, non-uniform transmission paths inside electronic equipment is central to the analysis of many EMC problems. Historically, much of this analysis has been based on modeling the transmission paths as transmission lines, using what are know as the telegrapher equations. There is a tremendous archive of knowledge regarding analytical and numerical techniques for solving and applying such transmission-line models. However, the increased complexity of circuits in modern systems and the need for greater accuracy has led to a need for better models. H. Haase, J. Nitsch, and T. Steinmetz describe such a model, which they term the Transmission-Line Super Theory. It is a full-wave theory, capable of modeling very complex geometries and conduction-path parameters, and it includes such effects as radiation losses and non-TEM coupling at higher frequencies. However, because the basic equations of the theory can be cast in the form of the telegrapher equations, most of the existing techniques for solving such equations and for applying the solutions can be used. In many applications, the new approach is also computationally more efficient than other full-wave methods. The authors illustrate the use of their approach with a variety of examples, and compare their results to those obtained with other methods. This is one of the Commission E *Reviews*.

The URSI Scientific Committee on Telecommunications (SCT) has taken an important step in its evolution. In a report on SCT activities in this issue, Martin Hall, the Chair of the SCT, describes a recent meeting of the URSI/ITU-R Network. This was held in Geneva, in conjunction with the meetings of Working Parties of ITU-R Study Group 7. This is important not only because of the relevance of the work of URSI to ITU and vice versa, but also because of the value in raising the visibility of URSI. You need to read this report. Furthermore, if you can contribute to this effort – either by becoming involved, or via suggestions – you need to do that, too.

Coordinated Universal Time (UTC) and International Atomic Time (TAI) are two widely used international definitions of time, and they differ because of the variable rotation of the Earth. The practice has been to insert a "leap second" from time to time, so as to keep the absolute value of the difference of the two times within a prescribed limit. A proposal has been made to do away with this practice. Both an URSI Working Group on the Leap Second, and a Special Rapporteur Group of the International Telecommunication Union (ITU), are studying the potential consequences of such a change. The ITU group has invited URSI participation in their study. The URSI Working Group needs your input – and, in particular, the input of the official representatives to the URSI Commissions – in order to fulfill their mission. A questionnaire appears in this issue. If you are aware of any systems that might be affected by the leap-second issue, or if you have any relevant information, please respond.

There is also a letter to the URSI community from one of the Young Scientists at the 2002 General Assembly in this issue. Read it: you may discover that URSI's contributions can extend beyond science.

Because this is the December issue of the *Bulletin*, it contains a directory of all of those officially involved in URSI, including their positions and current contact information. Please check the information, and send any corrections to the URSI Secretariat. This directory has always made keeping the December issue a necessity. However, now that we will be having some of the *Reviews of Radio Science* in every issue, you will hopefully find even more reasons to keep *every* issue!

Happy New Year

The new year will come shortly after you receive this issue, according to many calendars. Looking at the year past, I'm grateful for the excellent efforts of those who help to make the *Bulletin* a reality: Paul Lagasse, Inge Lievens, Inge Heleu, John Volakis, Phil Wilkinson, and all of our Associate Editors. I'm also grateful for being allowed to edit the *Bulletin*, something that I really enjoy doing. I hope that in the new year you will find peace, health, success, and interesting and rewarding radio science. When you do, I hope you'll consider using these pages to share it with the URSI community.

Ross

In Memoriam

Yela Stevanovitch
1926 - 2003

Mrs. Ielena (Yela) Stevanovitch-Bogitch was interpreter and later Administrative and Executive Secretary of URSI from January 1958 until the end of 1990. She passed away on 10 August at the age of 77.

Complex organisations such as URSI are anonymous. During the many years which she devoted to URSI Yela Stevanovitch became the human face of URSI. Countless radioscientists found in her a most friendly and helpful guide when attending the General Assembly or when requiring information related to our Union.

I became Secretary General after Yela Stevanovitch had retired as Executive Secretary of our Union and I therefore had not the opportunity to work extensively with her. Nevertheless she was ever ready to give me help and advice. To the end of her life the well-being and evolution of URSI remained one of her primary concerns.

Many of her URSI friends wished to contribute to this obituary. Their remembrances are reproduced below. I hereby wish to thank all these colleagues for their kind, personal words of appreciation.

P. Lagasse, Secretary General

Yela was the corporate conscience and memory of URSI. Hired and trained by that master of SECRETARY GENERALS, Col. Herbays in 19xx, she quickly became the keeper of the records, the friend of the members representatives through her fluency in languages, the supporter of the officers, and the delightful hostess of URSI.

The distinguished Col. Herbays hired Yela sight-unseen and what a great move that was for Yela served faithfully and effectively for so many URSI meeting cycles, preparing agendas, back—up materials and reports, and distributing them ahead of time, a remarkable feat !

Yela was a loyal friend to so many members including those in Eastern Europe, a sweet lady who cared for the young scientists whom she loved, a gourmet cook who ran the International Union of Gastronomy. This responsibility she took most seriously, keeping records of the meetings (in her home and around the times of Board meetings); listing, the dozen or so attendees , seven—course menus with a cheese board that rivaled the best in France and desserts that can only be described as decadent, wines by sources and vintages (the wines were selected by Morgan Minnis, long-time Secretary General of URSI). Somehow Yela managed all of this in addition to her busy schedule of Board activities, a minor miracle.

For all of the time that Morgan Minnis was Secretary General they worked together closely in the URSI Office, sharing space, a love of gourmet food and fine wines but nothing further in their personal lives to the disappointment of several generations of officers. My wife, Elva , and I became dear friends of Yela and remained so for more than forty years. We grieve at her passing.

W.E. Gordon, Honorary President of URSI

I was deeply grieved on receiving the sad news of passing of my dear friend and great adviser, Mrs. Yela Stevanovitch, on 10th August. Although I knew that she had been ill and in a rather serious condition for some time, it was a great shock for me to learn her death.

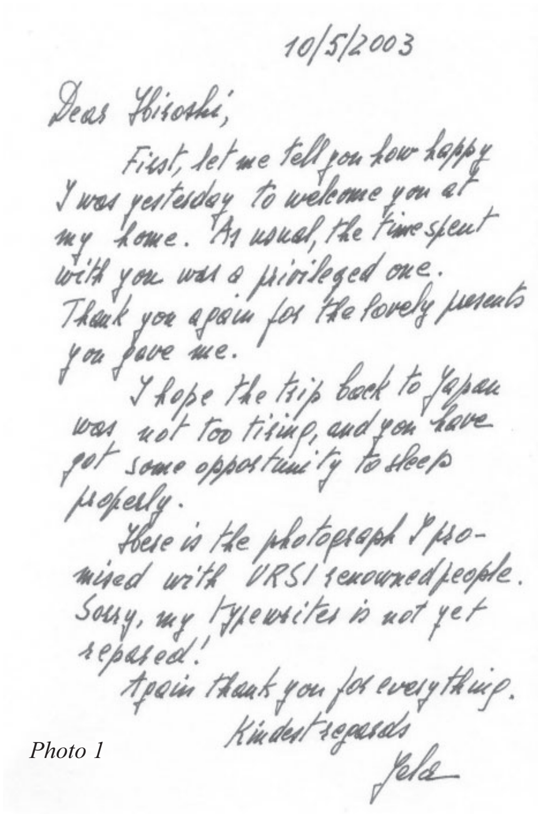

10/5/2003

Dear Hiroshi,

First, let me tell you how happy I was yesterday to welcome you at my home. As usual, the time spent with you was a privileged one. Thank you again for the lovely presents you gave me.

I hope the trip back to Japan was not too tiring, and you have got some opportunity to sleep properly.

Here is the photograph I promised with URSI renowned people. Sorry, my typewriter is not yet repaired!

Again thank you for everything.

Kindest regards

Yela

Photo 1

I visited her home in May this year. Despite her condition, she was kind enough to invite me to her home and give me a wonderful time, Photo 1 is the last correspondence which I received from her in May of this year. Her hand-writings were always impressive and warm-hearted.

It was at the time of the General Assembly in Prague when I first met her in person. Since then she provided me much information about URSI and URSI scientists including senior members and members in the old days. I learned a lot about URSI history, both formal and informal ones, and other international bodies within ICSU.

Photo 2

Photo 2 is a cutout of a group photo taken at the time of the 13th General Assembly in London in 1960. She is standing in the back with Prof. W. E. Gordon and his wife and URSI officers at that time.

Photo 3 and 4 are working Yela at the 26th Lille General Assembly helping the Local Committee.

Photo 3

Photo 4

Photo 5

Photo 5 isYela being relaxed at home with myself. Yela was so devoted to URSI and URSI has been everything for her. Yela was a genius with languages and multi-lingual. Yela was a walking dictionary of URSI history. Yela supported Secretary Generals and Presidents/Officers and kept all URSI archived documents and records at home when she was URSI Secretary and even after her formal retirement from URSI. Yela was loved by many friends and the whole of URSI. Yela invited URSI families to her home and hosted a wonderful Gastronomy party. Yela provided much advice and encouragement to me when I served as URSI President. Yela will be remembered by all URSI radio scientists.

I imagine that she is now having a heart-warming reunion with old departed friends in the other world. May her soul rest in peace.

Hiroshi Matsumoto
20th President of URSI

Yela , une femme d'exception au service de la Science

Spontanée, l'œil vif, d'une grande disponibilité, polyglotte, passionnée…c'est certainement l'image de Yela qui s'impose aux membres de la communauté URSI qui l'ont approchée, notamment au cours des assemblées générales.

Au-delà de cette image se dessine une démarche étonnante. En effet, spécialiste de littérature comparée, elle s'est rapidement investie dans le monde de la science radioélectrique. Elle a tout de suite perçu la dimension de cette science qui a accompagné et souvent précédé les grands bouleversements; du vingtième siècle en matière de communication, de perception de l'univers et de l'environnement terrestre, de mesure du temps, de conquête spatiale ou d'instrumentation médicale. La science fascinait Yela pour sa dimension sociétale, mais également pour les hommes et les femmes, avec leurs qualités et leurs défauts, qui s'y consacraient. Président de l'URSI au moment où l'on célébrait le soixante quinzième anniversaire de l'URSI, j'ai pu mesurer, comme beaucoup d'autres ont pu le faire dans d'autres circonstances, son immense culture, sa vision synthétique de l'extraordinaire développement de laradioélectricité et son infaillible mémoire. Je lui suis infiniment reconnaissant du soutien qu'elle m'a apporté à cette occasion comme, d'ailleurs, au cours de toute la période durant laquelle je l'ai côtoyée.

Le sens de l'amitié, de la fidélité et de la générosité de Yela est une autre dimension qui la rendait particulièrement attachante. Cette dimension avait de multiples facettes qu'un seul élément suffit à illustrer : les réunions du club de «radiogastronomie» orchestrées par Yela et au cours desquelles, les radioastronomes, en particulier, savaient montrer que leurs aspirations n'étaient pas uniquement extra-terrestres.

Nous venons de perdre une grande amie qui a beaucoup œuvré pour la Science.

Pierre Bauer
18e Président de l'URSI

Yela Stevanovitch, who retired some years ago as URSI executive secretary after many years with the organization, was a great source of help and information on URSI matters for both officers and members and a close friend of many URSI personalities from around the world. A very intelligent and dedicated woman, skilled in several of the most important languages of URSI, she prepared position papers on scientific topics of interest to the URSI board and frequently advised new members of the board, commissions and ordinary members seeking her advice on what they should say or do in URSI. For people like me this included how it should be said in French. URSI was her life and her kindness and hospitality was extended also to our wives and children. Even long after her retirement meetings of the so-called (by URSI president Sam Silver) "Radiogastronomy Commission" continued to be held in her Brussels apartment. Those of us fortunate enough to attend these events and many others will dearly miss her.

Edward Jull
17th President of URSI

Embryonically in 1914, but officially from 1919, URSI has served as an important link between several groups of radioscientists, both physicists and engineers. They were few at the start, and the meetings of URSI gave them a chance to interact, a possibility which was hardly available elsewhere. Personal friendships were developed, and "go to URSI", in particular to the General Assemblies, became a very special occasion.

This situation prevailed undisturbed until an important mutation took place in the late seventies. The Secretariat of URSI – the coordination center- was run by the Secretary General and an Administrative Assistant. It became financially too difficult to maintain such a team, and the decision was made to transform the function of the Secretary General into a voluntary, honorary one.

This was a drastic reduction of the administration top, at a time when the number of radioscientists had increasedconsiderably as compared with the pre-WWII situation, and a substantial increase in the flow of information, towards and from the Secretariat, could be expected. This was also the time when fax made its first appearance, followed by e-mail, and the modest facilities of the Secretariat became fast obsolescent. An administrative upgrade could not be delayed much longer.

The URSI Board was scheduled to take over some of the functions of the Secretary General, leaving the latter in charge of the routine activities. This system started very slowly, given the geographical spread of the Board members. One important exception, however: the considerable help provided by the successive Treasurers.

The start of the new set-up was therefore difficult, since the new Secretary General could only devote one day a week to the Secretariat in Brussels, given a more than full-time load elsewhere. But we survived, although the preparation of the 1981 General Assembly was in full swing. The former Secretary General, Dr. Minnis, generously gave of his time to help run the accounts, and in a next step the function of Assistant Secretary General was created, in 1984, and Professor Delogne joined us to give us his energy, enthusiasm and scientific competence. But it is Ms. Stevanovitch who stood as a rock during that ten-year long transition. She initially prepared most letters and documents herself, came to Ghent regularly to have them signed, and was a source of priceless information about the past of our Union. In our regular sessions in Brussels I found her to be of constant good spirits, and strongly loyal to the URSI-image she had formed in the past. She was very much concerned with maintaining the family-like atmosphere of URSI, and I understand she even ran a "Union of Gastronomy" from her own home, where she received many an URSI member. It was at the General Assemblies, however, that her warm qualities came strongly to the fore. The Young Scientists Program has been vigorously rejuvenated at the 1981 General Assembly by Presidents Christiansen and Gordon (and equally vigorously expanded by their successors), and it was her joy to help and advise these younger colleagues when she had a chance to meet them in person.

Another group also benefited from her concerns. Easy contacts between scientists from different countries were still a problem in the eighties, and Ms. Stevanovitch's knowledge of Slavic languages remained essential in helping members from some of our Committees feel at home at URSI gatherings.

I worked more than ten years almost daily with Ms. Stevanovitch, and keep from that period the memory of a most cultured person, full of human qualities, and of considerable courage when confronted with adversity, which in the last war took dramatic forms. She was also of strong will and firmness of purpose in defending her ideas and principles.

J. Van Bladel
Secretary General, 1979-1993

Yela was a special part of my life. In speaking of her I must strike a personal note, since our relationship was intensely personal in nature, inspired at the outset by our mutual love of language. Upon our first meeting at Tokyo in 1963 she welcomed me warmly in Serbian, a language I had learned as a student, and then continued to communicate with me in that Slavic tongue when we would meet in later years. A letter from her following the Toronto Assembly was one of the most touching I have ever received. It began in Serbian and then continued in French as she expressed some of her most personal thoughts. The last part was in English as she indicated a long held desire to meet my wife Betty.

Yela was the vigorous woman who provided me with insights into the meaning and inner workings of URSI. Her photo albums from successive Assemblies and commentary thereon were not to be missed. During a working visit to IASB in Brussels in the 1990s, I was writing an article that touched upon the remarkable presentation in 1952 by J. Ratcliffe of Owen Storey's doctoral work on whistler propagation. It was Yela who found in the URSI archives the needed reporter's notes from that long-ago Assembly at Sydney.

On several occasions in the early 1990s I was privileged to experience Yela's legendary hospitality. If it were daytime, we might walk together in the nearby Forêt de Soignes, and I would invariably have the pleasure of tasting her excellent cuisine. Charming yet modest, Yela was among the least pretentious people I have known. When I finally was able to introduce her to Betty and my sons, she embraced them as she had me. She told us of the great personal losses she had suffered in life, doing so not in search of our sympathy but rather in appreciation of our desire to know her better.

During our final visit, in 2002, she made a point of giving me a number of books in Serbian from her library, as well as a copy in English of some scholarly work she had undertaken on the subject of Bosnia-Herzegovina and the historical background of the tragic conflict there. As we stood by the book case, she became aware of the sad look on my face. Smiling, she said "Nema veze!", repeating it several times with emphasis. It was her way of telling me in Serbian not to be so concerned, that her coming death was really not important.

What a truly wonderful person she was, and how important her life was to us all!

D. L. Carpenter

Au revoir, Yela !

Au moment où elle s'en est allée, je pense à Yela Stevanovitch en me rappelant tout ce que nous avons vécu ensemble et notre relation suivie, non seulement d'elle par rapport à moi, mais aussi par rapport à mon épouse Suzanne et à mes enfants.

J'ai rencontré Yela pour la première fois à l'A.G. de l'URSI à Lima (Pérou), en 1975. Nous avions sympathisé, à l'époque, en bonne connivence de circonstance mais sans plus, et nous le fîmes encore aux A.G. d'Helsinki (1978) et de Washington (1981).

Notre relation s'est très fort approfondie à partir de l'A.G. tenue à Florence en 1984. A cette occasion, sur décision du Bureau de l'URSI, j'avais été nommé Secrétaire Général Adjoint de l'Union, fonction que j'ai exercée jusqu'en 1990. Dans toute cette période de six ans, j'ai passé une journée par semaine au Secrétariat de l'URSI, à gérer les affaires de l'Union, en discussion constante avec Yela, mais en nous en référant toujours au Secrétaire-Général, Jean Van Bladel, pour la décision finale. C'est dans cette position que j'ai vraiment pu apprécier le rôle que tenait Yela dans la structure de l'URSI et aussi sa personnalité propre.

Ce rôle s'affirmait au plus haut point lors des Assemblées Générales de l'URSI. J'ai vécu à ses côtés celles de Florence (1984), Tel Aviv (1987) et Prague (1990). Une Assemblée Générale de l'URSI est, pour le Secrétariat, une période de très grande surcharge. On doit produire des agendas et procès-verbaux pour nombre de réunions, celles du Bureau, du Conseil, du Comité de Coordination. En outre, on doit introduire dans la discussion, nombre de communications entrantes, telles que tous les rapports venant des Commissions. Bref, il y a déjà de quoi occuper tous les membres du Secrétariat, chaque jour jusqu'au milieu de la nuit.

Ce qui m'a le plus impressionné, dans cette période, c'est que dans cet océan de surcharges, dont Yela était inévitablement la première victime, il y avait, en permanence, un bureau d'accueil chaleureux : celui que Yela maintenait ouvert pour tous les participants, en dehors des moments où elle était contrainte d'assister à des réunions. On venait trouver Yela à toute heure pour des problèmes les plus divers : un problème de visa, une réservation d'hôtel déficiente, une pénurie d'argent pour un participant venant d'une région exotique, une information sur le programme de telle ou telle Commission, voire un avis sur la manière de voter sur tel ou tel point au Conseil de l'URSI. Yela accueillait toutes ces visites avec une convivialité extrême et en leur donnant la priorité sur les travaux de secrétariat qu'elle devait assumer. Dans ce scenario, elle m'est un peu apparue comme la mère de l'URSI, c'est-à-dire la première personne à laquelle le scientifique moyen peut s'adresser, pour une information ou un conseil.

Mais ce que peu de personnes savent, c'est que en dehors des périodes d'Assemblée Générale, des scientifiques en difficulté, parce qu'ils manquaient de financements, s'adressaient souvent à Yela en quête de l'une ou l'autre aide. Ils ont toujours été bien accueillis. Il y en eut plusieurs que Yela a logés gratuitement chez elle lors de séjours à Bruxelles, parfois pendant plusieurs semaines. Nombre de responsables de l'URSI ont aussi séjourné chez elle. L'appartement de Yela était aussi, un peu, celui de l'URSI.

Il y a un dernier point que je voudrais évoquer, en parlant de Yela. C'est son parcours personnel, qui fut très difficile. Née à Gand, en Belgique, fille d'un médecin serbe et d'une épouse belge, elle y a passé son enfance avant de retourner en Serbie avec sa famille. Là-bas, elle a vécu durement les affres de la deuxième guerre modiale. Son frère, qui s'était engagé auprès des résistants serbes à l'occupant nazi, y laissa sa vie. Son père fut longuement emprisonné par le régime de Tito, devenu le maître du pays. Yela a géré ces problèmes à Belgrade avec beaucoup de courage, étant elle-même suspecte aux yeux du régime. Un jour cependant, elle a pu s'en échapper, en profitant des opportunités offertes par un congrès international où elle pouvait participer comme interprète. C'est dans ces circonstances qu'elle est arrvée à Bruxelles, où le Secrétaire Général de l'URSI, M. Herbays, l'a prise en charge et lui a offert un travail au Secrétariat de l'URSI. Elle a été toujours été très reconnaissante à l'URSI de l'avoir aidée dans un moment très difficile. Cela explique sans doute son très grand dévouement à notre Union et son attention particulière aux personnes en difficulté.

En dépit de ce parcours très difficile, Yela gardait un optimisme fondamental. Rendre service était une de ses raisons de vivre. Son plus grand plaisir était d'aider les jeunes ; beaucoup lui en sont reconnaissants. Nous garderons de Yela un souvenir ému.

Paul Delogne

Therapeutic Uses of Pulsed Magnetic-Field Exposure: A Review

Naomi M. Shupak

1. Introduction

Bioelectromagnetics is the study of the interaction between non-ionizing electromagnetic fields and biological systems. In the extremely low frequency (ELF, ≤ 300 Hz, [1, 2, 3]) part of the electromagnetic spectrum, experimental therapies have been emerging for a variety of medical conditions, such as non-union bone fractures, skin ulcers, migraines, and degenerative nerves. Pulsed electromagnetic fields have been used as therapeutic agents over the last 40 years, following convincing evidence that electric currents can accelerate bone formation [4]. Specifically, electromagnetic-field stimulation gained credibility as a therapy following observations that the application of physical stress on bones promoted the formation of very small electric currents that are related to bone formation. A similar mechanism has been observed for cartilage, whereby electrical stimulation of chondrocytes increased the synthesis of the major component of cartilage matrix, known as proteogylcans [5].

A subset of ELF electromagnetic fields, i.e., pulsed electromagnetic fields (PEMF), displays frequencies at the low end of the electromagnetic spectrum [6], from 6 Hz up to 500 Hz. Another characteristic of PEMF waveforms is their rate of change. High rates of change (e.g., Teslas/second) are able to induce significant biological currents in tissues, thereby enabling them to have greater biological effects than waveforms of lower rates of change, if the biological effect is dependent on the magnitude of the induced current [1].

Extremely low frequency fields are non-ionizing and athermal (defined as either inducing no significant heating of the tissue, or thermal heating below the naturally occurring thermal fluctuations in tissue [2]). The waveforms associated with PEMFs can be asymmetric, biphasic, and quasi-rectangular or quasi-triangular in shape [6]. However, most ELF sources of electromagnetic-field stimulation produce a sinusoidal waveform [1]. In 1979, the United States Food and Drug Administration (FDA) approved both quasi-rectangular and quasi-triangular waveforms as safe and efficacious forms of treatment of disorders associated with fractures [6]. Specific types of low-level EMFs have the ability to produce specific biological responses, depending on the parameters (e.g., magnitude, frequency, waveform) of the field [2]. Intermittent use of PEMF stimulation has been shown to produce superior outcome responses to continuous use [7].

There are two methods in which PEMF stimulation can be non-invasively applied to biological systems: capacitive or inductive coupling. Capacitive coupling does not involve any contact with the body. In contrast, direct coupling requires the placement of opposing electrodes in direct contact with the skin surface surrounding the tissue of interest [7]. For example, if PEMF therapy is desired for the long bone of one's right arm, the opposing electrodes would be placed on the skin on either side of the right arm, surrounding the bone of interest.

Inductive coupling does not require the electrodes to be in direct contact with the skin. Rather, the time-changing magnetic field of the PEMF induces an electric field (Faraday's Law of Induction), which, in turn, produces a current in the body's conductive tissue [7, 8, 9, 10].

Pulsed electromagnetic-field stimulation – used as a treatment for conditions such as non-union bone fractures, failed joint fusions, and congenital pseudarthroses – has yielded success rates of 70% to 95% in prospective and double-blind studies. Treatment times range from 20 minutes to 8-10 hours per day, depending on the condition to be treated and the field parameters used [11]. There is no

Naomi M. Shupak, Frank S. Prato, and Alex W. Thomas are with the University of Western Ontario (Medical Biophysics), Lawson Health Research Institute, St. Joseph's Health Care (London), 268 Grosvenor Street, London, Ontario, Canada N6A 4V2; Naomi M. Shupak: Tel: +1 (519) 646-6000 ext. 64682; Fax: +1 (519) 646-6135; E-mail: nshupak@lri.sjhc.london.on.ca; Frank S. Prato: +1 (519) 646-6000 ext. 64140; Fax: +1 (519) 646-6135; E-mail: prato@lri.sjhc.london.on.ca; Alex W. Thomas: Tel: +1 (519) 646-6000 ext. 64191; Fax: +1 (519) 646-6135; E-mail: athomas@lri.sjhc.london.on.ca

Editor's Note: This is one of the *Reviews of Radio Science*, invited by Commission K.

Study	Parameters	Effect of MF
Bassett et al. [18] (Beagle dogs)	2 mV/cm, 1.5 msec, 1 Hz, biphasic; 20 mV/cm, 0.15 msec, 65 Hz, biphasic	Accelerated bone repair
Bassett et al. [19] (Beagle dogs)	2 mV/cm, 1.5 msec, 1 Hz, biphasic; 20 mV/cm, 0.15 msec, 65 Hz, biphasic	Accelerated bone repair
Wilson & Jagadeesh [41] (Rats)	Diapulse; 65 μsec bursts, 80-600 pulses/sec	Increased speed of nerve regeneration
Bassett et al. [20]	ElectroBiology Inc.; quasi-rectangular, assymetrical, 300 μs pulse width; 75 Hz 12-16 hrs daily; 3-6 months	Promoted osteogenesis
De Haas et al. [23] (Rabbits)	0.1 Hz, 0.015 T; 1 Hz, 0.015 T; 4 Hz, 0.025 T 6 hrs/day; 5 days/week; 2 weeks	Not effective; healing initiated at 1 Hz but effect not maintained
Heckman et al. [13]	Electro-biology Inc., Fairfield, N.J. Min. 12 hrs/day; min 3-4 months	Healed 64.4% of ununited fractures
Barker et al. [22]	0.3 T/s, 15 Hz 12-16 hrs/day; 24 weeks	Established tibial unions (questionable effect)
Binder et al. [32]	73 $\pm$ 2 Hz; 2.7 mT (peak) 5-9 hrs daily; 4 weeks	Reduced pain, improved active range
Raji [42] (Rats)	Diapulse; 400 pulses/sec 15 min daily; 3.5 days, 1, 2, 3, 4, or 8 weeks	Acclerated rate of recovery of injured nerve; enhanced regeneration of damaged nerves
Kavaliers et al. [89] (Mice)	Rotating magnetic field, 1.5 G – 90.0 G Several exposure periods	Abolished morphine-induced analgesia
Devereaux et al. [33]	Single pulse of 200 μs, 15 Hz 8+ hrs daily; 1-2 days	No effect on lateral humeral epicondylitis
Kavaliers & Ossenkopp [97]	0.2 mT - 3.5 mT, 30min, 10 consecutive days	Reduced tolerance to morphine
Ossenkopp et al. [83] (Mice)	static: 1470 $\pm$ 0.2 G; radiofrequency: 6.25 MHz, 2 bursts (gaussian, square) every 100 msec pulsed: 8 x 10^3 G/sec (z), 10 x 10^3 G/sec (x, y) 22.5 min pre- and post-morphine injection	Attenuated morphine-induced analgesia
Frykman et al. [12]	Bi-osteogen, System Electro-biology Inc., Fairfield, N.J. 8-10 hrs daily; mean 4.3 months	Healed non-union scaphoid fractures
Prato et al. [86] (Mice)	static: 0.15 T; pulsed: 0.4 mT_{pk} - 0.9 mT_{pk} radiofrequency: Gaussian pulse, 2 and 4 ms widths 23.2 min, 62 MHz	Static component had no effect, radiofrequency component reduced, and pulsed component abolished morphine- induced analgesia
Kavaliers & Ossenkopp [88] (Snail)	0.1 mT - 0.8 mT; 0.5 Hz 15 - 30 min	Inhibited analgesia from opioid agonists
Sisken et al. [44] (Rat)	0.3 mT, 20 msec pulse, 2 Hz repetition 1 hour daily	Regeneration of sciatic nerve
Ieran et al. [38]	2.8 mT, 75 Hz, 1.3 msec 3-4 hrs daily; 90 days	Increased success rate of treating venous skin ulcers; reduced recurrence rate
Mooney [36] (Rabbits)	0.18 mT, 1.5 Hz	Increased success rate of interbody lumbar fusion established effectiveness of bone graft stimulation
Omote et al. [62] (Rats) (Cell culture)	4 mT, 200 Hz, pulse width 2.0 msec 1 hr (once) 4 mT, 250 Hz, pulse width 1.5 msec 2 hrs (once)	Increased survival of rats; survival greatest when PEMF and drug given in combination Colony formation suppressed; greater suppression with Combination PEMF & drug
Tabrah et al. [25]	2.85 mT (peak), 380 μsec quasirectangular, followed by 72 Hz, 6 msec quasitriangular wave 10 hrs daily; 12 weeks	Short-term increased bone mineral density
Bassett & Schink-Ascani [16]	Electo-Biology Inc. (Parsippany, NJ); amplitude set to deliver 1.5 mV/cm for normal cortical bone with periosteum 10-12 hrs daily; 3 months - 4 years	Healed congenital pseudarthrosis of the tibia
Bellossi & Desplaces [59] (Mice)	12 Hz, 9 mT 10 min, 3 non-consecutive days/wk from 2-3 wks after tumours appeared until death	Increased length of survival in early stage of cancer development
Mouchawar et al. [66] (Dogs)	Rectangular pulses 0.1 msec in duration at 50 Hz	Stimulated the heart
Sanseverino et al. [28]	50 Hz solenoid, 3 mT - 6 mT 15-40 min daily; 15 sessions	Removed pain, recovered joint mobility, maintained improved conditions of joints
Stiller et al. [9]	PELUT; ΔB = 2.2 mT; 3 part pulse (+, -, +) of 3.5 msec total width 3 hrs daily; 8 weeks (or earlier is healed); 12 wks total if improvement present at 8 wks	Decreased wound depth and pain intensity
Kanje et al. [43] (Rats)	60 μT or 300 μT, 2 pulse/sec 15 min-24 hrs/day; 1-7 days	Pretreatment increased regeneration of sciatic nerve (not all MFs were effective)
Kavaliers & Ossenkopp [84] (Snails)	0.1 mT - 0.8 mT; 0.5 Hz	Reduced opioid-induced analgesia following administration of naloxone
Roland et al. [48]	0.5 Hz - 17 Hz; 0.1 μT - ~0.15 μT 15 min daily; 1 week	Improved tinnitus
Betancur et al. [87] (Mice)	3 mT - 4 mT	Reduced analgesic effect
Fleming et al. [100] (Rats)	5 μT pulse burst; 1 sec on, 4 sec off 20 minutes	Increased analgesia
Grant et al. [65] (Rabbits)	2.8 mT, 75 Hz, single pulse (280V) 350 min	Lessened cortical ischemic oedema, reduced ischemic neuronal damage

Table 1: Summary of Magnetic Field Effects as Therapeutic Agents in Treatment

Hannan et al. [8] (Mice)	5.2 mT, 250 pulses/sec, 120 μsec ramped pulse 1 hr	Decreased tumour size when in combination with chemotherapy drugs
Jorgensen et al. [39]	1-250 MHz; 2-30 pulses/sec 15-30 min; repeated as necessary	Relief from pelvic pain
Del Seppia et al. [93] (Pigeons)	continuous + 70 μT to - 20 μT; sinusoidal	Hyperalgesia (heightened sensitivity) to painful electrical stimulation
Papi et al. [94]	continuous + 70 μT to - 20 μT; sinusoidal	Increased sensitivity to painful electrical stimulation
Konrad et al. [26]	5 mT, 50 Hz 20 min/session; 20 treatments total	Reduced pain and improved hip movements
Darendeliler et al. [17]	15 Hz, positive duration 200 μsec; 1.8 mT 8 hrs daily; 9 days	Accelerated rate of bone repair
Glazer et al. [35] (Rabbit)	peak (negative) 3 $\pm$ 1 T/sec; (positive) 9 $\pm$ 4 T/sec 26-msec pulse burst; 670 $\pm$ 10-msec burst interval 4 hrs daily; 6 weeks	Reduced the rate of pseudarthrosis
Godley [21]	Electro-biology Inc. (Parsippany, NJ) 10 hrs daily; 3 months	Enabled solid union of carpal scapoid
Harrison & Bassett [27]	PEMF coils 10 hrs nightly; 7.5 to 18.5 months	Not effective in treating Perthes' Disease
Liang et al. [63] (Mice) (Tissue culture)	5.25 mT, 250 pulses/sec, 120 μsec ramped pulse 1 hr weekly; 3 weeks 5.25 mT, 250 pulses/sec, 120 μsec ramped pulse 1 hr weekly; 3 weeks	Decreased tumour volume in combination with anti-cancer drug Enhanced potency of anti-cancer drug only when PEMF was prior to drug injection
Richards et al. [47]	5 μT - 10 μT, 4-13 Hz, 1 msec pulsed waves 10-24 hrs daily; 2 months	Improvement in performance tests; increased alpha EEG during a language task
Sartucci et al. [101]	0.5 Hz; 70 μT to -20 μT; 0.1 msec duration	Reduced pain thresholds and pain-related somatosensory evoked potentials
Thomas et al. [95] (Snail)	100 μT_{pk}, 0.4 T/s 15 min	Induced analgesia, and increased opioid- induced analgesia
DiCarlo et al. [68] (Chick embryos)	60 Hz; 4 μT, 6 μT, 8 μT, or 10 μT 20 min	Increased rate of survival (reduced anoxia- induced mortality)
Jankauskienė et al. [46]	1 mT, 80 kHz 30 min; 10 sessions	Improved soft tissue, reduced inflammation; did not affect visual signs or eye movements
Mann et al. [53]	900 MHz, pulsed with 217 Hz, 577 μsec width 8 hrs (1 night)	Cortisol slightly elevated; no change in growth/ luteinizing hormones, or melatonin
Thomas et al. [98] (Snail)	100 Tpk, 0.4 T/s 15 - 30 min daily; 6 - 9 days	Development of tolerance, and cross- tolerance to repeated MF exposures; effect reduced with novel environmental cues
Albertini et al. [74] (Rats)	Triangular waveform; 75 Hz; 30 mT	Reduced necrotic region of myocardial infarct
DiCarlo et al. [67] (Chick embryos)	60 Hz; 4 μT, 6 μT, 8 μT, or 10 μT 20 min	Increased rate of survival; induced stress response that protected embryo myocardium from anoxia-related mortality
Karasek et al. [57]	2.9 mT, 40 Hz, square impulse shape 20 min daily, 5 days/week; 3 weeks 0.025 mT - 0.08 mT, 200 Hz, complex saw-like impulse shape, bipolar 8 min twice daily, 5 days/week; 3 weeks	Significantly lowered rise in nocturnal melatonin Did not influence melatonin levels
Carmody et al. [73] (Cells)	60 Hz, 8 μT 20 minutes - several hours	Protection from ischemia-reperfusion injuries
Del Seppia et al. [85] (Mice)	hypogeomagnetic field: 4 μT Oscillating magnetic field: 20 μT - 70 μT 90 min in home cage; 30 min restrained	Suppressed stress-induced analgesia
de Seze et al. [61] (Mice)	100 mT, 0.8 Hz square-wave 8 hours daily	Decreased tumour growth;increased survival
Karasek et al. [58]	25 μT - 80 μT, 200 Hz, saw-like impulse shape 8 min twice daily, 5 days/week, 3 week	No effect on melatonin concentrations
Marks [34]	Spinal-Stim (Orthofix Inc., Richardson, TX) 4+ hrs daily, 4-6 months	Enhanced bone bridging in lumbar spinal fusion
Matsumoto et al. [24] (Rabbits)	0.2 mT/ 0.3 mT/ 0.8 mT; 100 Hz; width 25 μsec 4 or 8 hrs daily; 1, 2, or 4 weeks	Promoted bone formation
Jacobson et al. [30]	0.034 μT - 0.274 μT; 0.976 Hz - 7.7 Hz 6 min, 8 sessions; 2 weeks	Reduced knee pain due to osteoarthritis
Pipitone & Scott [14]	50 μT; 3 Hz, 7.8 Hz, or 20 Hz 10 min, 3 times daily; 6 weeks	Improvement from baseline in pain, stiffness, and physical disability
Prato et al. [79] (Mice)	200 μT_{pk}, 0.4 T/s	Increased movement under low intensity light; decreased movement under high intensity light
Thomas, Drost, & Prato [77]	200 μT_{pk}, 0.4 T/s	Improved standing balance
Thomas, White, et al. [78]	200 μT_{pk}, 0.4 T/s	Improved standing balance in fibromyalgics and controls to greater degree than in arthritics during eyes open; all groups had worse standing balance during eyes closed
Williams et al. [60] (Mice)	0, 10 mT, 15 mT, or 20 mT; 120 pulses/s 10 min daily	Reduced tumour growth and vascularization
Robison et al. [64] (Human cell lines)	0.15 $\pm$ 0.02 mT_{pk} sinusoidal, 120 W, 60 Hz 4, 12, or 24 hours	Decreased susceptibility to heat-induced apoptosis, leading to proliferation of cancer
Warman et al. [54]	200 μT - 300 μT; 50 Hz 2 hours; 1 night	Changed melatonin onset variability, but not average melatonin onset time

Note: Subjects were humans unless otherwise indicated.

Table 1: Summary of Magnetic Field Effects as Therapeutic Agents in Treatment (continued)

discomfort or known risk associated with this stimulation, it is non-invasive, and the cost of medical treatment is substantially reduced relative to the costs of surgery [2, 6, 7, 11]. The presence of implanted metals does not appear to affect the therapeutic ability of the PEMF exposure [10]. Furthermore, PEMF therapy is simple to use [2]: no surgical procedure is required, the PEMF stimulation can be performed in an office setting, there are no known complications, no anesthetic is required, and the length of treatment is comparable to bone-grafting procedures. However, these advantages of PEMF stimulation are qualified by the cooperation of the patient [12]. Specifically, the patient must sometimes use the PEMF stimulation device for upwards of 10 hours daily, must immobilize the fracture ends, and must ensure no weight-bearing [13].

Of particular concern when considering the use of PEMF stimulation as a clinically therapeutic agent are the health risks associated with exposure to such stimulation. While evidence for carcinogenic effects of magnetic fields (magnetic fields) is small, and there is no evidence supporting the direct damage of DNA by electromagnetic fields, there is some support that magnetic-field stimulation could act as a co-carcinogen in combination with a known genotoxic and/or non-genotoxic carcinogen. There is greater support for the possibility of teratogenic and reproductive effects of ELF magnetic fields [1]. Despite the ongoing debate over the safety of PEMF exposure, it is generally believed and accepted that brief exposure to the fields is safe. Nevertheless, there are still warnings for those with known cancers, those who are pregnant, and those with permanent pacemakers to avoid exposure sessions [7].

This review will examine the therapeutic benefits of PEMF stimulation as used in clinical and experimental settings. Procedures that involve electrode placement in tissue, i.e., capacitive coupling methods, will not be included in this review. Summaries of the discussed findings are provided in Table 1 (studies listed by publication date) and Table 2 (studies listed by disease/ condition category).

2. Musculoskeletal Disorders

To date, the only FDA approvals for the use of PEMF stimulation for clinical treatment are for therapeutically resistant problems of the musculoskeletal system, such as delayed-union bone fractures, failed joint fusions, and congenital pseudarthroses [6, 11, 14]. Several cellular mechanisms, including increases in growth factors, have been implicated as the possible causes of success from PEMF stimulation. For example, fracture non-unions, failed joint fusions, and congenital pseudarthroses are thought to be healed via increases in mineralization [6], angiogenesis, collagen production, and endochondral ossification that result from PEMF stimulation. Congenital pseudarthroses also show decreased osteoclasis following PEMF therapy [11].

2.1 Bone Repair

Bone repair requires the cooperation of bone-specific cell-types: osteoblasts and osteoclasts. Osteoblasts are involved in the formation of bone, while the main function of osteoclasts is in bone resorption. Generally, these two cell types are in normal balance, and the amount of bone is kept constant. When a fracture occurs, osteoblasts and osteoclasts work together to quicken the healing process. However, sometimes healing is not at an optimum, and non-unions result. These types of fractures require an additional stimulus, such as pulsed electromagnetic-stimulation, to assist in the healing process [15].

Pulsed electromagnetic-field stimulation has been shown to have an effect on bone repair via a number of different mechanisms. Firstly, PEMF has been shown to stimulate calcification of the fibrocartilage in the space between the bony segments. Second, the increased blood supply that arises due to PEMF's effects on ionic calcium channels have been implicated as a source of improved bone healing. Thirdly, PEMF has been suggested as having an inhibitory effect on the resorptive phase on wound repair, leading to the early formation of osteoids and calluses [16, 17]. A fourth mechanism by which PEMF is thought to have an effect on bone repair is through its influence on increasing the rate of bone formation by osteoblasts [15].

The degree to which PEMF stimulation is effective is dependent on several factors, including anatomic location, associated surgery, patient age, disability time, date of treatment initiation, adherence to treatment protocol, and infections. In general, non-unions in young adults are more easily stimulated to heal than those in older adults, and stimulation has been found to be more effective if initiated within two years of onset of the original fracture [13].

Non-union fractures are those fractures in which healing does not occur within six months of injury. These fractures represent 3% of all long-bone fractures, and result in a tremendous amount of discomfort and pain. The use of PEMF stimulation as a treatment for non-unions has been very successful, with success rates reaching 80% [7, 12]. The amount of time required prior to having this treatment prescribed is slowly being reduced from its original requirement of nine months following injury. Furthermore, the successful results obtained from this treatment have prompted discussions of the use of these fields for treatment of ordinary fractures. It is anticipated that PEMF stimulation on ordinary fractures would reduce the amount of time that a cast must be worn [7].

The first study to report successful application of PEMF stimulation was conducted by Bassett et al. Using 43 beagle dogs with surgically produced bilateral fibular osteotomies, these researchers were able to demonstrate a non-invasive acceleration of the repair process in the dogs

Disease	Author	Ref.	Effect of MF
Bone			
Osteotomy	Bassett et al.	[18]	Accelerated fibula bone repair
	Bassett et al.	[19]	Accelerated fibula bone repair
	De Haas et al.	[23]	Quickened initiation of long bone healing; did not sig. reduce time for solid union
	Darendeliler et al.	[17]	Increased new bone growth
Non-union bone fracture	Bassett et al.	[20]	Osteogenesis
	Heckman et al.	[13]	Enhanced bone healing
	Barker et al.	[22]	Established tibial unions; not sig. different from controls
	Frykman et al.	[12]	Healed non-union scaphoid fractures
	Godley	[21]	Enabled solid union of carpal scaphoid
Congenital Pseudarthrosis	Bassett et al.	[16]	Healed tibial congenital pseudarthrosis
Bone formation	Matsumoto et al.	[24]	Increased bone contact and bone area with the implant
Osteoporosis	Tabrah et al.	[25]	Initial increase in bone density followed by steady decline
Hip Arthroplasty	Konrad et al.	[26]	Improvement in pain ratings and hip movements
Perthes Disease	Harrison et al.	[27]	No significant difference from controls
Joint			
Joint Disorders	Sanseverino et al.	[28]	Decreased pain ratings and improved mobility of joint
Rheumatoid Arthritis	Ganguly et al.	[29]	Enhanced improvements in pain, swelling, tenderness, and joint function among seronegative relative to seropositive patients
Osteoarthritis	Pipitone et al.	[14]	Improvements in pain, stiffness, and physical disability relative to baseline
	Jacobson et al.	[30]	Greater reduction in pain
Rotator Cuff Tendinitis	Binder et al.	[32]	Decrease in pain ratings, increase in active range
Lateral Epicondylitis	Devereaux et al.	[33]	No significant benefit
Spinal Fusions			
Spinal fusions	Marks	[34]	Enhanced successful bony bridging
Pseudarthrosis	Glazer et al.	[35]	Enhanced solid union, increased stiffness, increased maximum load before fusion failure
Interbody lumbar fusions	Mooney	[36]	Improved success rate of solid fusion
Ulcers			
Venous leg ulcers	Ieran et al.	[38]	Healed ulcers for prolonged period; prevented recurrence
	Stiller et al.	[9]	Decreased wound surface area, wound depth; increased healthy granulation tissue
	Flemming et al.	[37]	Insufficient evidence from reviewed studies to warrant use of PEMF stimulation
Pelvic Pain			
Pelvic Pain	Jorgensen et al.	[39]	Quickened return to normal activities, prevented need for surgery
Nerves			
Median-ulnar nerve	Wilson et al.	[41]	Stimulated and quickened nerve regeneration
Peroneal nerve	Raji	[42]	Quickened toe-spreading reflex, enabled nerve regeneration
Sciatic nerve	Sisken et al.	[44]	Regeneration of nerve
	Kanje et al.	[43]	Enhanced regeneration of nerve
Endocrine ophthalmopathy	Jankauskienė et al.	[46]	Reduced soft tissue involvement and proptosis, improved corneal and optic nerve function
Neurological Disorders			
Multiple Sclerosis	Richards et al.	[47]	Improvement in performance scales;increased alpha EEG during language tasks
Tinnitus	Roland et al.	[48]	Improvements in symptoms; reductions in sensation levels
Neuroendocrine System			
Hormone production	Mann et al.	[53]	Altered cortisol secretion pattern
Melatonin levels	Karasek et al.	[57]	Reduced melatonin profile depending on pulse parameters
	Karasek et al.	[58]	No influence on melatonin concentrations
	Warman et al.	[54]	Changed melatonin onset variability, but not average melatonin onset time
Cancer			
Mammary carcinoma	Bellossi et al.	[59]	Increased length of survival
	Williams et al.	[60]	Reduced tumour growth/ vascularization
KMT-17 / KDH-8 tumours	Omote et al.	[62]	Increased survival rates, decreased colony formation, especially in combination with drug therapy
A431/ HT-29 cell lines	Hannan et al.	[8]	Reduced mean tumour volume, esp. in combination with anti-cancer drugs
Subline KB-ChR-8-5-11	Liang et al.	[63]	Reduced tumour size and enhanced survival
HL-60, HL-60R, and Raji cell lines	Robison et al.	[64]	Decreased susceptibility to heat-induced apoptosis, enabling proliferation of cancerous cell lines
Benzo(a)pyrene- induced tumours	de Seze et al.	[61]	Decreased rates of tumour growth; increased survival
Cerebral Ischemia (Stroke)			
Focal ischemia	Grant et al.	[65]	Reduced extent of cortical oedema, and areas of neocortex and neostriatum
Coronary Protection			
Cardiac Stimulation	Mouchawar et al.	[66]	12 kJ required to achieve closed-chest ectopic beats
Myocardial Protection	DiCarlo et al.	[68]	Incresed survival rates following cardiac anoxia damage
	Albertini et al.	[74]	Reduced necrotic region of myocardial infarct
	DiCarlo et al.	[67]	Increased survival rates following cardiac anoxia damage
	Carmody et al.	[73]	Protection from ischemic-reperfusion injury
Psychophysiological Regulation			
Human Standing Balance	Prato et al.	[79]	Increased movement under low Intensity light; decreased movement under high intensity light
	Thomas, Drost, ...	[77]	Improved standing balance
	Thomas, White,...	[78]	Improved standing balance in fibromyalgics and controls to greater degree than in arthritics during eyes open;all groups had worse standing balance during eyes closed

Table 2: Efficacy of Magnetic Field Therapy, by Disease Category

Pain	Kavaliers et al.	[89]	Abolished morphine-induced analgesia
	Kavaliers & …	[97]	Reduced tolerance to morphine
	Ossenkopp et al.	[83]	Attenuated morphine-induced analgesia in mice
	Prato et al.	[86]	Static component had no effect, radiofrequency component reduced, and pulsed component of MF abolished morphine-induced analgesia
	Kavaliers & …	[88]	Inhibited analgesia from opioid agonists
	Kavaliers & …	[84]	Reduced opioid-induced analgesia following administration of naloxone
	Betancur et al.	[87]	Reduced analgesic effect
	Fleming et al.	[100]	Increased analgesia
	Del Seppia et al.	[93]	Hyperalgesia (heightened sensitivity) to painful electrical stimulation
	Papi et al.	[94]	Increased sensitivity to painful electrical stimulation
	Sartucci et al.	[101]	Reduced pain thresholds and pain-related somatosensory evoked potentials
	Thomas et al.	[95]	Induced analgesia, and increased opioid-induced analgesia
	Thomas et al.	[98]	Development of tolerance and cross-tolerance to repeated MF exposures; effect reduced with presentation of novel environmental cues
	Del Seppia et al.	[85]	Suppressed stress-induced analgesia

Table 2: Efficacy of Magnetic Field Therapy, by Disease Category (Continued)

following 28 days of exposure to low-frequency, low-intensity PEMFs (2 mV/cm, 1.5 ms, 1 Hz, biphasic; or 20 mV/cm, 0.15 ms, 65 Hz, biphasic). The 65 Hz PEMF was more effective in improving healing (i.e., producing new bone tissue) than was the lower-frequency field [18, 19].

2.1.1 Non-Unions

Bassett, Pilla, and Pawluk [20] reported the first account of a therapeutic benefit of ELF PEMFs in humans. These researchers reported that PEMF stimulation (300 is pulse width; 75 Hz) on surgically resistant non-unions led to osteogenesis as a result of the therapy. Twenty-five of the 29 patients in the study displayed radiographic evidence of bone formation following one month of stimulation. Furthermore, these researchers were able to prevent several individuals who were recommended for amputations from these painful and debilitating procedures.

Following the success of Bassett et al. [20], further research was conducted investigating PEMF stimulation on fracture healing. Heckman et al. [13], for example, reported a 64.4% success rate in 149 patients who used PEMF stimulation to treat non-unions. For patients who maintained intensive use of the stimulation for three months, effectiveness was seen in 85% of patients. Frykman et al. also reported success of PEMF stimulation. These researchers reported an 80% success rate among 44 patients with non-unions of the scaphoid (a small bone in the wrist joint) treated with PEMF stimulation, and advocated PEMF stimulation as an alternative method for treating non-union scaphoid fractures when long-arm cast treatment proves ineffective [12]. This finding was replicated in 1997 in a case study of a 12-year-old boy with a non-united carpal scaphoid fracture who was successfully treated with PEMF stimulation, such that union of the fracture was established following treatment [21]. The use of PEMF stimulation appears to be effective, and a reasonable choice of treatment, among individuals suffering from non-unions [13].

A more recent reporting by Traina et al. [10] of the successful application of PEMF exposure for the treatment of non-unions claimed a 74% healing rate, with age of patient, site of fracture, type of non-union, and presence of infection as significant factors influencing the results. The presence of infection of the bone tissue or surrounding soft tissue was previously reported to not have an effect on the treatment outcome [10].

The early success of PEMF treatment of non-unions was not replicated in every study. For example, PEMF stimulation (0.3 T/s burst waveform, 15 Hz) was not shown to be effective in the treatment of un-united tibia fractures at 12 months post-injury. Specifically, Barker et al. [22] found that five of the nine patients in the active treatment group, relative to five of the seven patients in the placebo group, displayed united fractures at the end of the 24-week experiment. These data suggest the need for further research; yet, this study included only 16 patients, and so there was very little statistical power to detect a significant difference. Also, the induced electric fields were much lower in this study than in the original work by Bassett [20].

2.1.2 Congenital Pseudoarthrosis

Pulsed electromagnetic-field stimulation has also been shown to have clinical efficacy for the treatment of congenital Pseudoarthrosis [16]. This treatment modality aims at bone consolidation, as well as prevention of re-fracture and misalignment of the bones involved [10]. Specifically, PEMF (8 T/s, 20 pulses repeated at 15 Hz) stimulation, along with immobilization of the fractured area, was found to have an 80% or greater success rate for Type I and Type II lesions (gaps less than 5 mm wide) for which no operations had yet been performed. Type III lesions (lesions which are atrophic, spindled, and had gaps in excess of 5 mm wide) were not as responsive to PEMF stimulation, displaying a 7% success rate in response to treatment that included only PEMF, and an overall 19% success rate for treatments that also included operations. The lesion types were defined according to the lesion's appearance on X-ray photographs [16]. The success of treatment of congenital pseudoarthrosis with PEMF stimulation was outstanding since in the past, amputation was the most frequent outcome for this disorder [6].

2.1.3 Osteotomies

Pulsed electromagnetic field stimulation has been shown to have an additional use in bone repair – one that has yet to be approved by the FDA. Treatment of osteotomies (misaligned bones) in guinea pigs with PEMF therapy (15 Hz, 200 is unipolar pulse, 1.8 mT, 3 T/s) has resulted in increased new bone growth in the gap caused by the osteotomy relative to placebo group animals, where loose connective tissue filled the osteotomy sites. This study provides implications to humans about the possibilities of using PEMFs to quicken craniofacial healing [17]. However, disapproval of PEMF stimulation was provided by De Haas et al. [23], who found that recently osteotomized long bones of rabbits given PEMF stimulation experienced a quicker initiation of the healing process, but did not have a significantly reduced time for solid union relative to control rabbits.

The pulse parameters of a magnetic field as well as its duration of use are important characteristics that have been shown to influence the effectiveness of PEMF stimulation. Matsumoto et al. [24] investigated the bone formation surrounding dental implants inserted into the femur of rabbits, and found that bone contact with the implant was greater among PEMF-treated (100 Hz, rise times of 8 T/s, 12 T/s, and 32 T/s for 0.2 mT, 0.3 mT, and 0.8 mT peak, respectively) animals relative to controls. Among treated rabbits, 0.2 mT and 0.3 mT fields had significantly greater bone contact and bone area than the 0.8 mT-treated femurs. No significant difference was observed for bone contact or bone area for those femurs treated four hours/day as opposed to eight hours/day. Furthermore, it was found that two weeks of exposure had a significantly greater effect than one week; yet, the measured outcomes were not significantly lower at two weeks than they were following four weeks of exposure. This study indicated the need to select the proper magnetic-field intensity, duration, and length of treatment to maximize outcome [24].

2.2 Other Orthopedic Disorders

2.2.1 Osteoporosis

Osteoporosis, the most common skeletal disorder, is associated with decreased bone mass. Consequences of this condition include the inability of the skeleton to resist stresses of everyday life, resulting in numerous fractures. The beneficial application of PEMF stimulation in healing non-union bone fractures suggested the possibility that such treatments might be beneficial to patients with osteoporosis. Twenty post-menopausal women participated in an investigation of the effectiveness of PEMF therapy in increasing bone density. During twelve weeks of daily 72 Hz pulsating magnetic field exposure (380 ìs quasirectangular wave, followed by 6 ms quasitriangular wave), bone densities of exposed bone regions increased; however, during the 36 weeks following treatment, bone densities decreased significantly. These rebound results suggest the immediate effectiveness of PEMF therapy, and indicate the need for continued treatment to ensure prolonged increased bone density [25]. A decrease in initial improvement is not exclusive to PEMF treatment; any treatment (including drug therapy) given to improve symptoms associated with osteoporosis is expected to show declines following its removal.

2.2.2 Hip Arthroplasty

Hip arthroplasties are required when individuals are suffering from hip problems. A common side effect of such surgeries, however, is the loosening of the prosthesis that occurs in 15% - 25% of patients within 10 years of the surgery. The successful application of PEMF therapy in orthopedic disorders prompted Konrad et al. [26] to consider its use in a non-blinded, uncontrolled study investigating the treatment of twenty-four patients suffering from aseptic loosening of the hip prostheses. Patients were assessed for levels of pain and hip movements prior to and following exposure to magnetic fields (50 Hz, 5 mT). No patients were randomized to a sham condition. Significant improvements in pain ratings and all hip movements (except for flexion and extension) were noted following exposure sessions in patients suffering from loose hip replacement, but not for those patients suffering from severe pain due to gross loosening of the hip prostheses [26]. This suggests that PEMF therapy may only be beneficial in reducing mild-to-moderate pain associated with hip prostheses, but not severe pain levels.

2.2.3 Perthes Disease

While there have been good results found from the treatment of orthopedic disorders with PEMF, not all diseases or conditions have benefited from such treatment. For example, Perthes' disease, a condition in which young children suffer from a temporary loss of blood supply to the femoral head (the ball part of the hip joint) has not been shown to benefit from PEMF stimulation [27]. Twenty-two boys, randomized to either orthosis plus PEMF treatment or sham treatment, displayed no significant differences in treatment durations (an average of 12.5 months for those receiving PEMF versus an average of 12.0 months for those receiving sham). The treatment time was defined as the amount of time required for the upper femoral epiphysis (the top part of the femoral head) to be resistant to the deforming effects caused by weight-bearing. Based on this controlled study, there does not appear to be a significant effect of PEMF stimulation on the successful treatment of Perthes' disease.

However, there are inconsistencies in the literature with respect to the success of PEMF stimulation in treating diseases associated with the femoral head. For example, research investigating the ways in which PEMF stimulation enables repair of the dead bone associated with lack of blood supply to the femoral head has found that PEMF exposure enables repair of the dead bone by promoting ingrowth of new blood vessels, while maintaining a balance between the rate of dead bone removal and the formation of new bone [6]. Vallbona and Richards [4], commenting on studies using EMF stimulation to treat femoral-head necrosis, reported that this form of treatment resulted in successful progression for lesions located in the hips, according to both clinical (80% successes) and magnetic resonance (MR) imaging (76.6% successes) evaluations. The combined clinical and MR imaging success rate was reported as 63.3% for the lesions.

2.3 Summary of Orthopedic Literature

Pulsed electromagnetic field exposure has been applied to a variety of orthopedic pathologies, mostly with positive, successful indications. For example, Traina et al. [10] reported that PEMF therapy was a successful modality of treatment of congenital pseudoarthrosis, pseudoarthrosis, delayed union, fracture at risk, recent fracture, bone grafts, vertebral arthrosis, and avascular necrosis. Limb lengthening, however, was not successfully achieved through the use of PEMF stimulation. The reader is directed to the review prepared by Traina et al. [10] on bone healing through pulsed electromagnetic-field exposure and other means of biophysics enhancement for a more comprehensive analysis of bone healing.

3. Rheumatological Disorders

3.1 Joint Diseases

Pulsed electromagnetic-field therapy has been shown to be effective in treating joint diseases; yet, the degree of its success depends on the specific joint disease in question. Specifically, joint diseases involving only one joint, as well as single traumata (suffering from acute lesions), show significant improvement following PEMF stimulation. In contrast, disorders involving multiple joints (e.g., polyarthrosis, rheumatoid arthritis) are much more resistant to the effects of PEMF stimulation, and show less improvement following treatment sessions. In a large 11-year experimental study, 3014 patients suffering from a joint disease were treated with extremely low frequency, low-intensity sinusoidal magnetic fields (0.6 T/s - 1.2 T/s). Patients were given one 15 - 40-minute session daily for 10 - 15 days to assess the effects of the pulsed magnetic field exposure on healing of the joints and associated pain levels. These patients – except females who were pregnant or menstruating, and individuals who carried a pacemaker – were exposed to the magnetic fields. Control patients (in addition to the 3014 patients) were included and provided with sham treatment. Of the 3014 subjects who received PEMF exposure, 78.8% showed good results (i.e., pain disappearance, 40% - 50% increase in degrees of freedom of the sick joint, maintenance of benefit for at least three months, decrease in thermal irradiation of the affected joint after magnetic-field exposure). The best results were obtained with patients who participated in therapeutic exercises following magnetic-field therapy, and maintained control of body weight and bone mineralization. Control patients reported a complete absence of any benefit when (unknowingly) exposed to sham treatment; upon subsequent exposure to the active PEMF unit, these controls obtained the same results as the patients who were exposed to the active unit [28].

3.1.1 Rheumatoid Arthritis

Rheumatoid arthritis (RA) is a chronic condition in which an individual suffers from inflammation of the joints, resulting in feelings of pain, stiffness, and swelling. There is no known cause of this disorder, but it has been implicated as being autoimmune in nature. In testing individuals for the presence of rheumatoid arthritis, screening can be conducted for an antibody known as the rheumatoid factor (RF). The rheumatoid factor is present in the blood of 80% of adults suffering from rheumatoid arthritis [29]; however, its presence or absence does not necessarily indicate that one has rheumatoid arthritis. Individuals who possess the rheumatoid factor are classified as serological-positive, while those lacking the antibody are categorized as serological-negative.

Gunguly et al. [29] conducted a study investigating the effectiveness of PEMF stimulation in reducing pain, tenderness, swelling, joint functional disability, and joint spasm with deformity in 35 patients suffering from rheumatoid polyarthritis (multiple joint disorders). Patients in this study were assessed according to serological grouping. Results indicated that those individuals lacking the rheumatoid factor (i.e., patients who were serological-negative) showed earlier responses to the PEMF (rectangular pulse) for pain and swelling, and a much earlier improvement for pain, tenderness, and joint functional disability relative to serological-positive individuals. The same trend appeared for joint spasm with deformity; however, the overall treatment effect for this symptom was low for both groups. These findings provide empirical support for clinicians to treat individuals with and without the rheumatoid factor differently, as PEMF was not shown to be as effective a therapy for those possessing the antibody [29].

3.1.2 Osteoarthritis

Osteoarthritis is the most common rheumatic disorder, affecting older people in industrial countries [5]. It is characterized by degeneration of articular cartilage (cartilage at a joint), and the presence of hypertrophic (enlargement of organ due to increase in size of constituent cells) tissues [30]. Those suffering from the disorder experience pain, swelling, tenderness, and stiffness in the weight-bearing joints of the lower extremities [5]. Approximately 80% of the population over 75 years of age displays radiological signs of osteoarthritis, with 40% - 80% of these individuals also having clinical symptoms of the disease [14, 30].

Treatment for osteoarthritis has begun to shift away from drug therapies – which have, in large part, been found to be ineffective and toxic – and towards more unconventional modes of healing [5]. This shift has resulted despite the firm position of the American College of Rheumatology that there is currently inadequate scientific documentation to warrant the use of PEMF therapy for treatment of osteoarthritis of the hips and knees [14]. Nevertheless, PEMF stimulation has been gaining increasing support as a treatment for osteoarthritis. It has been suggested that magnetic fields are beneficial in the treatment of osteoarthritis because they suppress inflammatory responses at the level of the cell membrane [31].

An attempt to demonstrate the clinical importance of magnetic-pulse treatment for knee osteoarthritis was conducted by Pipitone and Scott [14]. These authors found no significant improvement of magnetic-field-treated patients (unipolar pulse, 7.8 Hz in morning, 3 Hz in evening; < 50 T/s) relative to placebo-treated patients at the end of the study. However, the authors did find that magnetic-field-treated patients reported significant improvements in a questionnaire assessing pain, stiffness, and physical disability at the end of the study relative to their baseline scores on these measures. In contrast, no significant changes were observed for placebo-treated patients in these measures between baseline and the end of the study. This work suggests that PEMF stimulation should be included as a part of the treatment protocol for individuals suffering from osteoarthritis; however, further experimentation using different magnetic devices, treatment populations, and experimental protocol should be considered.

3.1.3 Rotator-Cuff Tendinitis

Rotator-cuff tendinitis, inflammation of one or more of the muscles that holds the ball of the shoulder joint tightly against the socket, is a common cause of shoulder pain among adults. Conventional treatments, such as corticosteroid injections, are not always effective; therefore, alternative therapies have been evaluated. A randomized double-blind experiment designed to assess the effect of PEMF stimulation [73 $\pm$ 2 Hz; 2.7 mT_{pk}, 7.9 T/s] on individuals suffering from rotator-cuff tendonitis was conducted. The design of this experiment consisted of three phases. During the first phase, one group of patients received PEMF treatment, while the other group received sham treatment. The second phase involved the administration of PEMF exposure for *both* groups of patients. In the third phase, no PEMF stimulation was given to either group. This design allowed for obvious group differences to be detected upon the introduction of the second phase, and also enabled all subjects to receive the PEMF treatment following four weeks (the beginning of second phase), as opposed to only offering such therapy to the treatment group. Upon presentation of PEMF stimulation to the control group at the beginning of the second phase, a remarkable decrease in pain ratings and an increase in active range were noted. These scores were in the direction of those of the treatment group, with no significant group differences present following the four-week mark of the study. These findings demonstrate the ability of PEMF stimulation to reduce pain and increase activity among individuals suffering from rotator-cuff tendinitis, and implicate such therapy for individuals who suffer from the disorder, and are unresponsive to, or noncompliant with the administration of, corticosteroid injections. Overall, Binder et al. found that more than 70% of all patients in this study improved following PEMF therapy [32].

3.1.4 Lateral Humeral Epicondylitis

The success of PEMF therapy in treating rotator-cuff tendinitis prompted rheumatologists to consider the use of such therapy for other chronic tendon lesions, such as lateral humeral epicondylitis (better known as "tennis elbow"). A randomized, double-blind assessment of the effectiveness of PEMF therapy in treating this condition (a minimum of eight weeks of treatment) in 30 patients failed to find a significant beneficial effect of PEMF stimulation (single pulse, 200 ìs duration, 15 Hz) to warrant its use over placebo conditions. This conclusion may be related to the 53% spontaneous healing found among patients in the placebo group, or to the use of different pulses in treating lateral humeral epicondylitis relative to other rheumatological disorders [33].

4. Spinal Fusions

Spinal fusions occur when an individual is suffering from a painful vertebral segment, and wishes for the motion at the vertebral region to be reduced to help alleviate the pain. This type of surgery is invasive, and is used only after more conservative methods of treatment have been explored (e.g., bed rest, drug therapy, exercise, massage) [34]. Once spinal fusions are deemed medically necessary, the surgical team wants to ensure that recovery will be as quick as possible, and that minimal pain will be endured. One method in which to achieve these goals is through the use of PEMF stimulation. Marks [34] found that spinal fusions for discogenic low back pain were successful (i.e., incorporation of the graft, no radiolucency between graft and vertebral bone, no motion at level of fusion) in 97.6% of the surgeries of patients in the PEMF stimulation group, as opposed to the low 52.6% success rate among patients in the unstimulated group, indicating that PEMF stimulation allows for bony bridging in lumbar spinal fusions. Furthermore, successful spinal fusions correlated with good or excellent clinical outcomes [34].

A complication of spinal fusions arises when an individual also suffers from Pseudoarthrosis, the failure of a union to develop in fusion. The use of PEMF therapy to reduce Pseudoarthrosis has been shown to be effective in a rabbit fusion model [35]. Twenty adult white rabbits were randomly assigned to either a PEMF or a sham exposure for four hours daily for six weeks. Characteristics of the electromagnetic field included asymmetric rise and fall times (3 ± 1 T/s and 9 ± 4 T/s) using a 26-ms pulse burst, a 670 ± 10-ms burst interval, and a pulse rise and fall time of 400 ns. The animals were euthanised at six weeks, at which time radiologic and histologic samples were taken. Radiographic analysis indicated that six of the 10 animals in the placebo group, and eight of the 10 animals in the PEMF group, had solid fusions. In the rabbits that demonstrated solid fusion, there was a significant increase in stiffness of the fusion mass, a significant increase in area under the load-displacement curve (representing energy absorbed by each motion segment), as well as a significant increase in the maximum load before fusion failure among the PEMF-exposed animals relative to the placebo controls [35]. The implication of these findings to human studies is of importance, as this study provided preliminary support for the idea that exposure to PEMFs can reduce Pseudoarthrosis, thereby reducing pain among human patients with lower back pain.

4.1 Interbody Lumbar Fusions

Interbody lumbar fusions are performed to help release stress from a damaged disk that has caused a pinched nerve root. The rates of lumbar fusion are unpredictable; however, following evidence that PEMFs have the ability to aid in bone formation, it has been shown that the presence of these fields has a significant effect on spinal fusions. Using a double-blind prospective approach, Mooney [36] assessed the success of spinal fusions in 195 patients who were undergoing initial attempts at interbody spinal fusions. Success rates were defined as radiographic evidence of solid fusion. For those patients who complied with the methodology of using the brace for at least eight hours each day, there was a success rate of 92.2% in the active treatment group (PEMF, 0.18 mT, 1.5 Hz). This rate was significantly higher than the 67.9% success rate found among patients in the placebo group. The patients' age, sex, fusion level, number of grafts, graft type, or internal fixation did not affect these success rates. Smoking made very little difference, yet showed a decreased trend in success rates for both active and placebo group patients [36]. It should be noted that there is controversy as to whether interbody lumbar fusions are an orthopedic indication.

5. Soft-Tissue Regeneration

5.1 Venous Leg Ulcers

Leg ulceration is a chronic, recurring condition, affecting more women than men, and increasing in prevalence with increasing age. Venous leg ulcers are caused by a blockage in the veins of the legs. Compression can heal most of these ulcers; however, it is not an effective form of treatment for all such sores [37]. Pulsed electromagnetic-field stimulation has been investigated as a therapy for wound healing following results that PEMFs can promote healing by potentially increasing collagen synthesis, angiogenesis, and bacteriostasis [9, 37].

The use of PEMF stimulation to reduce the size and eliminate pain associated with venous leg ulcers was investigated in a double-blind study of patients suffering from skin lesions present for at least three months [38]. Using a 2.8-mT magnetic field with a 75-Hz frequency and pulse width of 1.3 ms over a treatment protocol of 90 days, these researchers found a significantly higher success rate (66% versus 32%) among patients exposed to the active PEMF device relative to those exposed to identical dummy devices. Furthermore, the effect of the field exposure was prolonged, evident at follow-up of at least one year, and protected the patient from ulcer recurrence. These findings suggest that PEMF stimulation is a useful complement to the treatment protocol for venous leg ulcers [38].

A prospective, multi-center, double-blind, randomized study was conducted to assess the efficacy of a portable PEMF stimulation device, PELUT (pulsed electromagnetic limb ulcer therapy). The PELUT device (bi-directional $2.2\,mT_{pk}$, three-part pulse of 3.5 ms total width, induces a low-level, non-thermal electrical field of 0.06 mV/cm in the skin above the wound dressing) was modeled after devices that have been successful in treating non-union fractures. Subjects suffering from recalcitrant venous stasis ulcers were randomized into either treatment or placebo group conditions, and were assessed at baseline, four weeks, eight weeks, and 12 weeks from the start of the experiment. All subjects were also given standard wound dressings as part of the treatment protocol. At week eight, relative to placebo group subjects, those individuals treated with the PELUT exhibited a 47.7% (significant) decrease in wound surface area, a significant decrease in wound depth, and a 15% increase in healthy granulation tissue. Those patients who had shown improvement at the eight-week mark, and chose to remain in the treatment program for an additional four weeks, exhibited further improvement, showing a 66% decrease in wound surface area at that time. The investigators' global assessments of the ulcers revealed a 50% improvement among those in the treatment group relative to a 0% improvement rate among the ulcers in the placebo group. None of the ulcers on subjects in the treatment group worsened following treatment; however, 54% of the ulcers in the placebo group worsened over the course of the eight weeks [9].

A review conducted by Flemming and Cullum [37] to investigate the effectiveness of PEMF in treating venous leg ulcers reported that, to date, there is insufficient evidence to warrant the clinical use of PEMF stimulation for the treatment of such ulcers. However, given the results reported in Stiller et al. [9], there is a need to perform further investigations into the true ability of PEMF stimulation in treating these ulcers.

6. Pelvic Pain

Another useful clinical application of PEMF radio-frequency (RF) stimulation is for the treatment of pain arising from pelvic disorders such as dysmenorrhoea, endometriosis, ruptured ovarian cyst, and acute lower urinary tract infection. In a study involving a total of 20 episodes of pain arising from pelvic disorders, pain was reduced following PEMF stimulation in 90% of the cases (i.e., 18 episodes). Pulsed electromagnetic stimulation involved brief 15-minute – 30-minute exposures to short pulses (1.0 MHz - 250 MHz; 2 - 30 pulses/s). The pain relief was evident following PEMF stimulation, and permitted a quicker return to normal life activities and prevented surgery. Patients suffering from the remaining two episodes of pain did not report pain relief following treatment. Recurrence of the pain condition occurred in one, or possibly two, of the treated episodes, and there were no adverse side effects reported either during or following treatment [39].

7. Nerves

Investigations into possible therapies and treatments for damaged nerves are essential, as these injuries can have detrimental and devastating effects in humans. However, human research is not always the best first approach for introducing and subsequently assessing nerve damage. Rather, animal models provide an excellent avenue for establishing an injury to a nerve to enable an understanding into what methods are successful in the repair of the injury. Animal studies investigating repair of damaged peripheral nerves have focused on the use of PEMF exposure sessions to aid in the regeneration of the nerve [40].

Wilson and Jagadeesh [41] conducted an experiment designed to assess regeneration of the median-ulnar nerve in the upper forelimb of 132 rats using PEMF (Diapulse Corporation of America; 65-ms pulse bursts) and sham treatments. Nerve-conduction studies indicated a return to nerve conduction of degenerated nerves following Diapulse treatment, but not following sham treatment. Histology slides revealed regenerating nerve fibers 30 days post-surgery in PEMF-treated rats; slides taken 60 days post-surgery in control rats showed evidence of regeneration, but not to the level found in the treated rats at 30 days post-surgery. Taken together, these results indicated that PEMF treatment is effective in stimulating and quickening the regeneration of the median-ulnar nerve in rats [41].

Further research into treating injured nerves with PEMF treatment investigated a nerve that is fairly important to humans: the peroneal nerve. Located in the leg and used for walking, when damaged, the peroneal nerve prevents individuals from lifting their foot and moving their toes. Raji [42] conducted an animal study investigating the degeneration and regeneration of this nerve using PEMFs. These researchers inflicted injury to the left peroneal nerve of male Lewis rats to assess the effects of both PEMF (Diapulse; 400 pulses/s) and sham treatments on the recovery of the rat's injured leg. Regeneration of functionally complete motor nerves was assessed via a test of reflex spreading of the toes upon being lowered suddenly to the ground. Results from the test suggest the beneficial usage of Diapulse, as the toe-spreading reflex was significantly quicker to appear in treated as opposed to untreated animals. Furthermore, microscope slides revealed accelerated progressive improvement in the appearance of transverse sections of the nerve, as well as increases in the number of nerve fibers, among magnetic-field-treated animals relative to rats in the sham group. These results suggest that PEMF therapy is beneficial in aiding the regeneration of the peroneal nerve in male rats [42].

Continued research on nerve repair and PEMF treatment has enabled investigations into other nerves of interest. In particular, the largest nerve in the body, the sciatic nerve, has followed the success of previous research, and has shown enhanced regeneration following exposure to PEMFs relative to animals (e.g., male and female rats) given sham treatment [43]. Sisken et al. [44] have seen regeneration in the sciatic nerve after a crush lesion following one hour of exposure (0.3 mT, 20 ms pulse, 2-Hz repetition) daily; the regeneration did not improve significantly with longer exposure periods. Furthermore, rats pre-treated with 0.38 T/s PEMFs (20 ms pulse, 2 Hz) were shown to have enhanced regeneration of the sciatic nerve after a crush lesion, while those exposed to 60 ìT fields did not experience this effect. This indicates that the regeneration process might be receptive to specific fields [43]. Overall, these results suggest that PEMF treatment can be used to successfully repair the sciatic nerve.

The animal studies conducted on nerve repair and PEMF treatment, considering nerves from both the arms and the legs, all converged on the finding that PEMF therapy was effective in nerve regeneration relative to results obtained from animals given sham treatment. The regeneration rate following PEMF exposure was enhanced to the same degree as obtained by other treatment methods, including conditioning lesions, hormones, and growth factors [45].

7.1 Endocrine Ophthalmopathy

Endocrine ophthalmopathy is considered an organ-specific autoimmune disorder, caused by an abnormality in immune-response mechanisms. Possible treatments for this disorder include corticosteroids and nonsteroidal anti-inflammatory drugs to reduce the inflammation of the eye (an identifying characteristic of this condition). When these drugs are ineffective, alternative forms of treatment are required. The success of PEMF stimulation in improving metabolic processes in tissues and organs led to the study of the effectiveness of PEMF therapy in treating endocrine ophthalmopathy [46]. Following exposure to magnetic fields of 1 mT with pulses emitted at a frequency of

8.0×10^4 Hz, patients diagnosed with endocrine ophthalmopathy enjoyed reductions in soft-tissue involvement and proptosis (displacement of the eyeball). Limitations in ocular movements were reduced, while corneal and optic-nerve function improved following magnetic-field exposure; these measures did not, however, reach statistical significance. The study showed that PEMF therapy is only useful for those suffering from endocrine ophthalmopathy who show signs of soft-tissue involvement; nonetheless, given the gravity of this disorder, the evidence for the usefulness of and necessity for a non-invasive treatment method is great [46]. Further work is required to determine the significance of PEMF exposure on treating diseases such as endocrine opthalmopathy; a Pubmed search yielded this paper as the only one investigating such effects.

8. Neurological Disorders

8.1 Multiple Sclerosis

The findings that PEMF stimulation was successful in improving nerve conduction and regeneration indicates a possibility that its use might be effective in treating disorders of the central nervous system, such as multiple sclerosis (MS), for example. Multiple sclerosis is a neuro-degenerative disorder in which the myelin sheath surrounding neurons is damaged, and nerve conduction is slowed. In a randomized, double-blind study, Richards et al. [47] found significant improvement in performance scales (assessing bladder control, cognitive function, fatigue level, hand function, mobility, sensation, spasticity, and vision) among magnetic-field-exposed patients (PEMF: 5 - 10 μT, 4 Hz - 13 Hz, 10 - 24 hours daily, two months) relative to non-exposed patients. All subscales of the performance test, except for those of hand function and sensation, as well as the combined performance (all eight tests) were significantly improved among the PEMF-exposed individuals. Electroencephalograph recordings indicated significant improvements among the PEMF-treated individuals between pre- and post-exposure for six of the 19 electrodes, as well as increased alpha EEG during a language task among MS patients exposed to the magnetic fields relative to MS patients who were not exposed to the magnetic fields. No significant differences between pre- and post-treatment scores were found for the test of clinical ratings. These findings suggested that PEMF therapy is a beneficial short-term treatment for individuals suffering from MS [47].

8.2 Auditory Disorders: Tinnitus

Tinnitus, more commonly known as "ringing in the ears," is a disorder of the auditory system in which a bodily condition, such as disturbances of the auditory nerve, causes the affected individual to hear sensations of noises (e.g., ringing) that are only audible to that individual. The high prevalence of this condition warrants alternative methods, such as PEMF stimulation, to be considered as possible treatments [48].

A double-blind randomized trial assessing the effectiveness of PEMF stimulation as a treatment for tinnitus found significant improvements in symptoms and significant reductions in sensation levels among the group of patients treated with the active PEMF device (0.5 Hz - 17 Hz; 0.1 - ~0.15 ìT). Overall, significantly more PEMF-group patients (45%) than placebo-group patients (9%) reported subjective improvement throughout the trial [48]. The study thus provided another useful and efficacious application of PEMF stimulation, and submitted evidence that PEMF therapy should be considered among other therapies for use among individuals suffering from tinnitus.

8.3 Psychiatric Disorders: Affective Disease

Transcranial magnetic stimulation (TMS), a safe and non-invasive method of exciting neurons through strong, brief, and focused [49] magnetic-field pulses, is currently the only ethically approved technique of modulating neuronal activity in the human brain. This method of stimulation works via the principle of induction: a capacitor is discharged to enable a strong current to pass through a coil placed over the scalp [50]. The strength of the induced current is a function of the rate of change of the magnetic field, which is affected by the current in the coil. The coils used today have a magnetic field peak intensity of 1.5 T to 2 T at the face of the coil, and neurons can be activated as far as 1.5 cm to 2.0 cm from the surface of the coil in the cortex [51]. The magnetic-field intensity used in TMS is many orders of magnitude larger than that present in ELF magnetic-field exposure, i.e., of the order of 10,000 T/s, as compared to maxima around 10 T/s.

Single-pulse TMS has been distinguished from repetitive TMS (rTMS) in that the latter is a modification of the former in which the magnetic field is repeated over a small time interval, allowing the stimulation of nerves during their refractory period. The multiple pulses that exist in rTMS are discharged through one coil using multiple stimulators, and are classified as fast rTMS if stimulation is greater than or equal to 1 Hz, and slow rTMS if stimulation is less than 1 Hz [49]. The use of rTMS has been considered for the treatment of psychiatric disorders such as depression, as it shares many of the behavioral and biochemical actions as other antidepressive treatments, such as electroconvulsive shock (ECT). Specifically, both treatments use transcranial brain stimulation; however, rTMS produces a localized effect, while ECT's effect is more generalized. Despite promising results with rTMS, its use has not yet produced evidence of beneficial results matching the effectiveness of the more-conventional treatment options [52].

9. Neuroendocrine System

The neuroendocrine system, a combination of hormone secretion and central nervous system activity, can be studied to investigate the biological effects of PEMFs [53]. To assess this link, the effects of an RF PEMF (modulated electromagnetic field) on hormone production were assessed in a healthy male population. Using a 900 MHz PEMF (217 Hz) set to provide a near-homogeneous field distribution, Mann et al. [53] determined nocturnal hormone profiles (growth hormone, luteinizing hormone, cortisol, melatonin) during both sham and RF PEMF exposure. The only significant difference in hormone secretions noted between the placebo and exposure trials was the significant interaction between field exposure and time, suggesting a different cortisol secretion pattern between the two sessions. No difference was reported between total cortisol production between the sham and exposure sessions, indicating a temporal difference in secretion of the hormone while under the influence of the RF PEMF [53]. Another study, designed to determine the effects of magnetic-field exposure on the human melatonin profile, used two-hour pulses of high-level circularly polarized 50 Hz magnetic fields (200 - 300μT) delivered at different circadian times [54]. Blood samples taken every 30 minutes to 60 minutes over a 17-hour overnight period provided multiple plasma melatonin measurements. Results from the study revealed that while no significant changes were present in average melatonin onset time following magnetic-field exposure, melatonin onset was significantly more variable following magnetic-field as opposed to sham exposure. The authors of the study discussed the possibility, on the basis of preliminary data, that the circadian time of the magnetic field might have an influence on the magnitude and direction of the observed response. This possibility might be the mediating link to explain why magnetic-field exposure has not been shown to consistently affect human melatonin profiles [54].

Further investigations of the effects of PEMFs on melatonin levels were conducted. Melatonin, a hormone derived from the pineal gland in the brain and controlled by the light-dark environment [55], is associated with pathological conditions – including cancer – when its levels are altered [56]. Levels of this hormone are generally high at night and low during the day [55]. Melatonin is believed to be important in synchronizing circadian rhythms [56], helping to induce sleep, reducing insomnia, eliminating jet lag, and has been speculated to be a contributor to anti-inflammatory and analgesic responses, as well as to soft-tissue repair [57]. As such, determining ways in which to modify melatonin levels is important to helping with these ailments that melatonin is thought to "cure." The presence of melatonin helps to retard the growth of tumors; however, exposure to ELF PEMFs has an inhibitory effect on the production of melatonin from the pineal glands at night, resulting in increased growth of tumor cells [56].

The ability of melatonin to reduce tumor growth may be a function of its role as hydroxyl (• OH) and peroxyl (ROO •) radical scavengers. Free radicals can be toxic and can damage DNA, leading to cancer. Melatonin's antioxidant properties, present through its indole functional group, enable the protection of DNA from oxidative damage (through less free radical attack on the DNA), resulting in reduced incidence of cancer [56]. Since it has been shown that magnetic-field exposure can suppress melatonin secretion, and it has also been shown that melatonin, as a hormone, acts to stop cancer growth, it may be possible to design specific magnetic fields to stimulate melatonin secretion as a treatment for cancer patients [31].

Karasek et al. [57] utilized two PEMFs (2.9 mT, 40 Hz, square impulse shape, bipolar; 0.025 - 0.08 mT, 200 Hz, saw-like impulse shape, bipolar) to assess whether exposure to either had an effect on melatonin levels in men suffering from low back pain. Results from that experiment revealed a significantly reduced melatonin profile following exposure to the 2.9 mT pulse, but no significant difference relative to baseline when exposed to the 0.025 - 0.08 mT pulses. These findings suggested that melatonin levels can be altered by specific PEMF parameters [57], and implied that further research should be conducted to further elucidate the exact "best" parameters for altering melatonin levels in humans.

Further research conducted by Karasek et al. [58], investigating whether the effect of melatonin concentrations in patients with low back pain could be influenced by magnetic-field exposures of different characteristics (e.g., different magnitudes), revealed negative results: chronic exposure to magnetic fields varying in magnitude between 25 and 80μT and having a frequency of 200 Hz did not influence human serum melatonin concentrations. However, those magnetic-field amplitudes were lower than those used by Karasek et al. [57].

10. Cancer

Cancer research is essential, since this disease affects a large proportion of the population, and is one of the major causes of death in North America. Given the promising results of PEMF stimulation in treating other disorders and human conditions, Bellossi and Desplaces [59] conducted an experiment investigating the effects of PEMF exposure on survival rates in C3H/Bi female mice with mammary carcinoma. Using a 9-mT PEMF, set at either 12 Hz or 460 Hz, these researchers found increased length of survival during the early stages of the disease when the mice were exposed to the 12-Hz magnetic field, and increased length of survival during the late stages of the disease when exposed to the 460-Hz field [59]. Williams et al. [60] conducted further work assessing the effects of therapeutic EMF on mammary carcinoma vascularization and growth in C3H/HeJ mice. These researchers found that daily 10-min sessions of 10-, 15-, or 20-mT pulsating magnetic field (120 pulses/s) significantly reduced tumor growth and the extent of vascularization relative to mice not exposed to the magnetic field. The ability of magnetic-field exposure to prolong survival was replicated in later work conducted by de Seze et al., using tumor-induced male and female mice. These researchers found that eight hours of daily exposure to the 100-mT, 0.8-Hz square-wave magnetic field resulted in significantly decreased rates of tumor growth and increased survival [61]. These three studies indicated that survival and tumor growth can be positively influenced by magnetic-field exposure.

In addition to using PEMF stimulation as a treatment for cancer growth, it is also possible to use this therapy as an adjunct to drug therapy. A combination treatment of pulsing magnetic fields (PMF) and an anti-tumor drug, mitomycin C (MMC), was shown to be successful in treating two experimentally-induced tumors [62]. Either the KMT-17 or the KDH-8 tumor cells were implanted subcutaneously into the right thigh of a male rat. Seven days following implantation, an intravenous injection of MMC was given to the rat; one hour later, PEMFs (2 T/s, 200 Hz) were applied over the thigh region. Rats were placed into one of four experimental groups: no treatment, MMC-only, pulsed-magnetic-field-only, or a combination of MMC and pulsed magnetic field. Survival rates of the KMT-17 implanted rats at 90 days were 0% for the untreated group, 34% in the MMC-only group; 47% in the pulsed-magnetic-field-only group, and 77% in the combination group. None of the rats implanted with the KDH-8 tumor survived to day 90; however, percentages of increased life span relative to untreated rats were 3.4% for the MMC-only group, 7.6% for the pulsed-magnetic-field-only group, and 17.6% for the combination group. Analysis of the cultured cells treated in each of the three treatment groups revealed a significant decrease in colony formation in the combination group relative to either the MMC-only or pulsed-magnetic-field-only (2.7 T/s, 250 Hz) groups. These results indicated the ability of pulsed magnetic field treatment to enhance treatment above that provided solely by MMC injections, and offer hope for possible alternative treatments for cancer [62].

The combination treatment of pulsed magnetic stimulation and anti-tumor drugs has been used in further research following the promising, successful results obtained by Omote et al. [62]. Using an average field strength of $0.525\ mT_{rms}$, three different chemotherapeutic drugs (cisplatin, carboplatin, and doxorubicin), and either A431 or HT-29 human cell lines implanted into nude or NIH-III female mice, the results consistently showed that mean tumor volume was reduced by the combination treatment (i.e., drug + pulsed magnetic field group). Specifically, the volumes of the tumors in combined-treatment mice were 52%, 34%, and 35% of those found in the cisplatin, carboplatin, and doxorubicin drug-only treatment groups, respectively. This consistent finding demonstrates the generality of pulsed magnetic field augmentation of anti-tumor drug effects [8].

Liang et al. [63] conducted more complex investigations of the combined effect of pulsed magnetic field and drug therapy. These researchers investigated the effects of the combined treatment (i.e., Daunorubicin + pulsed magnetic field) approach on a multi-drug-resistant (MDR) human carcinoma subline KB-Ch^R-8-5-11. For the in vivo part of the study, female mice were inoculated with the KB- Ch^R-8-5-11 cells, and subsequently treated with one hour of pulsed magnetic field treatment (44 T/s, 250 pulses/s) and intravenous injection of Daunorubicin. The only significant differences in tumor volume were between the pulsed-magnetic-field-only and pulsed magnetic field + drug groups at both 39 and 42 days [63]. Thus, it appeared that the combination effect was significantly better at reducing tumor size relative to either treatment alone. The in vitro study revealed that the efficacy of Daunorubicin was enhanced when pulsed magnetic field (44 T/s, 250 pulses/s) was given before the drug was injected, but not when the pulsed magnetic field was given post-injection [63]. These findings provide additional support for the common trend among cancer research that a combination treatment of pulsed magnetic field and drug works best at reducing tumor volume and enhancing survival.

Despite these encouraging results regarding the beneficial effect of PEMF exposure on cancer reduction, the effect of such exposure sessions has not always been found to be positive. Robison et al. [64] have shown that electromagnetic field exposure (54 mT/s, 60 Hz) for 4, 12, or 24 hours resulted in decreased susceptibility to heat-induced apoptosis for three human cancer cell lines, indicating that the cancerous cell lines were able to proliferate. Furthermore, these exposure sessions also resulted in time-dependent decreased DNA repair rates among two of the three cell lines, allowing for propagation of the damaged DNA. Thus, there are conflicting results with respect to the effect of electromagnetic field exposure on cancer, possibly related to the significantly different characteristics of the PEMF exposures (for example, the study by Robison et al. [64] had a much lower T/s than the positive studies).

11. Cerebral Ischemia (Stroke)

The clinical implications of determining a model to protect against cerebral ischemia are important, since strokes have devastating and sometimes life-threatening effects on many individuals in society. Given this importance, Grant et al. [65] designed an experiment to assess the effects of low-frequency PEMF exposure on cerebral injury in a rabbit model of focal ischemia. Twelve male white rabbits underwent occlusion of the left internal carotid, proximal left anterior cerebral, and proximal left middle cerebral arteries for two hours, followed by four hours of reperfusion. Six of these rabbits subsequently underwent treatment, which included PEMF exposure (2.8 mT, 75 Hz) beginning 10 minutes following the onset of ischemia until the end of reperfusion. At the end of the six hours, the 12 rabbits were sacrificed, and magnetic-resonance-imaging (MRI) studies, as well as histological examinations, took place. The MRI studies revealed high-intensity lesions in the anterior and ventral cortical regions in the middle cerebral artery. PEMF exposure appeared to significantly reduce the extent of cortical oedema at the anterior level by 65% relative to controls. Histology slides revealed ischemic neuronal damage (IND) in the lateral neocortex and neostriatum within the middle cerebral artery ipsilateral to the occlusions. Subsequent to PEMF exposure, the areas of neocortex at the anterior level and the ischemic neuronal damage in the neostriatum were significantly reduced by 69% and 43%, respectively, relative to controls. These results suggest that exposure to PEMFs following focal cerebral ischemia can protect against the development of neuronal damage in the neocortex and neostriatum [65].

The success of combination treatment of pulsed magnetic fields and drugs for cancer treatment might be of benefit to researchers investigating possible therapies for cerebral ischemia. Specifically, given the effectiveness of the combined treatment in cancer, treatment for strokes may also be enhanced by the combined effect of drugs that are effective in treating acute focal ischemia [e.g., N-methyl-D-aspartate (NMDA) antagonists] and PEMF exposure [65]. The success of this approach can possibly be due to the enhanced ability of drugs in the presence of magnetic-field exposure to get across the blood-brain barrier.

12. Coronary Protection

12.1 Cardiac Stimulation

Stimulation of the heart is a necessary medical intervention to prevent coronary failure. Magnetic stimulators are capable of stimulating nerves; however, if the stimulation is too great, cardiac arrhythmias, or alterations in the rhythm of the heartbeat, can occur. Magnetic stimulation of the heart is preferred over stimulation with electrodes in direct contact with the skin since it is a less painful method of achieving the same result. To assess a method in which magnetic-field stimulation can be achieved without causing harm, Mouchawar et al. [66] investigated the threshold for cardiac stimulation by magnetic fields in 11 dogs. The PEMF was delivered via two coplanar coils placed on the surface above which the heart was located in the dogs. To induce a reversible and temporary cardiac arrest in the dogs, the researchers used rectangular pulsed magnetic fields (0.1 ms; 50 Hz) to stimulate the dogs' right vagus nerve. Once arrest was established (after approximately 3 s), electroencephalogram (ECG) and blood-pressure recordings were taken. If the PEMF coils produced an ectopic beat after the dog was in induced cardiac arrest, the voltage was reduced in decrements of 10% until the PEMF no longer evoked ventricular contractions. If, however, no ectopic beat was produced, the voltage was increased by 10% increments until such a beat was produced. The threshold was then defined as the voltage at which 10% less did not stimulate the heart. Results from the study indicated that an average energy of 12 kJ was required to achieve closed-chest ectopic beats via a PEMF. These findings acknowledge the importance of determining safe levels of magnetic fields, and suggest that it is possible to determine safety parameters for PEMF, such as those produced by MRI scanners [66].

12.2 Myocardial Protection

In addition to determining safe levels of PEMF stimulation for the heart, the determination of protective benefits of PEMF treatment for the myocardium would be of great importance to clinicians seeking ways in which to inhibit/ attenuate damage to the heart muscle following reduced oxygen to the area. DiCarlo et al. [67] showed that chick embryos (fertilized White Leghorn eggs) exposed to low-frequency (4-, 6-, 8-, and 10-μT; 60 Hz) PEMFs prior to exposure to an anoxia chamber had significantly increased survival rates (68.7%) relative to the survival rates of control embryos (39.6%) following cardiac anoxia damage. Anoxia was achieved by maintaining oxygen levels below 1% during the experiment. The embryos were subsequently re-exposed to ambient oxygen levels (21%) at the time at which 15% - 45% of control embryo hearts were still beating. Survival was objectively determined as the presence of a heart beat [68]. Further investigations revealed that the protection was due to the PEMF itself, and not due to thermal heating. This research provides encouraging results for human clinical studies, suggesting that preconditioning a human with exposure to PEMF stimulation prior to surgery and transplantation might minimize myocardial damage [67].

Human research, investigating methods in which the myocardium can be protected, is essential to enable potential longevity of human lives. Ischemia (interruption of blood flow) - reperfusion (reintroduction of blood flow) injuries to organs, such as the heart, have potential detrimental effects such as lack of oxygen that can kill ischemic cells, and subsequent reperfusion can introduce harmful oxygen radicals into the organ. Preconditioning a tissue with a non-lethal ischemia-reperfusion (I/R) can help protect the tissue from later, more fatal I/R events. Preconditioning a vital organ by inducing mild heat shock to the tissue or by exposing the tissue to electromagnetic fields helps to protect the organ from subsequent heat shocks [67, 69]. Heat-shock proteins produce heat-shock preconditioning; these proteins act to protect the cell from excess heat, free oxygen radicals, and I/R, and are important for a cell's survival [70, 71]. Heat-shock proteins produced in the presence of PEMFs [72] provide an alternative to other induction methods that are harmful and use non-localized stimuli, such as hyperthermia, or are controversial, such as gene transfection. The production of heat-shock proteins in specific cells is likely dependent on the magnetic-field susceptibility of those cells. For example, cardiomyocytes appear to be consistently stimulated during 60 Hz, 8 ìT magnetic-field exposure [67, 73, 74]. The magnetic-field exposure time required to provide protection from I/R injuries is also cell-dependent, and ranges from 20 minutes to several hours [73].

Heat-shock proteins are produced within the body, and provide the potential of protecting myocardial tissue from permanent damage due to I/R. However, a problem with the suggested use of PEMF exposure to induce production of heat-shock proteins is that clinically, patients are unlikely to present themselves prior to ischemia. Nonetheless, since most of the damage to the myocardial cells occurs during reperfusion, there is likely still to be a benefit of heat-shock protein production. Specifically, reperfusion therapy and transplantation cause injury that could be ameliorated with heat-shock proteins. It is still unknown whether cardioprotection is conferred by heat-shock proteins, or whether magnetic-field stimulation might be activating opiate agonists that then protect the cell from further damage [75]. Therefore, there is still much more work that must be done to determine the ultimate protector of cardiac cells, to ensure that the best possible, and most appropriate, treatment options are implemented to prevent further cardiac tissue damage.

13. Psychophysiological Regulation

13.1 Human Standing Balance

Pulsed electromagnetic-field stimulation has been shown to produce detectable physiological and behavioral effects in both animals and humans. The investigation of potential magnetic-field effects on human standing balance (postural sway) is important, since disturbances in this behavioral trait can indicate the presence of underlying diseases [76]. "Normal standing balance," defined as "the ability of a human to stand in a fixed position for a period of time [77]," is an automatic behavior in humans. When performed with "eyes open," little perturbations are noted in standing balance; however, this robust behavior is greatly affected when an individual is in the "eyes closed" state. Thomas et al. [77, 78] have extensively investigated this topic. Using a three-dimensional force plate to measure center-of-pressure movements, these researchers have included an objective measure of a behavioral response. Each subject in their studies was given four two-minute exposure conditions (eyes open/eyes closed, sham/magnetic field). Results from these studies suggested that specific ELF PEMF (200 μT_{pk} , 0.4 T/s; generated at head level) exposure has beneficial effects on standing balance, such that standing balance was improved significantly in both the "eyes-open" and "eyes-closed" conditions during magnetic-field exposure sessions relative to sham exposure sessions. The effect of PEMF exposure on standing balance appeared to be mediated by light intensity during the eyes-closed trials, as movement was significantly increased under low-intensity (0.12 W/m^2), and was decreased under high-intensity (0.51 W/m^2) light [79]. These results held for both genders and for all ages (range: 18 - 34 years), despite past findings that postural sway is sensitive to factors such as age and gender [76].

The influence of magnetic-field exposure on standing balance was affected by a subject's physical condition. Specifically, fibromyalgia patients (FM) and normal controls had similar standing balance during eyes open and sham exposure that was better than the standing balance recorded for rheumatoid-arthritis patients (RA). When eyes were closed, the postural sway of all three groups of subjects deteriorated, but to a greater degree in the two patient groups relative to the controls. Magnetic-field exposure was shown to improve the eyes-closed-to-eyes-open ratio in all three groups of subjects [78]. These results suggest that PEMF exposure has the ability to affect behavioral traits in both healthy controls and chronic pain patients.

14. Pain

Most of the therapeutic uses of magnetic-field exposure include a component of pain reduction; however, there are controversial reports in the literature regarding the effects of magnetic-field exposure on specific investigations of pain. Acute pain, or nociception, can be used as an outcome measure to determine sensitivity to stimuli. Nociception is a measure of an animal's or human's sensitivity to an adverse environmental stimulus. An understanding of how an organism responds to such stimuli enables researchers to determine its capacity to perform adaptive behaviors [80].

There is evidence to suggest that endogenous as well as exogenous opioid systems are affected by exposure to magnetic fields [80, 81, 82, 83, 84, 85]. Early investigations of the use of magnetic-field exposure on subsequent pain sensations revealed increases in pain following exposure sessions. Following knowledge that magnetic-resonance exposure can suppress analgesia in mice that have received morphine injections [83], Prato et al. [86] conducted a study to determine which of the various components of the magnetic field (static, time-varying, radio frequency) were responsible for the inhibitory effects of the exposure. The static component from the resistive magnet was 0.15 T; the time-varying component had peak magnetic fields of 0.4 mT and 0.9 mT, which corresponded to rise times of 2 ms and 3 ms, respectively; and the radio-frequency component at 6.25 MHz was a Gaussian-modulated pulse with widths of either 2 ms or 4 ms. Male mice were exposed to 23.2 min of one of the field components both before and after an injection of morphine sulphate (10 mg/kg), and analgesia was defined as the amount of time during which mice were on a hot surface (50 °C) before they displayed an aversive behavior (paw-lick, jump, etc). Results from the study indicated that exposure to the time-varying (pulsed) component of the magnetic field completely abolished, the radio-frequency component significantly reduced, and the static-field component had no effect on morphine-induced analgesia. These findings may have relevance to humans who have ingested drugs such as morphine, and are subsequently exposed to these components of the magnetic field during magnetic-resonance imaging [86].

Exposures to hypogeomagnetic and oscillating magnetic fields have also been shown to have inhibitory effects in male mice. Specifically, Del Seppia et al. [85] found that mice removed from the normal geomagnetic field and placed in mu-metal boxes showed suppressed stress-induced analgesia; these mice displayed significantly lower latencies than mice exposed to a normal geomagnetic field. Hypogeomagnetic-field exposed mice displayed an effect similar to that observed in mice after exposure to an oscillating magnetic field. These results suggest that in addition to time-varying PEMFs, the presence of hypogeomagnetic fields also has the ability to reduce stress-induced analgesia.

Further work investigating the inhibitory effect of magnetic-field exposure on analgesia in mice focused on the possible modulatory effect of light [87]. Mice, displaying stress-induced analgesia, were found to have significantly lower analgesic levels following stable magnetic-field exposure (3 - 4 mT) under white light, but unaltered analgesic levels following either red light or total darkness. These results replicated previous findings found using lower magnetic-field intensities [86], and suggest that magnetic-field exposure might exert its effect only under certain light-intensity conditions.

Other early work found similar results in the land snail, Cepaea nemoralis. Specifically, Kavaliers and Ossenkopp [88] determined that 15 - 30 min exposures to weak rotating magnetic fields (0.1 - 0.8 mT; 0.5 Hz) inhibited analgesia from opioid agonists. (Absence of analgesia was previously reported in mice following exposure to a similar magnetic field [89]). The latency of nociceptive responses (the elevation of the snail's anterior portion of its extended foot) was shown to increase following the administration of opioid agonists (morphine and U-50, 488H, respectively); however, the concurrent application of an opioid agonist and magnetic-field exposure resulted in significantly reduced nociceptive responses, indicating significant inhibitory effects of magnetic-field exposure on opioid-mediated analgesia. The reduction in opioid-induced analgesia apparent with the magnetic-field exposure sessions was similar to that observed following opioid-antagonist (naloxone) injections [88]. Exposing the snails to 0.1 mT_{rms} , 60 Hz magnetic fields yielded similar results, with reduced opioid-induced analgesia present following magnetic-field exposure sessions. This finding was upheld for a variety of magnetic-field exposure periods (0.5 - 120 hours), and the inhibitory effect was significantly greatest during the dark period of the snail's light-dark cycle [80]. Snails that received daily administrations of naloxone, an opioid antagonist, experienced increased opioid-induced analgesia in a manner similar to that apparent following the magnetic-field exposures [84]. A possible mediating variable that could explain the magnetic field's inhibitory effect on opioid-agonist analgesia is altered calcium channel activity. Calcium-channel antagonists, such as diltiazem, verapamil, and nifedipine, significantly reduced, but did not completely block the inhibitory effects of the magnetic fields on morphine-induced analgesia, while calcium-channel agonists, such as BAY K8644, further inhibited the effects of morphine-induced analgesia that were present with magnetic-field exposure [88]. Administration of either the calcium-channel antagonists or the calcium-channel agonists had no significant effect on the reductions in opioid-induced analgesia achieved by injections of naloxone. It is possible that magnetic-field exposure alters calcium-channel functioning, resulting in differential distribution of calcium ions. This finding was supported by research conducted by Fanelli et al. [90], who showed that exposure to static magnetic fields prevented apoptosis via the flux of calcium into U937 and CEM cells. McCreary et al. [91] provided further support for the change in calcium-ion concentrations following magnetic-field exposure; these authors reported significant changes in cytosolic calcium concentrations following exposure to alternating-current (AC), direct-current (DC), or a combination of AC/DC magnetic fields after cell cycle, pH of suspension medium, and response to monoclonal antibody were controlled. These findings support the possibility that redistribution of calcium ions may have an effect on the functioning of opiates such as morphine [92].

The inhibitory effect of exposure to magnetic fields on analgesic responses was a consistent finding among many researchers. Studies conducted on pigeons [93] found that exposure to weak, oscillating magnetic fields (sinusoidal; continuous induced magnetic flux between +70 and – 20 μT) resulted in hyperalgesia, or heightened sensitivity, to a painful electrical stimulation. The pigeons, when exposed to these specific magnetic-field parameters, displayed significantly decreased thresholds to the electrical stimuli following magnetic-field exposure. In comparison, control pigeons not exposed to the magnetic fields displayed significantly increased thresholds to the stimuli over time, attributable to the formation of stress-induced analgesia. Using the same magnetic-field parameters as in the study on pigeons, Papi et al. [94] reported that humans experienced increased sensitivity, observed via decreased thresholds, following magnetic-field exposure relative to the sham condition. Specifically, assessment of dental sensory threshold (DST), dental-pain threshold (DPT), cutaneous sensory threshold (CST), cutaneous pain threshold (CPT), and cutaneous tolerance value (CTV), revealed no significant change in value for any of these measurements between pre- and post-sham conditions. However, when the same measurements were assessed in the same subjects before and after magnetic-field exposure, significant decreases were observed in the DST, CPT, and CTV measurements post-exposure. These two studies investigating the use of sinusoidal magnetic field exposures on pain sensitivity in pigeons and humans extend past research in showing that in addition to pain sensitivity in animals, such sensitivity in humans is also negatively affected by magnetic-field exposure.

In contrast to these aforementioned studies, further research has discovered that exposure to magnetic fields does, in fact, have positive pain-relieving, anti-nociceptive, effects. For example, Thomas et al. [95] found that 15-min exposures to an ELFMF ($100\ \mu T_{pk}$, 0.4 T/s) in land snails induced analgesia, and increased opioid-induced analgesia, rather than producing inhibitory effects. Subsequent injection of an opioid antagonist, naloxone, resulted in a reduced, but not completely abolished, analgesia effect. These results demonstrate the anti-nociceptive action of a specific PEMF via an endogenous opioid mechanism. Specifically, the ability of naloxone to reduce, but not abolish, the analgesia effect suggests the presence of at least partial δ-opioid receptor mediation [96]. Furthermore, the ability of the specific PEMF – but not of the random or burstx PEMFs also tested in the study – to induce analgesia suggests that the opioid analgesia did not arise from a non-specific magnetic-field stress response, but rather seemed to be related to the specific ELF magnetic field pulse form [95].

Further investigation of the effects of the specific PEMF exposure on inducing and augmenting opioid-induced analgesia involved the development of tolerance. Tolerance is defined as reduced drug effectiveness that presents itself following repeated drug exposure. Kavaliers and Ossenkopp showed that tolerance to opioid agonists (e.g., morphine) was reduced if animals are exposed to rotating magnetic fields prior to morphine injections, for animals that had not developed complete tolerance, and that environmental cues provided by magnetic stimuli were important determinants of development of tolerance [97]. Tolerance is apparent in land snails following five to seven days of repeated administration of morphine, and can also extend to other, similar opioids, via an effect known as cross-tolerance [98]. Thomas et al. [98] studied the effects of tolerance to the δ-opioid receptor agonist DPDPE, (D-Pen^2, D-Pen^5) enkephalin in land snails, and found that the magnitude and duration of the magnetic-field-induced analgesia was reduced following repeated (six days - nine days) daily (15 or 30-min) exposures: an effect indicative of the development of tolerance. The same effect of tolerance was present if snails received the nociceptive testing (assessed via the hot-plate test of latency) each day, or only on the first and last days. The effect was nearly completely removed when the land snails were presented with novel environmental cues. Furthermore, snails that received repeated daily exposures of the specific PEMF ($100\ \mu T_{pk}$) displayed reduced sensitivity to the δ-opioid receptor agonist DPDPE. This reduced sensitivity provides evidence for the development of cross-tolerance of DPDPE to the opioid component of the PEMF [98]. Overall, these results provided insight into the development of tolerance and how magnetic-field exposure sessions can have (negative) effects similar to those of repeated drug administrations. This has great relevance for human clinical trials, as drug tolerance is known to be a problem among humans.

A discrepancy with respect to the effect of ELF magnetic-field exposure on land snails exists, as such exposure sessions have been shown to both increase [95, 96, 98] and decrease [88, 84, 92] analgesia. A possible mediating variable that explains the inconsistency in the literature is the presence of light, as opposed to dark, field conditions [99]. Prato et al. showed that the increases and decreases in opioid analgesia associated with magnetic-field exposure were consistent with the predictions of Lednev's parametric-resonance model (PRM) for the calcium ion [99]. Refer to Section 16.1 for a further explanation of potential mechanisms of action.

The results of increased analgesia following magnetic-field exposure extend beyond the work done on land snails. Briefly, it has also been shown that exposure to a pulsed magnetic field (5 μT burst firing pattern; 1 s on, 4 s off; 20 min) resulted in increased analgesia in female rats, as evaluated via flinch thresholds to electric shock. The analgesia seen was a 50% increase in flinch threshold, and was greater than that seen following the administration of a dose (4 mg/kg) of morphine [100].

In addition to animal research, human research has begun to reveal positive effects of magnetic-field exposure. Sartucci et al. [101] examined the effect of weak, oscillating magnetic-field exposure (constant-current rectangular pulses; 0.5 Hz; 0.1 ms duration; 70 to –20 μT) on human pain perception and pain-related somatosensory evoked potentials (SEPs). Pain thresholds were reduced, and pain-related SEPs were significantly reduced, following magnetic-field exposure; pain thresholds were significantly increased following sham sessions. These results provide the first evidence that human SEPs are influenced by magnetic-field exposure. Ongoing work in our lab is investigating other possible effects of pulsed magnetic-field exposure on human pain perception and analgesia.

15. Discussion and Concluding Remarks

This paper has discussed the effectiveness of magnetic-field stimulation as a treatment for a variety of health-related conditions. To date, of the articles included in this review, magnetic-field stimulation was shown to be effective for treatment of bone disorders (osteotomies, non-union bone fractures, congenital Pseudoarthrosis, bone formation, hip arthroplasty), joint disorders (including rheumatoid arthritis and osteoarthritis), rotator-cuff tendonitis, spinal fusions (including Pseudoarthrosis and interbody lumbar fusions), pelvic pain, neurological disorders (e.g., multiple sclerosis, tinnitus), nerve (median-ulnar, peroneal, sciatic) regeneration, endocrine ophthalmopathy, cancer, focal ischemia, cardiac and myocardial protection, and human standing balance. Stimulation was ineffective for treatment of Perthes Disease and lateral humeral epicondylitis. Magnetic-field stimulation is as yet inconclusive as an effective treatment for conditions such as osteoporosis, venous leg ulcers, imbalance of the neuroendocrine system (including hormone production and melatonin levels), and pain.

The preceding summary of results discussed in this paper indicates the great success of magnetic-field stimulation in treating a variety of conditions and disorders. Given the study outcomes, the next logical step in understanding what other medical conditions might benefit from this treatment requires a detailed analysis of the mechanisms of action that underlie this form of treatment. The following section will discuss possible mechanisms by which magnetic-field therapy is suggested to work.

15.1 Possible Mechanisms of Action

As can be appreciated from this review, there is a very significant body of literature that supports the idea that therapeutic effects can be achieved from ELF magnetic-field exposure. However, except for application to orthopedics (i.e. non-unions), these therapies have not been accepted as conventional medical practice. One of the reasons is that positive results are often not confirmed when a replication attempt is made, and different magnetic-field exposure conditions are often used. As there are infinite combinations of ELF magnetic-field parameters to choose from, the optimization of treatment regimens is very difficult given the lack of a predictive theoretical framework. This is made more difficult by the nature of the measured endpoints: changing one exposure parameter would require at least two exposure groups along with a sham control where patients must be treated for months (at hours per day), making such experiments strategically and financially almost impossible. Hence, it is not surprising that mechanism discovery has been difficult. However, progress has been made and new tools associated with molecular biology and medical imaging could dramatically accelerate the discovery of mechanism.

What do we mean by mechanism? In this field we are faced with a real challenge, because the mechanism to be discovered includes two discrete steps: a) the initial biophysical mechanism by which the ELF magnetic field is detected and converted to a biological signal; and b) the cascade of events by which the initial biological signal results in the behavioral/physiological event.

For the determination of the initial biophysical detection mechanism, it is generally accepted that the responding system can be treated as a black box. The parameters of the ELF magnetic field can be stepwise changed and the response measured. As there are infinite numbers of possible field combinations, it is helpful to start with some a priori concepts so that exposure conditions can be first set to discriminate between fundamentally different mechanisms, and then further experiments can select between similar mechanisms. For ELF magnetic fields with the parameters used in therapy that have been reviewed here, there are two fundamentally different biophysical transduction mechanisms: induced current and magnetic dipole. The induced current assumes that the time-changing magnetic field induces a current in the conductive tissue (Faraday's Law of Induction). In comparison, the applied magnetic fields could interact directly with the magnetic fields in the tissue associated with an endogenous magnet (e.g., magnetite) or with the magnetic moment produced by a nucleus, atom, or molecule [102]. Engstrom [103] and Engstrom and Fitzsimmons [104] have demonstrated that a limited number of experiments (i.e., five) would be needed. Perhaps the best example of this kind of approach has been undertaken by Prato et al. (see Table 3; [99, 105, 106, 107, 108, 109, 110, 111]). This work suggests that the magnetic fields were detected by a magnetic molecular dipole. However, in the work on snails, using a much different pulse, Thomas et al. [95, 96, 98] presented evidence suggesting that it is an induced-current mechanism. Hence, modification of opioid-like behaviors in land snails using two different magnetic fields (both in the ELF) may involve two very different mechanisms! Note that this work on land snails has been possible in large part because hundreds of animals could be studied in a few hours. A similar approach to study, for example, bone healing in humans would be all but impossible. A different approach is needed if significant mechanism discovery is to be achieved in the majority of therapeutic applications, and especially if validation is to be done in humans.

Fortunately, two significant developments over the last decade have made it possible to dissect the mechanisms, both at the detection/transduction stage and to follow the events to the final behavioral/physiological outcome. These are the combined advances in molecular biology and non-invasive imaging, resulting in the field of molecular imaging.

For example, in 1981 the first commercial bone-density units were being used to evaluate treatments for osteoporosis, but relatively large groups had to be followed for years because of the uncertainty in the measurements. Twenty years later, the success of treatment in a single woman can be determined in six to 12 months. Not only do such advances allow the evaluation of mechanism, but they also allow the fine-tuning of therapy for the individual patient. In the future, ELF magnetic-field therapy will be image-guided. For example, in the treatment of patients with unipolar depression with transcranial magnetic stimulation, positron-emission tomography studies of brain blood flow and metabolism can predict the effectiveness of different magnetic-field parameters, the targeting of different brain structures, and the effectiveness of therapy in the individual patient [112]. These imaging methods are powerful. For example, Huber et al. [113] demonstrated that subtle differences in brain microwave irradiation resulted in significant differences in EEG and regional cerebral blood flow as measured with PET. In the future, advances in molecular imaging, such as the identification of number and activity of opioid receptors [114, 115], will allow

Experiment	Mechanism				Reference
	Induced Current	Free Radical	Magnetite	Parametric Resonance	
Variation of B_{AC} at 60 Hz	x	-	-	√	Prato et al. 1995 [108]
Variation of frequency for B_{AC} and B_{DC}	x	x	-	√	Prato et al. 1995 [108]
Variation of angle between B_{AC} and B_{DC}	x	-	x	√	Prato et al. 1996a [109]
Variation B_{AC} and B_{DC} at 30 Hz	x	x	x	√	Prato et al. 2000 [102]
Variation of angle between B_{AC} and B_{DC} in light and dark	-	-	x	-	Prato et al. 1996b [110]
Investigation of light/dark effects at 30, 60, 120 Hz	x	x	-	√	Prato et al. 1997 [111]
Investigation of light/dark effects during day/night	-	-	-	√	Prato et al. 1998 [112]
Role of nitric oxide synthase and related light/dark effects	-	-	-	√	Kavaliers et al. 1998 [113], and Kavaliers & Prato 1999 [114]

√ mechanism supported
x mechanism not supported
- mechanisms neither supported nor unsupported

Table 3: Summary of Evidence Supporting the Parametric Resonance Model as the Detection Mechanism Associated with ELF Magnetic Field Modulation of Opioid-Induced Analgesia

individual tailoring of pulsed ELF PEMFs in the treatment of pain.

Non-invasive anatomical, functional and molecular imaging will provide the platform by which elucidation of mechanisms will be possible and optimization of the treatment for the individual will be routine; these advances will result in a very significant acceptance of magnetic-field therapy for a wide variety of conditions.

15.2 Conclusion

There are many questions that require answers prior to the general acceptance of magnetic-field therapy as a primary treatment, rather than its use mainly as an adjunct therapy. For example, controlled, randomized, and double-blind studies must be used to assess optimal magnetic-field conditions and average duration of effect [4] in producing the best possible treatment. Furthermore, the cost-effectiveness of this form of therapy with respect to more traditional treatment protocols (e.g., non-steroidal anti-inflammatory drugs, analgesics, and massage) must be evaluated prior to use.

Difficulties in bioelectromagnetic research include the inability to reproduce and replicate work conducted in other laboratories. Furthermore, the lack of concrete mechanisms of action has impeded research regarding therapeutics [2]. Through continued research, and more solidified mechanisms of action, it is hoped that the therapeutic value currently associated with some ELF magnetic fields will become a mainstream intervention.

16. References

1. J. Juutilainen and S. Lang, "Genotoxic, Carcinogenic and Teratogenic Effects of Electromagnetic Fields: Introduction and Overview," *Mutation Research*, **387**, 1997, pp. 165-171.

2. B. Rubik, "Bioelectromagnetics & the Future of Medicine," *Administrative Radiology Journal*, **16**, 8, 1997, pp. 38-46.

3. C. Polk and E. Postow (eds.), *CRC Handbook of Biological Effects of Electromagnetic Fields*, Boca Raton, FL, CRC Press, 1986.

4. C. Vallbona and T. Richards, "Evolution of Magnetic Therapy from Alternative to Traditional Medicine," *Physical Medicine and Rehabilitation Clinics of North America*, **10**, 3, 1999, pp. 729-754.

5. J. Hulme, V. Robinson, R. DeBie, G. Wells, M. Judd, and P. Tugwell, "Electromagnetic Fields for the Treatment of Osteoarthritis," *(Cochrane Review), Cochrane Library*, **3**, Oxford, Update Software, 2002.

6. C. A. Bassett, "Fundamental and Practical Aspects of Therapeutic Uses of Pulsed Electromagnetic Fields (PEMFs)," *Critical Reviews in Biomedical Engineering*, **17**, 5, 1989, pp. 451-529.

7. D. H. Trock, "Electromagnetic Fields and Magnets: Investigational Treatment for Musculoskeletal Disorders," *Rheumatic Disease Clinics of North America*, **26**, 1, 2000, pp. 51-62.

8. C. J. Hannan Jr., Y. Liang, J. D. Allison, C. G. Pantazis, and J. R. Searle, "Chemotherapy of Human Carcinoma Xenografts during Pulsed Magnetic Field Exposure," *Anticancer Research*, **14**, 1994, pp. 1521-1524.

9. M. J. Stiller, G. H. Pak, J. L. Shupack, S. Thaler, C. Kenny, and L. Jondreau, "A Portable Pulsed Electromagnetic Field (PEMF) Device to Enhance Healing of Recalcitrant Venous Ulcers: A Double-blind, Placebo-controlled Clinical Trial," *British Journal of Dermatology*, **127**, 1992, pp. 147-154.

10. G. C. Traina, L. Romanini, F. Benazzo, R. Cadossi, V. Canè, A. Chiabrera, M. Marcer, N. Marchetti, and F. S. Snatori, "Use of Electric and Magnetic Stimulation in Orthopaedics and Traumatology: Consensus Conference," *Italian Journal of Orthopaedics and Traumatology*, **24**, 1, 1998, pp. 1-31.

11. C. A. L. Bassett, "Beneficial Effects of Electromagnetic Fields," *Journal of Cellular Biochemistry*, **51**, 1993, pp. 387-393.

12. G. K. Frykman, J. Taleisnik, G. Peters, R. Kaufman, B. Helal, V. E. Wood, and R. S. Unsell, "Treatment of Nonunited Scaphoid Fractures by Pulsed Electromagnetic Field and Cast," *The Journal of Hand Surgery*, **11A**, 1986, pp. 334-349.

13. J. D. Heckman, A. J. Ingram, R. D. Loyd, J. V. Luck Jr., and P. W. Mayer, "Nonunion Treatment with Pulsed Electromagnetic Fields," *Clinical Orthopaedics and Related Research*, **161**, 1981, pp. 58-66.

14. N. Pipitone and D. L. Scott, "Magnetic Pulse Treatment for Knee Osteoarthritis: A Randomised, Double-blind, Placebo-controlled Study," *Current Medical Research and Opinions*, **17**, 3, 2001, pp. 190-196.

15. R. A. Luben, "Effects of Low-energy Electromagnetic Fields (pulsed and DC) on Membrane Signal Transduction Processes in Biological Systems," *Health Physics*, **61**, 1, 1991, pp. 15-28.

16. C. A. L. Bassett and M. Schink-Ascani, "Long-term Pulsed Electromagnetic Field (PEMF) Results in Congenital Pseudarthrosis," *Calcified Tissue International*, **49**, 1991, pp. 216-220.

17. M. A. Darendeliler, A. Darendeliler, and P. M. Sinclair, "Effects of Static Magnetic and Pulsed Electromagnetic Fields on Bone Healing," *International Journal of Adult Orthodontic and Orthognathic Surgery*, **12**, 1, 1997, pp. 43-53.

18. C. A. L. Bassett, R. J. Pawluk, and A. A. Pilla, "Acceleration of Fracture Repair by Electromagnetic Fields: A Surgically Non-invasive Method," *Annals of the New York Academy of Sciences*, **238**, 1974, pp. 242-262.

19. C. A. L. Bassett, R. J. Pawluk, and A. A. Pilla, "Augmentation of Bone Repair by Inductively Coupled Electromagnetic Fields," *Science*, **184**, 136, 1974, pp. 575-577.

20. C. A. L. Bassett, A. A. Pilla, and R. J. Pawluk, "A Non-operative Salvage of Surgically-Resistant Pseudarthroses and Non-unions by Pulsing Electromagnetic Fields," *Clinical Orthopaedics and Related Research*, **124**, 1977, pp. 128-143.

21. D. R. Godley, "Nonunited Carpal Scaphoid Fracture in a Child: Treatment with Pulsed Electromagnetic Field Stimulation," *Orthopedics*, **20**, 8, 1997, pp. 718-719.

22. A. T. Barker, R. A. Dixon, W. J. Sharrard, and M. L. Sutcliffe, "Pulsed Magnetic Field Therapy for Tibial Non-union: Interim Results of a Double-blind Study," *Lancet*, **1**, 8384, 1984, pp. 994-996.

23. G. De Haas, M. A. Lazarovici, and D. M. Morrison, "The Effect of Low Frequency Magnetic Fields on the Healing of the Osteotomized Rabbit Radius," *Clinical Orthopaedics and Related Research*, **145**, 1979, pp. 245-251.

24. H. Matsumoto, M. Ochi, Y. Abiko, Y. Hirose, T. Kaku, K. Sakaguchi, "Pulsed Electromagnetic Fields Promote Bone Formation around Dental Implants Inserted into the Femur of Rabbits," *Clinical Oral Implants Research*, **11**, 2000, pp. 354-360.

25. F. Tabrah, M. Hoffmeier, F. Gilbert Jr., S. Batkin, and C. A. L. Bassett, "Bone Density Changes in Osteoporosis-prone Women Exposed to Pulsed Electromagnetic Fields (PEMFs)," *Journal of Bone and Mineral Research*, **5**, 5, 1990, pp. 437-442.

26. K. Konrad, K. Sevcic, K. Fõldes, E. Piroska, and E. Molnár, "Therapy with Pulsed Electromagnetic Fields in Aseptic Loosening of Total Hip Prostheses: A Prospective Study," *Clinical Rheumatology*, **15**, 4, 1996, pp. 325-328.

27. M. H. M. Harrison and C. A. L. Bassett (deceased), "The Results of a Double-blind Trial of Pulsed Electromagnetic Frequency in the Treatment of Perthes' Disease," *Journal of Pediatric Orthopaedics*, **17**, 1997, pp. 264-265.

28. E. R. Sanseverino, A. Vannini, and P. Castellacci, "Therapeutic Effects of Pulsed Magnetic Fields on Joint Diseases," *Panminerva Medica*, **34**, 4, 1992, pp. 187-196.

29. K. S. Gunguly, A. K. Sarkar, A. K. Datta, and A. Rakshit, "A Study of the Effects of Pulsed Electromagnetic Field Therapy with Respect to Serological Grouping in Rheumatoid Arthritis," *Journal of the Indian Medical Association*, **96**, 9, 1998, pp. 272-275.

30. J. I. Jacobson, R. Gorman, W. S. Yamanashi, B. B. Saxena, and L. Clayton, "Low-amplitude, Extremely Low Frequency Magnetic Fields for the Treatment of Osteoarthritic Knees: A Double-blind Clinical Study," *Alternative Therapies*, **7**, 5, 2001, pp. 54-69.

31. B. Rubik, R. O. Becker, R. G. Flower, C. F. Hazlewood, A. R. Liboff, and J. Walleczek, "Bioelectromagnetics: Applications in medicine," in B. M. Berman, D. B. Larson, et al., *Alternative Medicine, Expanding Medical Horizons*, NIH Publication No. 94-066, Washington, DC, US Government Printing Office, 1994.

32. A. Binder, G. Parr, B. Hazleman, and S. Fitton-Jackson, "Pulsed Electromagnetic Field Therapy of Persistent Rotator Cuff Tendinitis: A Double-blind Controlled Assessment," *The Lancet*, **1**, 8379, 1984, pp. 695-698.

33. M. D. Devereaux, B. L. Hazleman, and P. P. Thomas, "Chronic Lateral Humeral Epicondylitis - A Double-blind Controlled Assessment of Pulsed Electromagnetic Field Therapy," *Clinical and Experimental Rheumatology*, **3**, 1985, pp. 333-336.

34. R. A. Marks, "Spine Fusion for Discogenic Low Back Pain: Outcomes in Patients Treated with or without Pulsed Electromagnetic Field Stimulation," *Advances in Therapy*, **17**, 2, 2000, pp. 57-67.

35. P. A. Glazer, M. R. Heilmann, J. C. Lotz, and D. S. Bradford, "Use of Electromagnetic Fields in a Spinal Fusion: A Rabbit Model," *Spine*, **22**, 1997, pp. 2351-2356.

36. V. Mooney, "A Randomized Double-blind Prospective Study of the Efficacy of Pulsed Electromagnetic Fields for Interbody Lumbar Fusions," *Spine*, **15**, 7, 1990, pp. 708-712.

37.K. Flemming and N. Cullum, "Electromagnetic Therapy for Treating Venous Leg Ulcers" *(Cochrane Review),. Cochrane Library*, **3**, Oxford, Update Software, 2002.

38.M. Ieran, S. Zaffuto, M. Bagnacani, M. Annovi, A. Moratti, and R. Cadossi, "Effect of Low Frequency Pulsing Electromagnetic Fields on Skin Ulcers of Venous Origin in Humans: A Double-blind Study," *Journal of Orthopaedic Research*, **8**, 2, 1990, pp. 276-282

39.W. A. Jorgensen, B. M. Frome, and C. Wallach, "Electrochemical Therapy of Pelvic Pain: Effects of Pulsed Electromagnetic Fields (PEMF) on Tissue Trauma," *The European Journal of Surgery*, **574** (Supplement), 1994, pp. 83-86.

40.B. F. Sisken, J. M. Jacob, and J. L. Walker, "Acute Treatment With Pulsed Electromagnetic Fields and Its Effect on Fast Axonal Transport in Normal and Regenerating Nerve," *Journal of Neuroscience Research*, **42**, 1995, pp. 692-699.

41.D. H. Wilson and P. Jagadeesh, "Experimental Regeneration in Peripheral Nerves and the Spinal Cord in Laboratory Animals Exposed to a Pulsed Electromagnetic Field," *Paraplegia*, **14**, 1976, pp. 12-20.

42.A. M. Raji, "An Experimental Study of the Effects of Pulsed Electromagnetic Field (Diapulse) on Nerve Repair," *The Journal of Hand Surgery*, **9-B**, 2, 1984, pp. 105-112.

43.M. Kanje, A. Rusovan, B. Sisken, and G. Lundborg, "Pretreatment of Rats with Pulsed Electromagnetic Fields Enhances Regeneration of the Sciatic Nerve," *Bioelectromagnetics*, **14**, 1993, pp. 353-359.

44.B. F. Sisken, M. Kanje, G. Lundborg, E. Herbst, and W. Kurtz, "Stimulation of Rat Sciatic Nerve Regeneration with Pulsed Electromagnetic Fields," *Brain Research*, **485**, 1989, pp. 309-316.

45.B. F. Sisken, J. Walker, and M. Orgel, "Prospects on Clinical Applications of Electric Stimulation for Nerve Regeneration," *Journal of Cellular Biochemistry*, **52**, 1993, pp. 404-409.

46.J. Jankauskienĕ, A. Paunksnis, A. Bluþienĕ, and J. Saulgozis, "The Effect of Pulsed Electromagnetic Field on Patients with Endocrine Ophthalmopathy," *European Journal of Ophthalmology*, **8**, 4, 1998, pp. 253-257.

47.T. L. Richards, M. S. Lappin, J. Acosta-Urquidi, G. H. Kraft, A. C. Heide, F. W. Lawrie, T. E. Merrill, G. B. Melton, and C. A. Cunningham, "Double-blind Study of Pulsing Magnetic Field Effects on Multiple Sclerosis," *The Journal of Alternative and Complementary Medicine*, **3**, 1, 1997, pp. 21-29.

48.N. J. Roland, J. B. Hughes, M. B. Daley, J. A. Cook, A. S. Jones, and M. S. McCormick, "Electromagnetic Stimulation as a Treatment of Tinnitus: A Pilot Study," *Clinical Otolaryngology and Applied Sciences*, **18**, 1993, pp. 278-281.

49.M. S. George, F. R. Sallee, Z. Zahas, N. C. Oliver, and E. M. Wassermann, "Transcranial Magnetic Stimulation (TMS) as a Research Tool in Tourette Syndrome and Related Disorders," *Advances in Neurology*, **85**, 2001, pp. 225-235.

50.R. J. Ilmoniemi and J. Karhu, "Transcranial Magnetic Stimulation – Towards Navigated Targeting," *Business Briefing: Global Healthcare*, **3**, 2002, pp. 1-4.

51.M. S. George, E. M. Wassermann, and R. M. Post, "Transcranial Magnetic Stimulation: A Neuropsychiatric Tool for the 21st Century," *Journal of Neuropsychiatry*, **8**, 4, 1996, pp. 373-382.

52.E. M. Wassermann and S. H. Lisanby, "Therapeutic Application of Repetitive Transcranial Magnetic Stimulation: A Review," *Clinical Neurophysiology*, **112**, 2001, pp. 1367-1377.

53.K. Mann, P. Wagner, G. Brunn, F. Hassan, C. Hiemke, and J. Rõschke, "Effects of Pulsed High-frequency Electromagnetic Fields on the Neuroendocrine System," *Neuroendocrinology*, **67**, 1998, pp. 139-144.

54.G. R. Warman, H. Tripp, J. English, and J. Arendt, "Effects of 50 Hz EMF on the Human Melatonin Profile," in 24th Annual Bioelectromagnetics Meeting Abstract Book, 2002, (available from The Bioelectromagnetics Society, 2412 Cobblestone Way, Frederick, MD 21702 USA), p. 251.

55.R. J. Reiter, "A Review of Neuroendocrine and Neurochemical Changes Associated with Static and Extremely Low Frequency Electromagnetic Field Exposure," *Integrative Physiological and Behavioral Science*, **28**, 1, 1993, pp. 57-75.

56.R. J. Reiter, "Reported Biological Consequences Related to the Suppression of Melatonin by Electric and Magnetic Field Exposure," *Integrative Physiological and Behavioral Science*, **30**, 4, 1995, pp. 314-330.

57.M. Karasek, M. Woldanska-Okonska, J. Czernicki, K. Zylinska, and J. Swietoslawski, "Influence of Low-frequency Magnetic Field of Different Characteristics on Serum Melatonin Concentrations in Humans," *Advances in Experimental Medicine and Biology*, **460**, 1999, pp. 459-462.

58.M. Karasek, J. Czernicki, M. Woldanska-Okonska, K. Zylinska, and J. Swietoslawski, "Chronic Exposure to 25 - 80 μT, 200 Hz Magnetic Field Does Not Influence Serum Melatonin Concentrations in Patients with Low Back Pain," *Journal of Pineal Research*, **29**, 2000, pp. 81-85.

59.A. Bellossi and A. Desplaces, "Effect of a 9 mT Pulsed Magnetic Field on C3H/Bi Female Mice with Mammary Carcinoma: A Comparison between the 12 Hz and the 460 Hz Frequencies," *In Vivo*, **5**, 1991, pp. 39-40.

60.C. D. Williams, M. S. Markov, W. E. Hardman, and I. L. Cameron, "Therapeutic Electromagnetic Field Effects on Angiogenesis and Tumor Growth," *Anticancer Research*, **21**, 6A, 2001, pp. 3887-3891.

61.R. de Seze, S. Tuffet, J-M. Moreau, and B. Veyret, "Effects of 100 mT Time Varying Magnetic Fields on the Growth of Tumors in Mice," *Bioelectromagnetics*, **21**, 2000, pp. 107-111.

62.Y. Omote, M. Hosokawa, M. Komatsumoto, T. Namieno, S. Nakajima, Y. Kubo, and H. Kobayashi, "Treatment of Experimental Tumors with a Combination of a Pulsing Magnetic Field and an Antitumor Drug," *Japanese Journal of Cancer Research*, **81**, 1990, pp. 956-961.

63.Y. Liang, C. J. Hannan, B. K. Chang, and P. V. Schoenlein, "Enhanced Potency of Daunorubicin against Multidrug Resistant Subline KB-ChR-8-5-11 by a Pulsed Magnetic Field," *Anticancer Research*, **17**, 1997, pp. 2083-2088.

64.J. G. Robison, A. R. Pendleton, K. O. Monson, B. K. Murray, and K. L. O'Neill, "Decreased DNA Repair Rates and Protection from Heat Induced Apoptosis Mediated by Electromagnetic Field Exposure," *Bioelectromagnetics*, **23**, 2002, pp. 106-112.

65.G. Grant, R. Cadossi, and G. Steinberg, "Protection against Focal Cerebral Ischemia following Exposure to a Pulsed Electromagnetic Field," *Bioelectromagnetics*, **15**, 1994, pp. 205-216.

66. G. A. Mouchawar, J. D. Bourland, J. A. Nyenhuis, L. A. Geddes, K. S. Foster, J. T. Jones, and G. P. Graber, "Closed-chest Cardiac Stimulation with a Pulsed Magnetic Field," *Medical & Biological Engineering & Computing*, **30**, 1992, pp. 162-168.

67. A. L. DiCarlo, J. M. Farrell, and T. A. Litovitz, "Myocardial Protection Conferred by Electromagnetic Fields," *Circulation*, **99**, 6, 1999, pp. 813-816.

68. A. L. DiCarlo, J. M. Farrell, and T. A. Litovitz, "A Simple Experiment to Study Electromagnetic Field Effects: Protection Induced by Short-term Exposures to 60 Hz Magnetic Fields," *Bioelectromagnetics*, **19**, 1998, pp. 498-500.

69. J. M. Shallom, A. L. DiCarlo, D. Ko, L. M. Penafiel, A. Nakai, and T.A. Litovitz, "Microwave Exposure Induces HSP70 and Confers Protection Against Hypoxia in Chick Embryos," *Journal of Cellular Biochemistry*, **86**, 2002, pp. 490-496.

70. L. H. E. H. Snoeckx, R. N. Cornelussen, F. A. Van Nieuwenhoven, R. S. Reneman, and G. J. Van der Vusse, "Heat Shock Proteins and Cardiovascular Pathophysiology," *Physiological Reviews*, **81**, 2001, pp. 1461-1497.

71. M. Vayssier and B. S. Polla, "Heat Shock Proteins Chaperoning Life and Death," *Cell Stress & Chaperones*, **3**, 4, 1998, pp. 221-227.

72. H. Lin, M. Blank, and R. Goodman, "A Magnetic Field-Responsive Domain in the Human HSP70 Promoter," *Journal of Cellular Biochemistry*, **75**, 1999, pp. 170-176.

73. S. Carmody, X. L. Wu, H. Lin, M. Blank, H. Skopicki, and R. Goodman, "Cytoprotection by Electromagnetic Field-Induced HSP70: A Model for Clinical Application," *Journal of Cellular Biochemistry*, **79**, 2000, pp. 453-459.

74. A. Albertini, P. Zucchini, G. Noera, R. Cadossi, C. P. Napoleone, and A. Pierangeli, "Protective Effect of Low Frequency Low Energy Pulsing Electromagnetic Fields on Acute Experimental Myocardial Infarcts in Rats," *Bioelectromagnetics*, **20**, 1999, pp. 372-377.

75. H. H. Patel, A. Hsu, and G. J. Gross, "Attenuation of Heat Shock-Induced Cardioprotection by Treatment with the Opiate Receptor Antagonist Naloxone," *American Journal of Physiology: Heart and Circulatory Physiology*, **282**, 2002, pp. H2011-H2017.

76. H. Kollegger, C. Baumgartner, C. Wõber, W. Oder, and L. Deecke, "Spontaneous Body Sway as a Function of Sex, Age, and Vision: Posturographic Study in 30 Healthy Adults," *European Neurology*, **32**, 1992, pp. 253-259.

77. A. W. Thomas, D. J. Drost, and F. S. Prato, "Human Subjects Exposed to a Specific Pulsed (200 μT) Magnetic Field: Effects on Normal Standing Balance," *Neuroscience Letters*, **297**, 2001, pp. 121-124.

78. A. W. Thomas, K. P. White, D. J. Drost, C. M. Cook, F. S. Prato, "A Comparison of Rheumatoid Arthritis and Fibromyalgia Patients and Healthy Controls Exposed to a Pulsed (200 μT) Magnetic Field: Effects on Normal Standing Balance," *Neuroscience Letters*, **309**, 2001, pp. 17-20.

79. F. S. Prato, A. W. Thomas, and C. M. Cook, "Human Standing Balance is Affected by Exposure to Pulsed ELF Magnetic Fields: Light Intensity-dependent Effects," *NeuroReport*, **12**, 7, 2001, pp. 1-5.

80. M. Kavaliers and K.-P. Ossenkopp, "Opioid Systems and Magnetic Field Effects in the Land Snail, Cepaea nemoralis," *Biological Bulletin*, **180**, 1991, pp. 301-309.

81. E. Choleris, C. Del Seppia, A. W. Thomas, P. Luschi, S. Ghione, G.R. Moran, and F. S. Prato, "Shielding, but not Zeroing of the Ambient Magnetic Field Reduces Stress-induced Analgesia in Mice," *Proceedings of the Royal Society of London, Series B: Biological Sciences*, **269**, 2002, pp. 193-201.

82. J. H. Jeong, K. B. Choi, B. C. Yi, C. H. Chun, K. -Y. Sung, J. -Y. Sung, Y. -M. Gimm, I. H. Huh, and U. D. Sohn, "Effects of Extremely Low Frequency Magnetic Fields on Pain Thresholds in Mice: Roles of Melatonin and Opioids," *Journal of Autonomic Pharmacology*, **20**, 2000, pp. 259-264.

83. K. -P. Ossenkopp, M. Kavaliers, F. S. Prato, G.C. Teskey, E. Sestini, and M. Hirst, "Exposure to Nuclear Magnetic Resonance Imaging Procedure Attenuates Morphine-induced Analgesia in Mice," *Life Sciences*, **37**, 16, 1985, pp. 1507-1514.

84. M. Kavaliers and K.-P. Ossenkopp, "Repeated Naloxone Treatments and Exposures to Weak 60-Hz Magnetic Fields have 'Analgesic' Effects in Snails," *Brain Research*, **620**, 1993, pp. 159-162.

85. C. Del Seppia, P. Luschi, S. Ghione, E. Crosio, E. Choleris, F. Papi, "Exposure to a Hypogeomagnetic Field or to Oscillating Magnetic Fields Similarly Reduce Stress-induced Analgesia in C57 Male Mice," *Life Sciences*, **66**, 14, 2000, pp. 1299-1306.

86. F. S. Prato, K.-P. Ossenkopp, M. Kavaliers, E. Sestini, and G. C. Teskey, "Attenuation of Morphine-induced Analgesia in Mice by Exposure to Magnetic Resonance Imaging: Separate Effects of the Static, Radiofrequency and Time-Varying Magnetic Fields," *Magnetic Resonance Imaging*, **5**, 1987, pp. 9-14.

87. C. Betancur, G. Dell'Omo, and E. Alleva, "Magnetic Field Effects on Stress-induced Analgesia in Mice: Modulation By Light," *Neuroscience Letters*, **182**, 1994, pp. 147-150.

88. M. Kavaliers and K.-P. Ossenkopp, "Magnetic Fields Inhibit Opioid-mediated 'Analgesic' Behaviours of the Terrestrial Snail, Cepaea nemoralis," *Journal of Comparative Physiology A*, **162**, 1988, pp. 551-558.

89. M. Kavaliers, K. –P. Ossenkopp, and M. Hirst, "Magnetic Fields Abolish the Enhanced Nocturnal Analgesic Response to Morphine in Mice," *Physiology & Behavior*, **32**, 2, 1984, pp. 261-264.

90. C. Fanelli, S. Coppola, R. Barone, C. Colussi, G. Gualandi, P. Volpe, and L. Ghibelli, "Magnetic Fields Increase Cell Survival by Inhibiting Apoptosis Via Modulation of Ca2+ Influx," *FASEB*, **13**, 1999, pp. 95-102.

91. C. R. McCreary, A. W. Thomas, and F. S. Prato, "Factors Confounding Cytosolic Calcium Measurements in Jurkat E6.1 Cells During Exposure to ELF Magnetic Fields," *Bioelectromagnetics*, **23**, 2002, pp. 315-328.

92. M. Kavaliers and K.-P. Ossenkopp, "Calcium Channel Involvement in Magnetic Field Inhibition of Morphine-induced Analgesia," *Naunyn-Schmiedeberg's Archives of Pharmacology*, **336**, 1987, pp. 308-315.

93. C. Del Seppia, S. Ghione, P. Luschi, and F. Papi, "Exposure to Oscillating Magnetic Fields Influences Sensitivity to Electri-

cal Stimuli. I. Experiments on Pigeons," *Bioelectromagnetics*, **16**, 1995, pp. 290-294.

94.F. Papi, S. Ghione, C. Rosa, C. Del Seppia, and P. Luschi, "Exposure to Oscillating Magnetic Fields Influences Sensitivity to Electrical Stimuli. II. Experiments on Humans ," *Bioelectromagnetics*, **16**, 1995, pp. 295-300.

95.. W. Thomas, M. Kavaliers, F. S. Prato, and K.-P. Ossenkopp, "Antinociceptive Effects of a Pulsed Magnetic Field in the Land Snail, Cepaea nemoralis," *Neuroscience Letters*, **222**, 1997a, pp. 107-110.

96.A. W. Thomas, M. Kavaliers, F. S. Prato, and K.-P. Ossenkopp, "Pulsed Magnetic Field Induced "Analgesia" in the Land Snail, Cepaea nemoralis, and the Effects of μ, d, and k Opioid Receptor Agonists/Antagonists," *Peptides*, **18**, 1997, pp. 703-709.

97.M. Kavaliers and K. -P. Ossenkopp, "Tolerance to Morphine-induced Analgesia in Mice: Magnetic Fields Function as Environmental Specific Cues and Reduce Tolerance Development," *Life Sciences*, **37**, 1985, pp. 1125-1135.

98.A. W. Thomas, M. Kavaliers, F. S. Prato, and K.-P. Ossenkopp, "Analgesic Effects of a Specific Pulsed Magnetic Field in the Land Snail, Cepaea nemoralis: Consequences of Repeated Exposures, Relations to Tolerance and Cross-Tolerance with DPDPE," *Peptides*, **19**, 2, 1998, pp. 333-342.

99.F. S. Prato, M. Kavaliers, and A. W. Thomas, "Extremely Low Frequency Magnetic Fields Can Either Increase or Decrease Analgaesia in the Land Snail Depending on Field and Light Conditions," *Bioelectromagnetics*, **21**, 2000, pp. 287-301.

100.J. L. Fleming, M. A. Persinger, and S. A. Koren, "Magnetic Pulses Elevate Nociceptive Thresholds: Comparisons with Opiate Receptor Compounds in Normal and Seizure-Induced Brain-Damaged Rats," *Electro- and Magnetobiology*, **13**, 1, 1994, pp. 67-75.

101.F. Sartucci, L. Bonfiglio, C. Del Seppia, P. Luschi, S. Ghione, L. Murri, and F. Papi, "Changes in Pain Perception and Pain-Related Somatosensory Evoked Potentials in Humans Produced by Exposure to Oscillating Magnetic Fields," *Brain Research*, **769**, 1997, pp. 362-366.

102.C. Polk, "Dosimetry of Extremely-Low-Frequency Magnetic Fields," *Bioelectromagnetics Supplement*, **1**, 1992, pp. 209-235.

103.S. Engstrom, "What is the Time Scale of Magnetic Field Interaction in Biological Systems?" *Bioelectromagnetics*, **18**, 1997, pp. 244-249.

104.S. Engstrom and R. Fitzsimmons, "Five Hypotheses to Examine the Nature of Magnetic Field Transduction in Biological Systems," *Bioelectromagnetics*, **29**, 1999, pp. 423-430.

105.F. S. Prato, J. J. L. Carson, K. -P. Ossenkopp, and M. Kavaliers, "Possible Mechanisms by which Extremely Low Frequency Magnetic Fields Affect Opioid Function," *FASEB*, **9**, 1995, pp. 807-814.

106.F. S. Prato, M. Kavaliers, and J. J. L. Carson, "Behavioural Evidence that Magnetic Field Effects in the Land Snail, Cepaea nemoralis, might not depend on Magnetite or Induced Electric Currents," *Bioelectromagnetics*, **17**, 1996, pp. 123-130.

107.F. S. Prato, M. Kavaliers, and J. J. L. Carson, "Behavioural Responses to Magnetic Fields by Land Snails are Dependent on Both Magnetic Field Direction and Light," *Proceedings of the Royal Society of London, Series B: Biological Sciences*, **263**, 1996, pp. 1437-1442.

108.F. S. Prato, M. Kavaliers, A. P. Cullen, and A. W. Thomas, "Light-dependent and independent Behavioural Effects of Extremely Low Frequency Magnetic Fields in a Land Snail are Consistent with a Parametric Resonance Mechanism," *Bioelectromagnetics*, **118**, 1997, pp. 284-291.

109.F. S. Prato, M. Kavaliers, A. W. Thomas, and K. -P. Ossenkopp, "Modulatory Actions of Light on the Behavioural Responses to Magnetic Fields by Land Snails Probably Occur at the Magnetic Field Detection Stage," *Proceedings of the Royal Society of London, Series B: Biological Sciences*, **265**, 1998, pp. 367-373.

110.M. Kavaliers, E. Choleris, F. S. Prato, and K. -P. Ossenkopp, "Evidence for the Involvement of Nitric Oxide and Nitric Oxide Synthase in the Modulation of the Opioid-induced Antinociception and the Inhibitory Effects of Exposure to 60-Hz Magnetic Fields in the Land Snail," *Brain Research*, **809**, 1998, pp. 50-57.

111.M. Kavaliers and F. S. Prato, "Light-dependent Effects of Magnetic Fields on Nitric Oxide Activation in the Land Snail," *NeuroReport*, **19**, 1999, pp. 1863-1867.

112.T. A. Kimbrell, R. T. Dunn, M. S. George, A. L. Danielson, M. W. Willis, J. D. Repella, B. E. Benson, P. Herscovitch, R. M. Post, and E. M. Wassermann, "Left Prefrontal-Repetitive Transcranial Magnetic Stimulation (rTMS) and Regional Cerebral Glucose Metabolism in Normal Volunteers," *Psychiatry Research*, **115**, 2002, pp. 101-113.

113.R. Huber, V. Treyer, A. A. Borbely, J. Schuderer, J. M. Gottselig, H. -P. Landolt, E. Werth, T. Berthold, N. Kuster, A. Buck, and P. Achermann, "Electromagnetic Fields Such as Those from Mobile Phones, Alter Regional Cerebral Blood Flow and Sleep and Waking EEG," *Journal of Sleep Research*, **11**, 2002, pp. 289-295.

114.P. Petrovic, E. Kalso, K. P. Petersson, and M. Ingvar, "Placebo and Opioid Analgesia Imaging A Shared Neuronal Network," *Science*, **295**, 2002, pp. 1737-1740.

115.J. K. Zubieta, Y. R. Smith, J. A. Bueller, Y. Xu, M. R. Kilbourn, D. M. Jewett, C. R. Meyer, R. A. Koeppe, and C. S. Stohler, "Regional Mu Opioid Receptor Regulation of Sensory and Affective Dimensions of Pain," *Science*, **293**, 2001, pp. 311-315.

Transmission-Line Super Theory: A New Approach to an Effective Calculation of Electromagnetic Interactions

H. Haase
J. Nitsch
T. Steinmetz

Abstract

Techniques are presented in this paper for the modeling of discontinuities and non-uniformities in transmission lines with the aid of extended telegrapher equations. Simple static models for risers, bends, wires through holes, and a wire crossing a slit are followed by a detailed derivation of the transmission-line super theory. With this theory, one can describe the coupling to and propagation along almost arbitrarily shaped nonuniform lines in a homogeneous medium. Also, methods for the numerical solution of the resulting extended telegrapher equations are presented, and are embedded into the context of network formulations, like EM topology. Eventually, several examples demonstrate the potential of the prescribed methods.

1. Introduction

In the last few years, a tremendous increase in EM sources could be observed, in particular because of the rapid growth and extension in the fields of communication and information technology. This development was accompanied by a rise in the susceptibility of more and more densely packed electronic devices.

In order to meet EMC requirements, or to ensure signal integrity, one has to thoroughly analyze new systems with respect to their electromagnetic behavior within a huge frequency range. In particular, this refers to wiring in complex systems and wiring harnesses, which collect and transport electromagnetic energy to manifoldly connected electronic devices. Generally, the cables are routed non-uniformly through the systems, and are excited by internal or external sources having frequency spectra up to several GHz. Therefore, an effective theory for describing linear structures at arbitrary frequencies is needed. This also includes taking into account nonuniform conductors, as well as the consideration of radiation effects. We know that the telegrapher equations represent an effective tool for modeling multiconductor lines with a dominating TEM mode at lower frequencies.

These "classical" transmission-line theories (TLT) historically go back to the nineteenth century, where the first kind of a transmission-line model was formulated by Kelvin [1]. Later, Kirchhoff [2] formulated a theory on the basis of an interaction theory at a distance, using two variables. These later became the electric scalar and magnetic vector potentials, respectively, in the studies by Heaviside [3] of "guided" propagation of electric signals along parallel conducting wires. From there, the transmission-line theory was subjected to permanent extensions by Mie [4] and Sommerfeld [5], with many excellent text books and reviews in the literature, e.g. [6-12].

Today, the transmission-line theory for a multiconductor transmission line is very often represented by the telegrapher equations in the form

$$\frac{\partial}{\partial \xi}\mathbf{v}(\xi,\omega) = \left(-\mathrm{j}\omega\mathbf{L}' - \mathbf{R}'\right)\mathbf{i}(\xi,\omega) + \mathbf{v}'_s(\xi,\omega), \quad (1)$$

$$\frac{\partial}{\partial \xi}\mathbf{i}(\xi,\omega) = \left(-\mathrm{j}\omega\mathbf{C}' - \mathbf{G}'\right)\mathbf{v}(\xi,\omega) + \mathbf{i}'_s(\xi,\omega). \quad (2)$$

The variables $\mathbf{v}$ and $\mathbf{i}$ are the voltage and current vectors, respectively, containing the voltages and currents of the individual conductors. The primary per-unit-length (p.u.l.) parameters, $\mathbf{L}'$, $\mathbf{C}'$, $\mathbf{R}'$, and $\mathbf{G}'$, are the p.u.l. inductance, p.u.l. capacitance, p.u.l. resistance, and p.u.l. conductance,

H. Haase, J. Nitsch, and T. Steinmetz are with the Institute for Fundamental Electrical Engineering and EMC, Otto-von-Guericke-University Magdeburg, PO Box 4120, 39016 Magdeburg, Germany
Tel.: +49 391-671-1090; Fax: +49 391-671-1236;
e-mail: heiko.haase@et.uni-magdeburg.de.

Editors Note: This is one of the *Reviews of Radio Science*, invited by Commission E.

respectively. The above equations are for harmonic excitation. We will stay in frequency domain throughout the paper. The parameters are usually calculated by solving a two-dimensional static field problem in the cross section of the transmission line. The quantities $\mathbf{v}'_s$ and $\mathbf{i}'_s$ are the source terms, and are determined from the field excitation of the line, depending on the coupling model [13-15].

Although the transmission-line model describes the electromagnetic behavior of interconnections only approximately, it remains – under the observation of its common restrictions (the quasi-TEM mode, and that the transverse dimensions of the interconnects are much smaller than the length of the conductors and the smallest characteristic wavelength) – an effective tool. This is mainly due to its simplicity and the possibility of a fast (numerical) solution. There is a host of engineering applications of the usual transmission-line theory.

Nevertheless, there is an urgent need to extend the classical transmission-line theory to a more general theory, but still keeping the structure of the equations. The reason for this is basically because one wants to take into account arbitrary field modes (including radiation) and non-uniformities, especially at high frequencies. Therefore, this article is devoted to these topics.

We will focus primarily on nonuniform lines in homogeneous, lossless media, i.e., the analysis of almost arbitrarily shaped, non-uniformly conducted conductors with the aid of telegrapher equations. This already includes very challenging problems, and we will not deal with nonuniform or lossy dielectrics. Some recent contributions to problems arising from these kinds of setups can be found, e.g., in [16].

In Section 2, we start with some practical improvements of the classical transmission-line theory, with emphasis on the consideration of discontinuities in the conduction of cables. These discontinuities enforce additional lumped elements in the description of equivalent circuits, which are determined from field-theoretical considerations. Risers at the line ends can be treated, e.g., as biconical antennas; an open end of a line becomes an additional end-capacitance; and a bend in the line is modeled with additional inductances and capacitances at the bend. The conduction of a transmission line through a circular aperture or across a slit is modeled by an extra admittance at the location of the aperture or by a voltage generator and an adapted impedance for the slit, respectively. Section 3 focuses on the derivation of new extended telegrapher equations for nonuniform multiconductor transmission lines directly from Maxwell's theory, without the restriction to the TEM mode. The solution of these (generalized) telegrapher equations is then the subject of Section 4. Here, emphasis is also placed on the connection of multiple multiconductor transmission lines in a network. Eventually, the next section presents some examples, with analytical or numerical solutions.

2. Discontinuities in the Conduction of Cables

In complex, real systems, the conduction of cables is not uniform, in general. Discontinuities and non-uniformities are very often present. Special measures have to be taken into account to observe these unusual properties, which are not foreseen in the usual, classical transmission-line theory. In this section, we treat non-uniformities in the conduction of cables, in particular, concerning the conductors themselves, as well as concerning the geometry of the reference conductor. One may introduce additional lumped elements in the transmission-line theory, or one can modify the current and voltage sources and/or the p.u.l. parameters.

2.1 Vertical Connection Rods

Usually vertical elements are not considered in classical transmission-line theory. However, the vertical elements have an influence on the behavior of the transmission line, and thus must be taken into account for an exact calculation. Basically, one can find two methods for dealing with the vertical connection elements in the literature, both based on work published in [17] and [18].

[19] suggested treating the vertical connection as a biconical antenna, as shown in Figure 1. For a TEM mode, this antenna has a *constant* characteristic impedance, given by

$$Z_c = \frac{\eta_0}{2\pi} \ln \frac{1}{\tan \frac{\beta}{2}} \tag{3}$$

$$\approx \frac{\eta_0}{2\pi} \ln \frac{2h}{a}, \tag{4}$$

where $\eta_0 = \sqrt{\mu_0/\varepsilon_0}$. Since a wire of radius a and height h above ground has the same characteristic impedance, it is possible to just extend the transmission line by its vertical part.

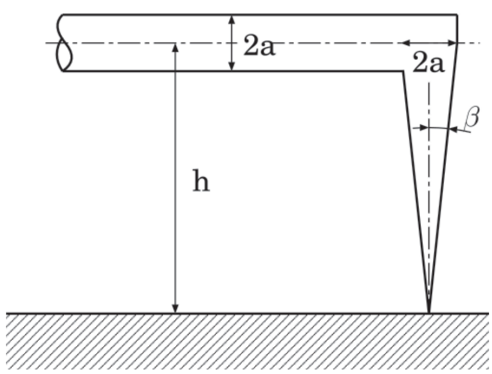

Figure 1. A vertical connection rod modeled as a biconical antenna.

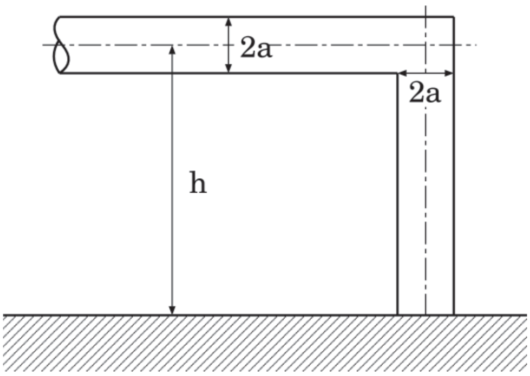

Figure 2. A vertical connection rod modeled as a cylindrical wire.

A different approach was shown in [17] and [20]. There, the vertical element was treated as a cylindrical wire (Figure 2). The height-dependent characteristic impedance of this type of connection then turns out to be [18]

$$Z_c\left(h'\right) \approx \frac{\eta_0}{2\pi} \ln \frac{2h'}{a}. \tag{5}$$

At low frequencies, i.e., $\lambda \gg h$, we can model the vertical rods with a transmission line of the same length, with average characteristic impedance

$$\overline{Z}_c = \frac{1}{h}\int_0^h Z_c\left(h'\right)dh' = \frac{\eta_0}{2\pi}\left[\ln\frac{2h}{a} - 1\right]. \tag{6}$$

However, this average characteristic impedance differs significantly from the characteristic impedance of the horizontal wire. One can not just extend the transmission line by the vertical rod, as suggested in [20] and [21], but rather a transmission line with the correct average characteristic impedance of the vertical element, Equation (6), should be connected.

Another possibility is to represent the vertical riser, including the termination impedance, Z_T, by its equivalent input impedance, $Z_{T_{\mathrm{eq}}}$ [20]:

$$Z_{T_{eq}} = \overline{Z}_C \frac{Z_T + \overline{Z}_C \tanh(\gamma h)}{\overline{Z}_C + Z_T \tanh(\gamma h)}. \tag{7}$$

For the response of vertical elements at the end of a transmission line, see also [22]. There, the model was extended to higher frequencies by introducing additional distributed voltage sources at the riser in the case of field coupling. An even more advanced technique was described in [23], where the coupling from the risers to the transmission line was additionally taken into account.

2.2 End Capacitance

In cases where a transmission line is finite and open-ended, we expect an increase of charge at the open end, leading to a local change of the p.u.l. capacitance which, for example, was obtained from an infinite line. Applying circuit theory, we can account for this change in the capacitance by the use of an additional capacitor that terminates the open end:

$$C^{\mathrm{end}} = \frac{2(h-a)\pi\varepsilon}{\left[\operatorname{arcosh}\left(\frac{h}{a}\right)\right]^2}. \tag{8}$$

This result was obtained by a quasi-static analysis [24]. An empirical approach gave a formula that refers to measurements [25], and took into consideration the capacitance of the end surface of the conductor:

$$C^{\mathrm{end}} \tag{9}$$

$$= \frac{2h\pi\varepsilon}{\operatorname{arcosh}\left(\frac{h}{a}\right)\left\{-3.954 + \sqrt{\left[2.564\operatorname{arcosh}\left(\frac{h}{a}\right)\right]^2 + (3.954)^2}\right\}}$$

A much more complicated approach to this problem was shown in [26-28]. There, the *Wiener-Hopf* method was used to get an exact solution for the open-ended transmission line. The result can then also be represented by an equivalent end impedance.

2.3 Bends in the Line Conductor

Practical layouts of cables very often contain bends. Since these act as inhomogeneities, they change the physical behavior of the line in their vicinities. One has to expect that the p.u.l. parameters will become dependent on the local coordinate around the region of the bend. Also, radiation will occur at very high frequencies. A reasonable approach to treating bends in a quasi-static approximation was performed by King [11] (see also references therein). There, a two-wire line (infinitely long) with a bend of an angle θ (the deviation from the straight line) at $\xi = 0$ was described by a one-dimensional EFIE (electric-field integral equation):

$$E_{x_1} - E_{x_2} = -\frac{j\omega\mu}{2\pi} i(\xi)\left[\int_{-\infty}^{0}\left(\frac{1}{R_1} - \frac{1}{R_2}\right)d\xi' \right.$$

$$\left. + \cos\theta \int_0^{\infty}\left(\frac{1}{R_{1_T}} - \frac{1}{R_{2_T}}\right)d\overline{\xi}'\right]$$

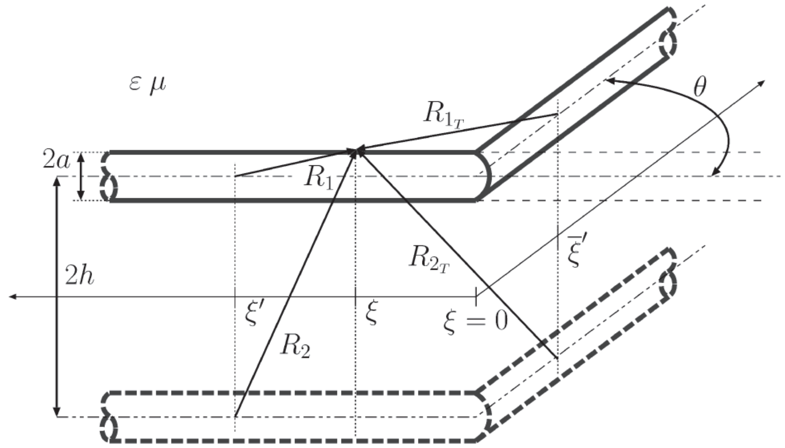

Figure 3. A transmission line with a bend.

$$-\frac{1}{2\pi\varepsilon}\frac{\partial q(\xi)}{\partial \xi}\left[\int_{-\infty}^{0}\left(\frac{1}{R_1}-\frac{1}{R_2}\right)d\xi' + \cos\theta\int_{0}^{\infty}\left(\frac{1}{R_{1_T}}-\frac{1}{R_{2_T}}\right)d\bar{\xi}'\right]. \qquad (10)$$

Here, R_1, R_2, R_{1_T}, and R_{2_T} are the distances as shown in Figure 3. They are given by

$$R_1 = \sqrt{(\xi-\xi')^2 + a^2}\,, \qquad (11)$$

$$R_2 = \sqrt{(\xi-\xi')^2 + (2h)^2}\,, \qquad (12)$$

$$R_{1_T} = \sqrt{\xi^2 + \bar{\xi}'^2 + 2|\xi|\bar{\xi}'\cos\theta + a^2}\,, \qquad (13)$$

$$R_{2_T} = \sqrt{\xi^2 + \bar{\xi}'^2 + 2|\xi|\bar{\xi}'\cos\theta + (2h)^2}\,. \qquad (14)$$

Since the tangential component of the electric-field strength vanishes on the surface of the conductor, Equation (10) can be easily transformed – together with the corresponding continuity equation – into the usual telegrapher equations with p.u.l. parameters that depend on the local coordinate, ξ [11]:

$$l_0(\xi) = \frac{\mu}{2\pi}\left[2\ln\frac{2h}{a} - \ln\frac{|\xi| + \sqrt{\xi^2+(2h)^2}}{|\xi| + \sqrt{\xi^2+a^2}} + \cos\theta\ln\frac{|\xi|\cos\theta + \sqrt{\xi^2+(2h)^2}}{|\xi|\cos\theta + \sqrt{\xi^2+a^2}}\right], \qquad (15)$$

$$c_0(\xi) = 2\pi\varepsilon\left[2\ln\frac{2h}{a} - \ln\frac{|\xi| + \sqrt{\xi^2+(2h)^2}}{|\xi| + \sqrt{\xi^2+a^2}} + \ln\frac{|\xi|\cos\theta + \sqrt{\xi^2+(2h)^2}}{|\xi|\cos\theta + \sqrt{\xi^2+a^2}}\right]^{-1}. \qquad (16)$$

If one is interested in the influence of the bend alone on the line parameters, compared to those of an infinitely long line, one has to subtract the inductance and capacitance p.u.l. of the uniform line from Equations (15) and (16), respectively. Further, if a representation of the bend in terms of lumped elements L_T and C_T in an equivalent circuit is desired, one has to integrate the mentioned differences of the line parameters as follows:

$$L_T = \int_0^{\infty}\left[l_0(\xi) - \frac{\mu}{\pi}\ln\frac{2h}{a}\right]d\xi\,, \qquad (17)$$

$$C_T = \int_0^{\infty}\left[c_0(\xi) - \pi\varepsilon\left(\ln\frac{2h}{a}\right)^{-1}\right]d\xi\,. \qquad (18)$$

The principal contribution for these integrals is in the range $|\xi| \le 10h$. Thus, if $\lambda \gg h$, modeling the bend by lumped elements is justified, and the equivalent circuit for the bent line looks like the one shown in Figure 4.

Using a wire line above a conducting ground for which $h = 10$ mm, $a = 1$ mm, and $\theta = 90°$, from Equations (17) and (18) one obtains the values $L_T = -1.831$ nH and $C_T = -29.215$ fF [21]. The negative values indicate that the line parameters in the neighborhood

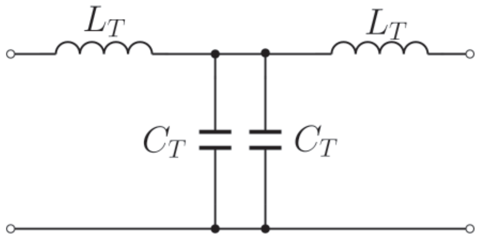

Figure 4. A two-port model of a bent line.

of the bend are smaller than those from an infinitely long straight line.

In [29, 30], it was shown in great detail how to obtain equivalent lumped-circuit elements for abrupt as well as smooth bends (modeled by an arc). A different approach was accomplished in [31]. There, extended telegrapher equations were derived to describe the current and potential on a bent wire. The approach even permitted describing the radiation. However, the p.u.l. parameters differed for forward- and backward-traveling waves.

2.4 Line Conduction through a Circular Aperture in a Metallic Screen

Systems that operate in harsh environments are often protected by metallic enclosures. However, apertures in the metallic walls are needed to connect different modules of a system. Thus, bundles of conductors, or even single wires, cross perforated metallic screens. They thereby introduce a discontinuity along the bundle, which forces a modification in the use of the multiconductor transmission-line model (see Figure 5). Therefore, it is important to model the problem of a wire running above a ground and passing a circular aperture in terms of an equivalent circuit that can be "inserted" into the description of a transmission line. This is the purpose of this subsection. We refer to [32] to achieve this goal, where, for the spectral representation of the current, $\tilde{I}_R(\alpha)$, flowing in the region to the right of the aperture ($\xi > 0$), the form

$$\tilde{I}_R(\alpha) = 2\pi^2 \omega \varepsilon a c_g G_g(\tau) \tag{19}$$

was derived. The function $G_g(\tau)$ is given by

$$G_g(\tau) = \frac{F(\tau) H_1^{(2)}(\tau a)}{\tau\left[H_0^{(2)}(2h\tau) - H_0^{(2)}(a\tau)\right]}, \tag{20}$$

with the function $F(\tau)$ being defined as

$$F(\tau) := J_0(a\tau)\left[H_0^{(2)}(a\tau) - H_0^{(2)}(b\tau)\right]$$

$$-H_0^{(2)}(2h\tau)\left[J_0(a\tau) - J_0(b\tau)\right]. \tag{21}$$

The current, $\tilde{I}_R(\alpha)$, is the Fourier transform of $I_R(\xi)$. The variable b denotes the radius of the circular aperture. The wavenumber is given by $k = \omega\sqrt{\mu\varepsilon}$, with ε and μ being the dielectric permittivity and magnetic permeability, respectively. Furthermore, τ evaluates to $\tau = \sqrt{k^2 - \alpha^2}$. The constant c_g is determined by imposing the continuity condition of the current at $\xi = 0$:

$$I_L(0) = I_R(0) = I_{L,\mathrm{TEM}}^i(0) = \frac{1}{\pi}\int_0^\infty \tilde{I}_R(\alpha)\, d\alpha. \tag{22}$$

Here, $I_L(\xi)$ is the current to the left of the screen, and $I_{L,\mathrm{TEM}}^i(\xi)$ represents the incident TEM current. We obtain

$$c_g = \frac{I_{L,\mathrm{TEM}}^i(0)}{2\pi\varepsilon\omega a \int_0^\infty G_g(\tau)\, d\alpha} \tag{23}$$

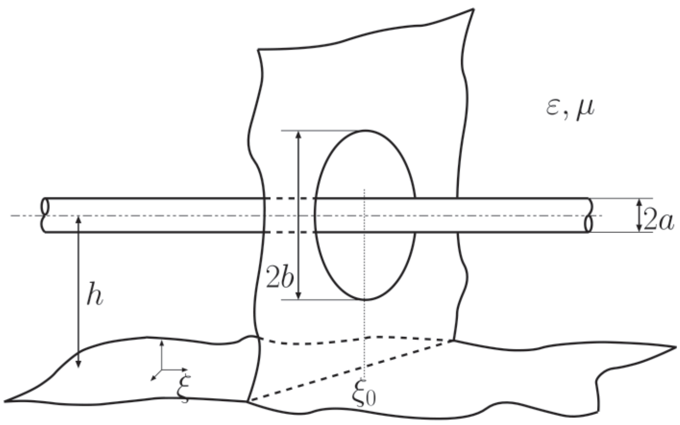

Figure 5. A transmission line through a circular aperture.

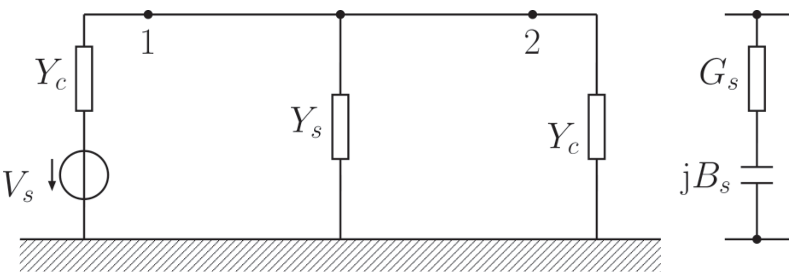

Figure 6. An equivalent circuit for a circular aperture in the absence of an external excitation.

An equivalent circuit for the TEM part of the current flowing along the wire can be derived from Equation (19). $\tilde{I}_R(\alpha)$ is decomposed into the sum of two terms that are related to the TEM mode and to the continuous modes of the current, respectively. Using Equations (19), (20), and (21), we get

$$\tilde{I}_R(\alpha) = \tilde{I}'_R(\alpha) + I''_R(\alpha) \tag{24}$$

The residue, R, of the function $\tilde{I}'_R(\alpha)$ at $\alpha = k$ is given by

$$R = \lim_{\alpha \to k} (\alpha - k)\tilde{I}_R(\alpha) = -j\frac{c_g}{Z_c}\ln\frac{b}{a} \tag{25}$$

Since the TEM part of the current is related to the singularities of $\tilde{I}'_R(\alpha)$ at $\alpha = \pm k$, we can write

$$\tilde{I}_{R,\mathrm{TEM}}(\alpha) = R\left(\frac{1}{\alpha - k} - \frac{1}{\alpha + k}\right) \tag{26}$$

It can be shown that $I_{R,\mathrm{TEM}}$ allows the following closed-form expression:

$$I_{R,\mathrm{TEM}}(\xi) = -jRe^{-jk\xi} = I^+_{R,\mathrm{TEM}}(0)e^{-jk\xi}, \tag{27}$$

with

$$I^+_{R,\mathrm{TEM}}(0) = \frac{c_g}{Z_c}\ln\frac{b}{a} \tag{28}$$

representing a TEM forward-traveling wave. Now, if we look at Figure 6, we may readily derive the entries of the scattering matrix for the corresponding scattering problem. Assuming the circuit is internally excited, the transmission coefficient, S_{21}, for the screen admittance Y_s becomes (for small k, such that radiation is omitted)

$$S_{21} = \frac{b_2}{a_1} = \frac{2Y_c}{Y_s + 2Y_c}. \tag{29}$$

The characteristic admittance is $Y_c = Z_c^{-1}$, a_1 represents the incoming wave from the left, and b_2 represents the outgoing wave on the right. For the TEM part of the current, we finally obtain

$$Y_s = G_s + jB_s = 2Y_c\left(\frac{I^i_{L,\mathrm{TEM}}(0)}{I^+_{R,\mathrm{TEM}}(0)} - 1\right), \tag{30}$$

where

$$\frac{I^i_{L,\mathrm{TEM}}(0)}{I^+_{R,\mathrm{TEM}}(0)} = \frac{2\pi kaZ_c}{\eta_0 \ln\frac{b}{a}}\int_0^\infty G_g(\tau)\,d\alpha\cdot \tag{31}$$

Numerical calculations of the real and imaginary parts of the screen admittance have shown that the action of the considered aperture essentially becomes noticeable by its lead-through capacitance at high frequencies [32]. For small values of a and b compared to the wavelength, the power losses mainly depend on the distance, h, between the wire and the ground plane, and not on the ratio $\left(\frac{b}{a}\right)$. The susceptance, B_s, mainly depends on the ratio $\left(\frac{b}{a}\right)$, and it increases as $\left(\frac{b}{a}\right)$ decreases.

2.5 Line Conduction Across a Slit

In the chassis of an automobile, for example, one may find conducting sheets that are welded together only at selected points. Thus, the slits that thereby occur in the metallic planes act as inhomogeneities for cables running across the slits, because the reference current below the conductor experiences a perturbation due to the slit. In order to handle this problem in the framework of transmission-line theory, one has to adequately model the slit in terms of an equivalent circuit. This is briefly described in the following. As a result, the slit is represented by a voltage, $V(\omega)$, and an input impedance, $Z(\omega)$, of a problem-adopted electric dipole [21].

On the basis of *Babinet's* principle, the problem is first transformed into a complementary structure. The duality principle is then used, where electric and magnetic quantities

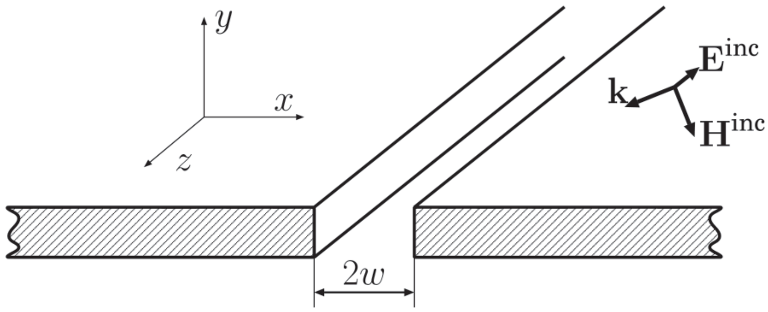

Figure 7. The geometry of an infinitely long slit of width $2w$ placed in a perfectly conducting plane.

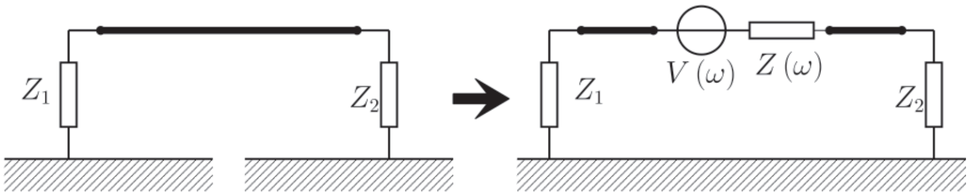

Figure 8. The equivalent circuit for a conductor crossing a slit.

are interchanged, and the slit is replaced by a narrow conducting strip of width $2w$. The integral equation for the *z*-directed surface current, $J_s(x)$, induced on a perfectly conducting strip by an axially invariant incident field that is transverse magnetic, is [33]

$$\int_{-w}^{w} J_s(x') H_0^{(2)}\left(k\left|x'-x\right|\right) \mathrm{d}x' = \frac{4}{k\eta_0} E_z^{\rm inc}(x). \quad (32)$$

At low frequencies ($|kw| \ll 1$), $E_z^{\rm inc}(x)$ is almost constant over the strip's cross section, and can be represented by its value on the *z* axis: $E_z^{\rm inc}(x) = E_z^{\rm inc}(0)$. Then, we obtain an analytical solution for the strip current [34]

$$J_s(x) = \frac{j2E_z^{\rm inc}(0)/\eta_0}{kw\left[\ln\left(\frac{\gamma kw}{4}\right) + j\frac{\pi}{2}\right]\sqrt{1-\left(\frac{x}{w}\right)^2}} \quad (33)$$

$$= \frac{J_s(0)}{\sqrt{1-\left(\frac{x}{w}\right)^2}}, \quad (34)$$

exhibiting the dependency of the current on the transverse coordinate, *x*. Here $\ln\gamma = 0.57722\ldots$ is *Euler's* constant. With this result, it is easy to calculate the total axial current, *I*, carried by the narrow strip:

$$I = \int_{-w}^{w} J_s(x)\,dx = J_s(0)\int_{-w}^{w} \frac{dx}{\sqrt{1-\left(\frac{x}{w}\right)^2}}$$

$$= J_s(0)(2w)\frac{\pi}{2}. \quad (35)$$

Note that we are dealing with the dual problem, and that we have estimated the total current in this problem. Thus, going back to our slit problem, instead of the current $J_s(0)$, we have to choose the electric field strength in the middle of the slit, $E_{\rm slit}$. The corresponding integration yields

$$V = \int_{-w}^{w} E_x(x)\,dx = E_{\rm slit}\int_{-w}^{w} \frac{dx}{\sqrt{1-\left(\frac{x}{w}\right)^2}}$$

$$= E_{\rm slit}(2w)\frac{\pi}{2}. \quad (36)$$

Remember, we wanted to transform a slit-crossing conductor into an equivalent-circuit model according to Figure 8. With the aid of Equation (36), we may estimate the voltage, $V(\omega)$, describing the potential difference across the slit. But we still have to determine the impedance, $Z(\omega)$, which represents, of course, a capacitance ($Z(\omega) = 1/\mathrm{j}\omega C$) for an open-ended slit.

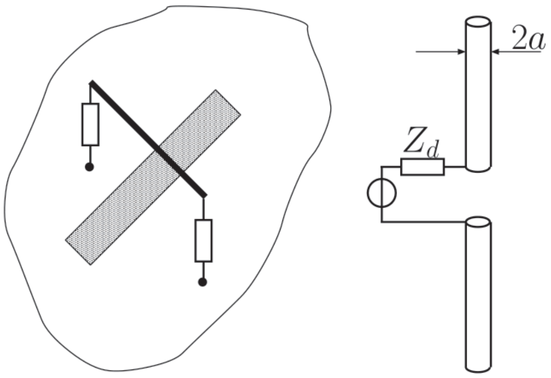

Figure 9. The dual representation of a slit: an electrical dipole with equivalent radius.

For a short-circuited slit in an ideally conducting plane, we proceed as follows. We first calculate the equivalent radius, a, of the above narrow strip by comparing the solution, Equation (35), with the corresponding solution for a perfectly conducting cylinder of infinite length, illuminated by a TM incident field. We obtain the well-known result [35]

$$a = \frac{\text{width}}{4} = \frac{w}{2} \cdot \tag{37}$$

Next, we observe that due to Babinet's principle, the relation [36]

$$Z_d Z = \frac{\eta_0^2}{4} \tag{38}$$

holds. Here, the impedance Z_d denotes the input impedance of an electric dipole of the same length as the slit and of equivalent radius a. Thus, a separate calculation is necessary to get Z_d.

Besides slits, there can also be (for example) holes in the ground plane. These cases are treated in [37]. Also, there the hole is modeled by a lumped equivalent circuit. More information can also be found in [38] and references therein.

2.6 Piecewise-Uniform Approximation of Nonuniform Transmission Lines

Only localized effects were considered in the previous sections. If we want to investigate a transmission line of nonuniform conduction, a method is used where the transmission line is approximated by piecewise-uniform sections [39, 40].

There, a nonuniform multiconductor line is modeled as a cascaded chain of many uniform transmission-line segments (see Figure 10). Within each segment, the p.u.l. parameters are constant, and are calculated as if the segment would be an infinitely long uniform transmission line. The solution for the nonuniform transmission line can then be obtained by calculating the product of the individual chain matrices of the uniform segments. When applying this method, the influence of the non-uniformity on the p.u.l. parameters is neglected, because the parameters are calculated the same way as for an infinitely long uniform line. They "do not know" anything about the non-uniformity of the line.

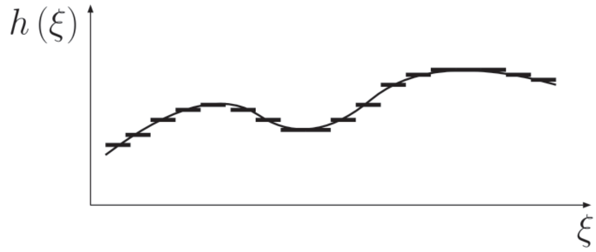

Figure 10. The approximation of a nonuniform transmission line by piecewise-uniform segments.

3. New Formulation of a Transmission-Line Theory

In this section, we will discuss the formulation of a very much extended, new transmission-line theory. This was originally introduced in [41] and then further developed [42-44]. Also, [45] and [46] contributed some ideas to a generalized transmission-line theory.

Above all, the improvements of the transmission-line theory concern all kinds of non-uniformities in the conduction of the conductors. These are taken into account right from the beginning of the derivation, and are therefore intrinsic to the theory. Thus, all physical effects occurring *due to the non-uniformities, such as radiation and higher order modes, are also reflected in the results*. Moreover, the new theory contains the classic transmission-line theory as a special case.

All calculations are done assuming harmonic excitation in the following. The basic procedure of the derivation can be divided into three parts. First, the mixed-potential field integral equation – sometimes also called the electric-field integral equation – is formulated. This equation is written in a special form that makes the following steps possible. Second, the unknown current distribution along the conductors is represented by a trial function, which is chosen such that it is a solution of a second-order differential equation, in general with non-constant coefficients. Then, the integral equation disintegrates into an ordinary second-order differential equation, which can be converted into two first-order ordinary differential equations. These become the telegrapher equations. Furthermore, one gets two integral equations: one for the determination of the coefficients, which become the per-unit-length parameters of the line; and one for the determination of the source terms in the telegrapher equations. The third step is the determination of the line parameters and the source terms by solving the two integral equations. Because there is no closed-form solution available for the general case, an iterative approach is used.

3.1 Formulation of the Integral Equation

3.1.1 Basic Equations from Maxwell's Theory

We start from well-known equations in electrodynamics that are often used in EM theory, e.g., for the derivation of numerical techniques, like the MoM or PEEC. The total electric field, $\mathbf{E}$, consists of a scattered and an incident part. The scattered portion results from the currents and charges in the conductors, while the incident part comes from one or more exterior sources:

$$\mathbf{E}-\mathbf{E}_{\text{inc}}=\mathbf{E}_{\text{scat}}\,. \tag{39}$$

The scattered field is now expressed by the scalar and the vector potentials ϕ and $\mathbf{A}$, respectively:

$$\mathbf{E}-\mathbf{E}_{\text{inc}}=-\nabla\phi-j\omega\mathbf{A}\,, \tag{40}$$

and the two potentials in the *Lorenz* gauge can be computed with the expressions

$$\mathbf{A}(\mathbf{x})=\mu\int_v \mathbf{J}(\mathbf{x}')G(\mathbf{x},\mathbf{x}')\,d^3x' \tag{41}$$

and

$$\phi(\mathbf{x})=\frac{1}{\varepsilon}\int_v \rho(\mathbf{x}')G(\mathbf{x},\mathbf{x}')\,d^3x'\,. \tag{42}$$

The sources, $\mathbf{J}$ and ρ, are the current and charge density, respectively, and $G(\mathbf{x},\mathbf{x}')$ is the *Green's* function, which, for free space, is

$$G(\mathbf{x},\mathbf{x}')=\frac{e^{-jk|\mathbf{x}-\mathbf{x}'|}}{4\pi|\mathbf{x}-\mathbf{x}'|}\,. \tag{43}$$

Here, other Green's functions can also be inserted to take into account ground planes, dielectrics, or cavities, for example. However, we will restrict ourselves to this rather simple free-space form.

3.1.2 Geometrical Characterization of the Conductors

We will apply the above equations to a multiconductor configuration, establishing a nonuniform transmission line with *n* conductors. In order to do that, the first thing that is needed is a local coordinate system for the conductors, and a precise mathematical representation of the geometry. The position of a conductor *i* is given by a space curve $\mathbf{C}_i(\xi)$, with the curve parameter ξ. All curves are scaled such that the parameter ξ is the same for every curve: it starts at ξ_0, the near ends of the conductors, and ends at ξ_l, which corresponds to the far ends. We can easily define the *Frenet* frame [47] for the curves, consisting of the tangential, normal, and binormal unit vectors. First, we need the tangential vector

$$\mathbf{T}_i=\frac{\partial\mathbf{C}_i}{\partial\xi}\,. \tag{44}$$

This is not a unit vector. Its length is

$$u_{ii}(\xi)=\left|\mathbf{T}_i(\xi)\right|, \tag{45}$$

and the unit vector $\mathbf{T}_i^u$ becomes

$$\mathbf{T}_i^u(\xi)=\frac{\mathbf{T}_i(\xi)}{u_{ii}(\xi)}\,. \tag{46}$$

The normal and binormal unit vectors are given by

$$\mathbf{N}_i^u=\frac{1}{\kappa_i u_{ii}}\frac{\partial\mathbf{T}_i^u}{\partial\xi} \tag{47}$$

and

$$\mathbf{B}_i^u=\mathbf{T}_i^u\times\mathbf{N}_i^u\,. \tag{48}$$

The variable κ_i is called the curvature of conductor *i* at position ξ:

$$\kappa_i(\xi)=\left|\frac{\partial\mathbf{T}_i^u}{\partial\xi}\right|\frac{1}{u_{ii}}\,. \tag{49}$$

We now establish a polar coordinate system in the plane that is spanned by the normal and the binormal vectors. Then, a point in that plane can be addressed by the coordinates (ξ,r,α) (see Figure 11):

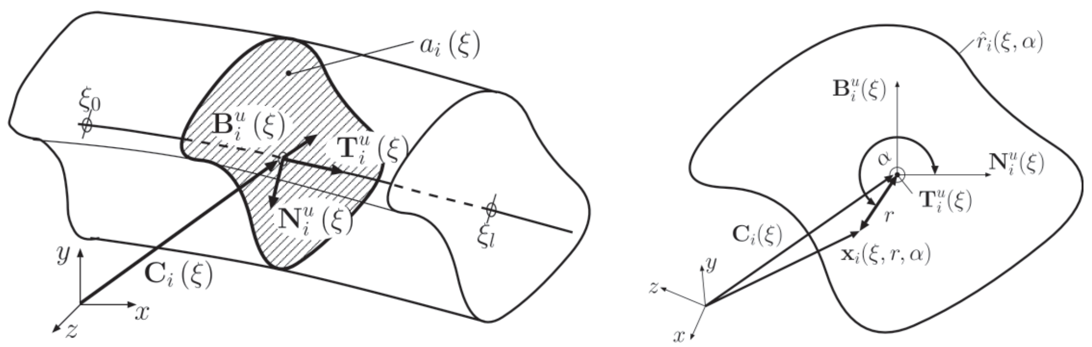

Figure 11. A wire with its local coordinate system.

$$\mathbf{x}_i(\xi,r,\alpha)=\mathbf{C}_i(\xi)+\mathbf{N}_i^u(\xi)\,r\cos\alpha+\mathbf{B}_i^u(\xi)\,r\sin\alpha, \tag{50}$$

where the angle α is in the interval $[0,2\pi]$, and the radius r is in the interval $[0,\hat{r}_i(\xi,\alpha)]$. The function $\hat{r}_i(\xi,\alpha)$ points to the surface of the conductor. This coordinate system is curvilinear and nonorthogonal, which usually is not very easy to handle. However, it is quite useful for our purposes.

After this short excursion into differential geometry, we will now focus on the further derivation of the integral equation.

3.1.3 Adaptation of the Equations to the Conductor Geometry

We will now give adapted expressions for the current and charge distribution. One important requirement we have to impose is for the current density, which cannot have a transverse component, i.e., the current density in a conductor always has to be parallel to its tangential vector. This is not always true in reality. Significant transverse components of the current density can occur at extremely high frequencies. In this case, a much more complicated theory would be needed to describe the fields, and we would not be able to carry on with our derivation. In the case of negligible transverse components, the current density can be represented as

$$\mathbf{J}\left[\mathbf{x}_i(\xi,r,\alpha)\right]=\mathbf{T}_i^u(\xi)\,i_i(\xi)\,d_{\mathbf{J}_i}(\xi,r,\alpha). \tag{51}$$

Note that this is a very general representation. No assumptions are made about the transverse distribution of the current density at this point.

In the same manner, the charge density can be represented with the aid of the charge per unit length, q_i:

$$\rho\left[\mathbf{x}_i(\xi,r,\alpha)\right]=q_i(\xi)\,d_{\rho_i}(\xi,r,\alpha)\cdot \tag{52}$$

The current, i_i, and the charge per unit length, q_i, are defined by the formulae

$$i_i(\xi):=\int_{a_i(\xi)}\mathbf{J}\left[\mathbf{x}_i(\xi,r,\alpha)\right]\mathbf{T}_i^u(\xi)\,da, \tag{53}$$

$$q_i(\xi):=\int_{a_i(\xi)}\rho\left[\mathbf{x}_i(\xi,r,\alpha)\right]da\cdot \tag{54}$$

The distribution functions are given formally by

$$d_{\mathbf{J}_i}(\xi,r,\alpha)=\frac{\mathbf{J}\left[\mathbf{x}_i(\xi,r,\alpha)\right]\mathbf{T}_i^u(\xi)}{i_i(\xi)\,u_{ii}(\xi)} \tag{55}$$

and

$$d_{\rho_i}(\xi,r,\alpha)=\frac{\rho\left[\mathbf{x}_i(\xi,r,\alpha)\right]}{q_i(\xi)}\cdot \tag{56}$$

These distributions have to be known or guessed in advance before any calculations are made. Often, some assumptions – such as a uniform or superficial current and charge distribution – lead to satisfying results. One could also use some kind of a perturbational approach to determine the distribution functions. However, this is not subject of this paper, and we assume that we know a reasonably good approximation of the current and charge distribution inside the conductors.

Ohm's law links the current density and the electric-field strength:

$$\mathbf{E}=\frac{1}{\sigma}\mathbf{J}\cdot \tag{57}$$

This is used to replace the total field strength in Equation (40), which is thought to be evaluated inside a conductor. The result is then dot multiplied with the tangential vector (not the unit vector), which extracts the tangential components of all quantities, multiplied with the length of the tangential vector

$$\frac{1}{\sigma} i_j d_{\mathbf{J}_j} - E_{\text{inc}_j} = -\frac{\partial \phi_j}{\partial \xi} - \mathrm{j}\omega A_j , \tag{58}$$

where

$$A_j = \mathbf{T}_j \bullet \mathbf{A} ,$$

$$E_{\text{inc}_j} = \mathbf{T}_j \bullet \mathbf{E}_{\text{inc}} , \tag{59}$$

$$\frac{\partial \phi_j}{\partial \xi} = \mathbf{T}_j \bullet \nabla \phi .$$

Eventually, from Equation (58) we calculate the average field strength *at the surface* of a conductor ($r = \hat{r}(\xi, \alpha)$). The result becomes

$$i_j(\xi) r_{jj}(\xi) - v_{\text{inc}_j}(\xi) + \frac{\partial \psi_j(\xi)}{\partial \xi}$$

$$= -\frac{j\omega}{2\pi} \int_0^{2\pi} A_j \left[\xi, \hat{r}_j(\xi,\alpha), \alpha\right] d\alpha \tag{60}$$

where

$$r_{jj}(\xi) = \frac{1}{2\pi} \int_0^{2\pi} \frac{1}{\sigma} d_{\mathbf{J}_j} \left[\xi, \hat{r}_j(\xi,\alpha), \alpha\right] d\alpha, \tag{61}$$

$$\psi_j(\xi) = \frac{1}{2\pi} \int_0^{2\pi} \phi_j \left[\xi, \hat{r}_j(\xi,\alpha), \alpha\right] d\alpha, \tag{62}$$

$$v_{\text{inc}_j}(\xi) = \frac{1}{2\pi} \int_0^{2\pi} E_{\text{inc}_j} \left[\xi, \hat{r}_j(\xi,\alpha), \alpha\right] d\alpha \tag{63}$$

Equation (60) is the basis for the first of the telegrapher equations: we just need to replace the vector potential A_j with a suitable expression. Equation (42), which gives us the scalar potential, will become the second telegrapher equation.

Both potentials are evaluated by integrating the product of the current or charge density, respectively, and the Green's functions over the volume. Those integrals can be reduced to integrals over the conductors. The potentials then become

$$\mathbf{A}(\mathbf{x}) = \mu \sum_{i=0}^{n} \int_{\xi_0}^{\xi_l} \int_{a_i(\xi')} G(\mathbf{x}, \mathbf{x}_i) d_{\mathbf{J}_i}(\mathbf{x}_i) \mathbf{T}_i(\xi')$$

$$i_i(\xi') \left[1 - r'\kappa_i(\xi') \cos\alpha'\right] da' \, d\xi' \tag{64}$$

and

$$\phi(\mathbf{x}) = \frac{1}{\varepsilon} \sum_{i=0}^{n} \int_{\xi_0}^{\xi_l} \int_{a_i(\xi')} G(\mathbf{x}, \mathbf{x}_i) d_{\rho_i}(\mathbf{x}_i) q_i(\xi')$$

$$u_{ii}(\xi') \left[1 - r'\kappa_i(\xi') \cos\alpha'\right] da' \, d\xi' \tag{65}$$

where the integration over the area a_i is an abbreviation for

$$\int_{a_i(\xi')} f\left[\mathbf{x}(\xi', r', \alpha')\right] da'$$

$$= \int_0^{2\pi} \int_0^{\hat{r}_i(\xi',\alpha')} f\left[\mathbf{x}(\xi', r', \alpha')\right] r' dr' \, d\alpha' \tag{66}$$

Equation (64) is now used to replace A_j in Equation (60), while Equation (65) is inserted into Equation (62). We then get two new equations for every conductor. All equations for all conductors can be combined to a very compact matrix formulation:

$$\frac{1}{j\omega} \left(\mathbf{ri} - \mathbf{v}_{\text{inc}} + \frac{\partial}{\partial \xi} \psi \right) = -\int_{\xi_0}^{\xi_l} \mathbf{k}_l(\xi, \xi') \mathbf{i}(\xi') d\xi' \tag{67}$$

$$\psi = \int_{\xi_0}^{\xi_l} \mathbf{k}_c(\xi, \xi') \mathbf{u}(\xi') \mathbf{q}(\xi') d\xi' . \tag{68}$$

The integral kernels, $\mathbf{k}_l$ and $\mathbf{k}_c$, are matrices of dimension $n \times n$. The elements of these matrices are given by the expressions

$$k_{l_{ji}}(\xi, \xi') = \frac{\mu}{2\pi} \int_0^{2\pi} \int_{a_i(\xi')} G(\mathbf{x}_j, \mathbf{x}_i) d_{\mathbf{J}_i}(\mathbf{x}_i) \mathbf{T}_j(\xi)$$

$$\mathbf{T}_i(\xi') \left[1 - r'\kappa_i(\xi') \cos\alpha'\right] da' \, d\alpha \tag{69}$$

and

$$k_{c_{ji}}(\xi, \xi') = \frac{1}{2\pi\varepsilon} \int_0^{2\pi} \int_{a_i(\xi')} G(\mathbf{x}_j, \mathbf{x}_i) d_{\rho_i}(\mathbf{x}_i)$$

$$\left[1 - r'\kappa_i(\xi') \cos\alpha'\right] da' \, d\alpha \tag{70}$$

For the above integration, the two spatial vectors have the following coordinate dependences:

$$\mathbf{x}_j = \mathbf{x}_j \left[\xi, \hat{r}_j(\xi,\alpha), \alpha\right], \tag{71}$$

$$\mathbf{x}_i = \mathbf{x}_i(\xi', r', \alpha') . \tag{72}$$

The variables $\mathbf{r}$ and $\mathbf{u}$ denote diagonal matrices, while the quantities $\mathbf{i}$, $\mathbf{q}$, ψ, and $\mathbf{v}_{\text{inc}}$ are column vectors:

$$\mathbf{i} = \begin{bmatrix} i_1 & \dots & i_n \end{bmatrix}^{\mathrm{T}}, \tag{73}$$

$$\mathbf{q} = \begin{bmatrix} q_1 & \dots & q_n \end{bmatrix}^{\mathrm{T}}, \tag{74}$$

$$\psi = \begin{bmatrix} \psi_1 & \dots & \psi_n \end{bmatrix}^{\mathrm{T}}, \tag{75}$$

$$\mathbf{v}_{\text{inc}} = \begin{bmatrix} v_{\text{inc}_1} & \dots & v_{\text{inc}_n} \end{bmatrix}^{\mathrm{T}}. \tag{76}$$

Equations (67) and (68) still have three unknowns ($\mathbf{i}$, $\mathbf{q}$, and ψ). We will use the continuity equation in order to eliminate $\mathbf{q}$. This equation ($\nabla \bullet \mathbf{J} = -j\omega\rho$) can be integrated over the cross-sectional area of a conductor. We then find a relation between the current and the charge per unit length:

$$\frac{\partial i_i}{\partial \xi} = -j\omega u_{ii} q_i + i_i b_{ii}, \tag{77}$$

where

$$b_{ii} = \int_{a_i(\xi)} \frac{\partial d_{\mathbf{J}_i}}{\partial \xi} da \cdot \tag{78}$$

The final integral equation, in super matrix notation, then reads

$$\begin{bmatrix} \frac{1}{j\omega}\left(\mathbf{r}\mathbf{i} - \mathbf{v}_{\text{inc}} + \frac{\partial}{\partial \xi}\psi(\xi)\right) \\ \mathrm{j}\omega\psi(\xi) \end{bmatrix}$$

$$= -\int_{\xi_0}^{\xi_l} \overline{\mathbf{K}}(\xi,\xi') \begin{bmatrix} \frac{\partial}{\partial \xi'}\mathbf{i}(\xi') \\ \mathbf{i}(\xi') \end{bmatrix} d\xi', \tag{79}$$

where the super matrix integral kernel is

$$\overline{\mathbf{K}}(\xi,\xi') = \begin{bmatrix} \mathbf{0} & \mathbf{k}_l(\xi,\xi') \\ \mathbf{k}_c(\xi,\xi') & -\mathbf{b}(\xi') \end{bmatrix}. \tag{80}$$

3.1.4 Thin-Wire Approximation

Very often, it is sufficient to think of the conductors as thin wires with a circular cross section. In that case, the integral kernels can be significantly simplified:

$$k_{l_{ij}}(\xi,\xi') := \mu \mathbf{T}_i(\xi') \bullet \mathbf{T}_j(\xi) G\left[\mathbf{C}_j(\xi), \mathbf{C}_i(\xi')\right], \tag{81}$$

$$k_{c_{ij}}(\xi,\xi') := \frac{1}{\varepsilon} G\left[\mathbf{C}_j(\xi), \mathbf{C}_i(\xi')\right], \tag{82}$$

$$b_{ii}(\xi,\xi') := 0 \cdot \tag{83}$$

If the spatial vectors $\mathbf{C}_j$ and $\mathbf{C}_i$ point to the same conductor, i.e., $i = j$, the coordinates for $\mathbf{C}_j$ are usually chosen on the surface of the wire.

3.2 Trial Function for the Current

We will now construct a trial function for the current, and insert it into the integral equations, Equations (79). The solution for the current can be expressed in the very general form

$$\mathbf{i}(\xi') = \mathbf{f}_0(\xi,\xi') + \mathbf{f}_1(\xi,\xi')\frac{\partial}{\partial \xi}\mathbf{i}(\xi) + \mathbf{f}_2(\xi,\xi')\mathbf{i}(\xi). \tag{84}$$

The function $\mathbf{f}_0$, which is a vector, and the functions $\mathbf{f}_1$ and $\mathbf{f}_2$, which are matrices, are so far unknown. They are determined by the solution of an ordinary differential equation of second order for the current vector $\mathbf{i}$. The term containing $\mathbf{f}_0$ resembles the inhomogeneous part of the solution, while the other two terms, involving $\mathbf{f}_1$ and $\mathbf{f}_2$, constitute the homogeneous solution. The current and its derivative at position ξ comprise the integration constants.

This is a very general approach for the current, because we do not specify the functions $\mathbf{f}_k, k = 0,1,2$. This approach can thus be used for every physical situation.

We can also calculate the derivative with respect to ξ' of Equation (84). The result of this can be combined with the expression itself into a super matrix notation

$$\begin{bmatrix} \frac{\partial}{\partial \xi'}\mathbf{i}(\xi') \\ \mathbf{i}(\xi') \end{bmatrix} = \begin{bmatrix} \frac{\partial}{\partial \xi'}\mathbf{f}_0 \\ \mathbf{f}_0 \end{bmatrix} + \underbrace{\begin{bmatrix} \frac{\partial}{\partial \xi'}\mathbf{f}_1 & \frac{\partial}{\partial \xi'}\mathbf{f}_2 \\ \mathbf{f}_1 & \mathbf{f}_2 \end{bmatrix}}_{\mathbf{F}} \begin{bmatrix} \frac{\partial}{\partial \xi}\mathbf{i}(\xi) \\ \mathbf{i}(\xi) \end{bmatrix} \tag{85}$$

However, this expression can be inserted into Equation (79). Because the current is now independent of the integration variable, it can be pulled out of the integral:

$$\begin{bmatrix} \frac{1}{j\omega}\left(\mathbf{r}\mathbf{i} - \mathbf{v}_{\text{inc}} + \frac{\partial}{\partial \xi}\psi(\xi)\right) \\ \mathrm{j}\omega\psi(\xi) \end{bmatrix} = -\overline{\mathbf{I}}(\xi) \begin{bmatrix} \frac{\partial}{\partial \xi}\mathbf{i}(\xi) \\ \mathbf{i}(\xi) \end{bmatrix} - \begin{bmatrix} \mathbf{I}_{10} \\ \mathbf{I}_{20} \end{bmatrix} \tag{86}$$

where

$$\overline{\mathbf{I}}(\xi)=\int_{\xi_0}^{\xi_l}\overline{\mathbf{K}}(\xi,\xi')\overline{\mathbf{F}}(\xi,\xi')\,d\xi' \tag{87}$$

$$\begin{bmatrix}\mathbf{I}_{10}\\ \mathbf{I}_{20}\end{bmatrix}=\int_{\xi_0}^{\xi_l}\overline{\mathbf{K}}(\xi,\xi')\begin{bmatrix}\dfrac{\partial}{\partial\xi'}\mathbf{f}_0(\xi,\xi')\\ \mathbf{f}_0(\xi,\xi')\end{bmatrix}d\xi'. \tag{88}$$

It is a matter of simple arithmetic operations to rearrange Equation (86) into

$$\frac{\partial}{\partial\xi}\begin{bmatrix}\psi\\ \mathbf{i}\end{bmatrix}=-j\omega\overline{\mathbf{P}}\begin{bmatrix}\psi\\ \mathbf{i}\end{bmatrix}+\begin{bmatrix}\psi'_s\\ \mathbf{i}'_s\end{bmatrix} \tag{89}$$

with the coefficient matrix

$$\mathrm{j}\omega\overline{\mathbf{P}}=\begin{bmatrix}\mathbf{1} & j\omega\mathbf{I}_{11}\\ \mathbf{0} & \mathbf{I}_{21}\end{bmatrix}^{-1}\begin{bmatrix}\mathbf{0} & j\omega\mathbf{I}_{12}+\mathbf{r}\\ j\omega\mathbf{1} & \mathbf{I}_{22}\end{bmatrix} \tag{90}$$

and the source terms

$$\begin{bmatrix}\psi'_s\\ \mathbf{i}'_s\end{bmatrix}=\begin{bmatrix}\mathbf{1} & j\omega\mathbf{I}_{11}\\ \mathbf{0} & \mathbf{I}_{21}\end{bmatrix}^{-1}\left(\begin{bmatrix}\mathbf{v}_{\mathrm{inc}}\\ \mathbf{0}\end{bmatrix}-\begin{bmatrix}j\omega\mathbf{1} & \mathbf{0}\\ \mathbf{0} & \mathbf{1}\end{bmatrix}\begin{bmatrix}\mathbf{I}_{10}\\ \mathbf{I}_{20}\end{bmatrix}\right) \tag{91}$$

which clearly can be identified as a system of coupled first-order differential equations. One could eliminate the vector ψ and get a second-order differential equation for the determination of $\mathbf{i}$, for which we already provided the general solution in Equation (84). Thus, the solution of Equation (89) should provide a way of determining the unknown functions $\mathbf{f}_0$, $\mathbf{f}_1$, and $\mathbf{f}_2$. Moreover, this equation exhibits the same mathematical structure as the telegrapher equations for nonuniform transmission lines, but still embodies Maxwell's theory, within the approximations we have made. Therefore, we call these equations generalized telegrapher equations, and the whole theory the *transmission-line super theory* (TLST). Because we have equations with the same structure as the classical telegrapher equations, all known procedures for the solution can be adopted.

3.3 Calculation of the Line Parameters and Source Terms

For the determination of the line parameters and the source terms, the expressions of Equations (90) and (91) must be evaluated using the results from Equations (87) and (88). However, those equations require the knowledge of the functions $\mathbf{f}_0$, $\mathbf{f}_1$, and $\mathbf{f}_2$, which will be determined here.

In order to do this, we anticipate the solution for the telegrapher equation, which will be given in more detail in Section 4. The general solution can be written as (see [48, 49])

$$\begin{bmatrix}\psi(\xi')\\ \mathbf{i}(\xi')\end{bmatrix}=\mathcal{M}_{\xi}^{\xi'}\left\{-j\omega\overline{\mathbf{P}}\right\}\begin{bmatrix}\psi(\xi)\\ \mathbf{i}(\xi)\end{bmatrix}$$

$$+\int_{\xi}^{\xi'}\mathcal{M}_{\zeta}^{\xi'}\left\{-j\omega\overline{\mathbf{P}}\right\}\begin{bmatrix}\psi'_s(\zeta)\\ \mathbf{i}'_s(\zeta)\end{bmatrix}d\zeta \tag{92}$$

From Equation (89), we can also find the expression

$$\begin{bmatrix}\dfrac{\partial}{\partial\xi}\mathbf{i}-\mathbf{i}'_s\\ \mathbf{i}\end{bmatrix}=-j\omega\overline{\mathbf{Q}}\begin{bmatrix}\psi\\ \mathbf{i}\end{bmatrix}, \tag{93}$$

where

$$\overline{\mathbf{Q}}=\begin{bmatrix}\mathbf{P}_{21} & \mathbf{P}_{22}\\ \mathbf{0} & -\dfrac{1}{j\omega}\mathbf{1}\end{bmatrix}, \tag{94}$$

which, if inserted into the solution, gives

$$\begin{bmatrix}\dfrac{\partial}{\partial\xi'}\mathbf{i}(\xi')-\mathbf{i}'_s(\xi')\\ \mathbf{i}(\xi')\end{bmatrix}$$

$$=\overline{\mathbf{Q}}(\xi')\mathcal{M}_{\xi}^{\xi'}\left\{-j\omega\overline{\mathbf{P}}\right\}\overline{\mathbf{Q}}(\xi)^{-1}\begin{bmatrix}\dfrac{\partial}{\partial\xi}\mathbf{i}(\xi)-\mathbf{i}'_s(\xi)\\ \mathbf{i}(\xi)\end{bmatrix}$$

$$-j\omega\overline{\mathbf{Q}}(\xi')\int_{\xi}^{\xi'}\mathcal{M}_{\zeta}^{\xi'}\left\{-j\omega\overline{\mathbf{P}}\right\}\begin{bmatrix}\psi'_s(\zeta)\\ \mathbf{i}'_s(\zeta)\end{bmatrix}d\zeta \tag{95}$$

By comparing the above expression with Equation (85), we can easily find expressions for $\mathbf{f}_k$, which then can be used to calculate the parameters and the source terms.

3.3.1 Line Parameters

From the comparison of Equation (95) with Equation (85), we find

$$\overline{\mathbf{F}}=\overline{\mathbf{Q}}(\xi')\mathcal{M}_{\xi}^{\xi'}\left\{-j\omega\overline{\mathbf{P}}\right\}\overline{\mathbf{Q}}(\xi)^{-1} \tag{96}$$

By using some properties of the product integral (see [48]), this expression can be rewritten as

$$\bar{\mathbf{F}} = \mathcal{M}_{\xi}^{\xi'}\underbrace{\left\{-\mathrm{j}\omega\bar{\mathbf{Q}}\bar{\mathbf{P}}\bar{\mathbf{Q}}^{-1} + \mathcal{D}\left\{\bar{\mathbf{Q}}\right\}\right\}}_{-\mathrm{j}\omega\bar{\mathbf{P}}^{\star}}, \qquad (97)$$

with the product derivative $\mathcal{D}\{\bar{\mathbf{Q}}\}$. With the aid of Equations (90) and (94), the argument is expressed with elements from the matrix $\bar{\mathbf{I}}$:

$$-\mathrm{j}\omega\bar{\mathbf{P}}^{\star}$$

$$= \begin{bmatrix} \mathbf{I}_{21} & \mathbf{0} \\ \mathbf{0} & \mathbf{1} \end{bmatrix}^{-1} \begin{bmatrix} -\omega^2\mathbf{I}_{11} - \mathbf{I}_{22}\dfrac{\partial\mathbf{I}_{21}}{\partial\xi} & -\omega^2\mathbf{I}_{12} + j\omega\mathbf{r}\dfrac{\partial\mathbf{I}_{22}}{\partial\xi} \\ \mathbf{1} & \mathbf{0} \end{bmatrix} \qquad (98)$$

Then, Equation (87) can be written as

$$\bar{\mathbf{I}}(\xi) = \int_{\xi_0}^{\xi_l} \bar{\mathbf{K}}(\xi,\xi')\mathcal{M}_{\xi}^{\xi'}\left\{-j\omega\bar{\mathbf{P}}^{\star}\right\}d\xi'. \qquad (99)$$

The only unknowns in this equation are the elements of the matrix $\bar{\mathbf{I}}$. Unfortunately, we are not able to explicitly solve for $\bar{\mathbf{I}}$; however, we suggest an iterative procedure to obtain an approximate solution. Once $\bar{\mathbf{I}}$ is known, we can easily determine the line parameters by applying Equation (90).

For the iterative solution of Equation (99), we start with a simple approximation for $\bar{\mathbf{I}}$: $\bar{\mathbf{I}}^{(0)}$. With that we are able to evaluate Equation (99), which then gives us a new approximation for $\bar{\mathbf{I}}$, namely $\bar{\mathbf{I}}^{(1)}$. Thus, the iteration procedure is

$$\bar{\mathbf{I}}^{(n+1)} = \bar{\mathbf{L}}\left\{\bar{\mathbf{I}}^{(n)}\right\}, \qquad (100)$$

where the operator $\bar{\mathbf{L}}\{..\}$ is given by Equation (99). We are currently not able to prove the convergence of the procedure for the general case; however, practical examples already showed a very good convergence after one iteration [41]. Moreover, the procedure gives the exact results for examples where closed-form solutions exist, e.g., a uniform transmission line (see Section 5.1). In order to start the iteration, we need some starting values, $\bar{\mathbf{I}}^{(0)}$. These values are obtained by an approximate calculation of the first term of the Taylor expansion of $\bar{\mathbf{I}}$, i.e.,

$$\bar{\mathbf{I}}(\xi,\omega) = \bar{\mathbf{I}}_0(\xi) + \omega\bar{\mathbf{I}}_1(\xi) + \ldots \qquad (101)$$

and

$$\bar{\mathbf{I}}^{(0)}(\xi) = \bar{\mathbf{I}}_0(\xi)\cdot \qquad (102)$$

The $\bar{\mathbf{I}}_0$ term can be calculated by evaluating Equation (99) at a frequency of $\omega = 0$, which is rather simple. If $\omega = 0$, one gets

$$-\mathrm{j}\omega\bar{\mathbf{P}}^{\star}\Big|_{\omega=0} = \begin{bmatrix} -\mathbf{I}_{21}^{-1}\left(\mathbf{I}_{22} + \dfrac{\partial\mathbf{I}_{21}}{\partial\xi}\right) & -\mathbf{I}_{21}^{-1}\dfrac{\partial\mathbf{I}_{22}}{\partial\xi} \\ \mathbf{1} & 0 \end{bmatrix}. \qquad (103)$$

The first terms of the product integral of this expression then become

$$\mathcal{M}_{\xi}^{\xi'}\left\{-\mathrm{j}\omega\bar{\mathbf{P}}^{\star}\right\}\Big|_{\omega=0}$$

$$= \bar{\mathbf{1}} + \begin{bmatrix} -\int_{\xi}^{\xi'}\mathbf{I}_{21}^{-1}\left(\mathbf{I}_{22} + \dfrac{\partial\mathbf{I}_{21}}{\partial\eta}\right)d\eta & -\int_{\xi}^{\xi'}\mathbf{I}_{21}^{-1}\dfrac{\partial\mathbf{I}_{22}}{\partial\eta}d\eta \\ (\xi'-\xi)\mathbf{1} & \mathbf{0} \end{bmatrix} + \ldots \qquad (104)$$

We only take the first term (unit matrix) for the calculation of the starting parameters, because that is all we know right now. For the first term of the expansion of $\bar{\mathbf{I}}$, we then find

$$\bar{\mathbf{I}}_0(\xi) \approx \int_{\xi_0}^{\xi_l}\bar{\mathbf{K}}(\xi,\xi')d\xi'\Big|_{\omega=0} \qquad (105)$$

$$\approx \begin{bmatrix} \mathbf{0} & \int_{\xi_0}^{\xi_l}\mathbf{k}_l(\xi,\xi')d\xi' \\ \int_{\xi_0}^{\xi_l}\mathbf{k}_c(\xi,\xi')d\xi' & -\int_{\xi_0}^{\xi_l}\mathbf{b}(\xi')d\xi' \end{bmatrix}\Bigg|_{\omega=0} \qquad (106)$$

We might mention here that for a TEM mode propagation along the transmission line, the term $\bar{\mathbf{I}}_0$ is the only term that does not vanish. Moreover, the approximate result for $\bar{\mathbf{I}}_0$ given above is exact in this case. For a transmission line with a dominant TEM mode, higher-order terms will be small, and the solution calculated with only $\bar{\mathbf{I}}_0$ taken into account is still a very good approximation. If the propagating waves deviate more and more from a TEM mode and higher-order modes appear, then the higher-order terms of $\bar{\mathbf{I}}$ also become important; however, the solution using only $\bar{\mathbf{I}}_0$ still gives quite good results, as we will illustrate in the examples section (Section 5).

The same applies to $\bar{\mathbf{P}}^{\star}$, which as well might be expanded into a series. The expansion coefficients are related to the coefficients of $\bar{\mathbf{I}}$, as given by Equation (98):

$$\bar{\mathbf{P}}^{\star}(\xi,\omega) = \bar{\mathbf{P}}_0^{\star}(\xi) + \omega\bar{\mathbf{P}}_1^{\star}(\xi) + \omega^2\bar{\mathbf{P}}_2^{\star}(\xi) + \ldots \qquad (107)$$

Thus, the product integral in Equation (99) can be expressed as

$$\mathcal{M}_{\xi}^{\xi'}\left\{-j\omega\bar{\mathbf{P}}^{\star}\right\}$$

$$= \mathcal{M}_{\xi}^{\xi'} \left\{ -j\omega \left(\bar{\mathbf{P}}_0^{\star} + \omega \bar{\mathbf{P}}_1^{\star}(\xi) + \omega^2 \bar{\mathbf{P}}_2^{\star}(\xi) + \ldots \right) \right\} \tag{108}$$

$$= \mathcal{M}_{\xi}^{\xi'} \left\{ -j\omega \bar{\mathbf{P}}_0^{\star} \right\} \mathcal{M}_{\xi}^{\xi'} \left\{ \bar{\mathrm{S}} \right\}, \tag{109}$$

with

$$\bar{\mathbf{S}}(\zeta) = -j\omega \mathcal{M}_{\xi}^{\zeta} \left\{ -j\omega \bar{\mathbf{P}}_0^{\star} \right\}^{-1}$$

$$\left(\omega \bar{\mathbf{P}}_1^{\star}(\zeta) + \omega^2 \bar{\mathbf{P}}_2^{\star}(\zeta) + \ldots \right) \mathcal{M}_{\xi}^{\zeta} \left\{ -j\omega \bar{\mathbf{P}}_0^{\star} \right\} \tag{110}$$

Then, for a TEM mode, $\mathcal{M}_{\xi}^{\xi'} \{ \bar{\mathbf{S}} \}$ becomes a unity matrix, and deviates only slowly from this result if we get higher-order modes. Thus, as a first approximation, we can just omit the second factor in Equation (109).

With these results, we can now calculate the second approximation for $\bar{\mathbf{I}}$, $\bar{\mathbf{I}}^{(1)}$. This does not correspond to the second term in the series expansion: it is $\bar{\mathbf{I}}$ after one iteration.

$$\bar{\mathbf{I}}^{(1)} = \int_{\xi_0}^{\xi_l} \bar{\mathbf{K}}(\xi, \xi') \mathcal{M}_{\xi}^{\xi'} \left\{ -j\omega \bar{\mathbf{P}}_0^{\star} \right\} d\xi' . \tag{111}$$

The outcome of the last equation can then be used to calculate the parameters, which can then be used to solve the telegrapher equations. For all examples calculated so far, the solutions of the extended telegrapher equations using the first iteration parameters were more or less identical to either measurements or comparative MoM calculations. This also included conductor arrangements that were more like antennas than transmission lines. More is shown in Section 5.

3.3.2 Source Terms

We will now focus on the determination of the source terms, ψ_s' and $\mathbf{i}_s'$. In contrast to the classical transmission-line theory, in the general case these terms cannot be calculated directly from the incident fields, but are given by the solution of an integral equation. This equation can also be solved iteratively. For practical examples, one iteration was usually enough to get very accurate results.

In order to determine the sources, we must evaluate Equation (91), which requires knowledge of $\mathbf{I}_{10}$ and $\mathbf{I}_{20}$. These variables can be calculated with the aid of Equation (88).

Equivalently to the determination of $\mathbf{f}_1$ and $\mathbf{f}_2$, we can also find an expression for the vector $\mathbf{f}_0$ and its derivative by comparing Equation (85) with Equation (95). The result becomes

$$\begin{bmatrix} \frac{\partial}{\partial \xi'} \mathbf{f}_0(\xi, \xi') \\ \mathbf{f}_0(\xi, \xi') \end{bmatrix} = \begin{bmatrix} \mathbf{i}_s'(\xi') \\ \mathbf{0} \end{bmatrix} - \mathcal{M}_{\xi}^{\xi'} \left\{ -j\omega \bar{\mathbf{P}}^{\star} \right\} \begin{bmatrix} \mathbf{i}_s'(\xi) \\ \mathbf{0} \end{bmatrix}$$

$$+ \int_{\xi}^{\xi'} \mathcal{M}_{\zeta}^{\xi'} \left\{ -j\omega \bar{\mathbf{P}}^{\star} \right\} \left\{ -j\omega \bar{\mathbf{Q}}(\zeta) \right\} \begin{bmatrix} \psi_s'(\zeta) \\ \mathbf{i}_s'(\zeta) \end{bmatrix} d\zeta \tag{112}$$

With this and with Equation (88) inserted into Equation (91), we get an implicit formula for the determination of ψ_s' and $\mathbf{i}_s'$.

$$\begin{bmatrix} \psi'_s \\ \mathbf{i}'_s \end{bmatrix} = \begin{bmatrix} \mathbf{1} & j\omega \mathbf{I}_{11} \\ \mathbf{0} & \mathbf{I}_{21} \end{bmatrix}^{-1} \left\{ \begin{bmatrix} \mathbf{v}_{\text{inc}} \\ \mathbf{0} \end{bmatrix} \right.$$

$$\left. - \begin{bmatrix} j\omega \mathbf{1} & \mathbf{0} \\ \mathbf{0} & \mathbf{1} \end{bmatrix} \int_{\xi_0}^{\xi_l} \bar{\mathbf{K}}(\xi, \xi') \begin{bmatrix} \frac{\partial}{\partial \xi'} \mathbf{f}_0(\xi, \xi') \\ \mathbf{f}_0(\xi, \xi') \end{bmatrix} d\xi' \right\} \tag{113}$$

An iterative procedure is suggested to solve for the unknowns. First, calculate Equation (112) with some starting values for ψ_s' and $\mathbf{i}_s'$, e.g., $\psi_s'^{(0)}$ and $\mathbf{i}_s'^{(0)}$. These results can then be used to calculate new values for ψ_s' and $\mathbf{i}_s'$ using Equation (113), e.g., $\psi_s'^{(1)}$ and $\mathbf{i}_s'^{(1)}$, which then can be used again to evaluate Equation (112). This can be repeated until some convergence is achieved. As starting values, we might use vanishing sources, i.e., $\psi_s'^{(0)} = 0$, $\mathbf{i}_s'^{(0)} = 0$. Then, after one iteration, we find

$$\psi_s'^{(1)} = \mathbf{v}_{\text{inc}} , \tag{114}$$

$$\mathbf{i}_s'^{(1)} = \mathbf{0} . \tag{115}$$

It is interesting to note that this is the value what we would use in the classical transmission-line-theory approach. If we use these first-iteration values in the transmission-line super theory in real examples, results comparable to the MoM solution can be obtained (see the examples in Section 5).

3.4 Discussion of the Extended Theory, Line Parameters, and Source Terms

The transmission-line super theory is a method where Maxwell's equations (with some minor simplifications and assumptions), applied to a nonuniform transmission line, are transformed to *generalized telegrapher equations*. These generalized telegrapher equations describe the behavior of the current and the average scalar potential along the nonuniform transmission line. In contrast to the classical transmission-line theory, not only the (quasi) TEM mode, but all field modes, are taken into account, and thus the intrinsic physical behavior is reflected. Even the radiation is properly modeled. The mathematical structure of the generalized telegrapher equations is the same as the structure of the classical telegrapher equations for nonuniform transmission lines. Thus, the procedures to solve those equations can be adopted.

It is necessary to switch from the voltage to the average potential because, in the general case, the voltage does depend on the integration path, and therefore looses its character as a local quantity. The scalar potential, however, is given in a unique way at every point. Although it has no physical meaning, it is a good replacement for the voltage, because if we have sections on the transmission line that only support the TEM mode, the potential becomes the voltage (in the Lorenz gauge).

The line parameters as well as the source terms differ from the quantities in the classical theory. The parameters usually become complex valued and frequency dependent, even for a lossless line. The reasons for this are the different modes that may appear at different frequencies, thus changing the parameters. The imaginary parts of the parameters can be interpreted as parts of the radiation resistance. For instance, for the parameter that corresponds to the per-unit-length inductance, one gets

$$j\omega P_{12} = j\omega\Re\{P_{12}\} + j\, j\omega\Im\{P_{12}\} \qquad (116)$$

$$= j\omega\Re\{P_{12}\} \underbrace{-\omega\Im\{P_{12}\}}_{\text{acts like a resistor}} \cdot \qquad (117)$$

The source terms cannot be determined directly from the incident fields; rather, these terms also contain properties of the transmission lines. This is obvious because when the line is nonuniform, the coupling at one point of the line is usually influenced by other parts of that line.

The parameters account only for one part of the radiation, namely, that part that is due to the non-uniformity of the transmission lines. The other contribution that is due to the field scattering is included in the sources. This can be seen on the first two examples in Section 5. The first example is a uniform transmission line, which only radiates if it is illuminated with an electric field that has components in the direction of the wire. The generalized parameters in this case are frequency independent and real, and thus do not indicate any radiation. The source terms, however, lead to a current distribution on the wire that clearly implies radiation (see also [50]). On the other hand, the parameters of a semi-infinite line with a vertical termination become frequency dependent and complex. Thus, they support radiation. This happens even if the line is excited by a local source at infinity, where no scattering appears.

4. Solution of the Telegrapher Equations and Transmission-Line Networks

This section focuses on the solution of the (extended) telegrapher equations, as well as the application of this solution to computing the response of networks of multiple multiconductor transmission lines and cables. The first part gives a short review of solution methods for the telegrapher equations with non-constant parameters. The general solution is first demonstrated, then various numerical techniques are shown. The results are then used to calculate admittance or scattering matrices that can be incorporated into a higher-level network formulation.

4.1 Solution of the Telegrapher Equations

With the techniques described in Sections 2 and 3, one can compute the per-unit-length parameters for arbitrary nonuniform transmission lines. The voltage-current formulation is often used, but there are other representations of the transmission-line equations. For instance, a description with "waves" is very popular, where the voltage and current are combined into a new wave quantity. All the different representations can be converted into each other by similarity transformations of the telegrapher equations and when written in matrix form, lead to a non-homogeneous first-order differential matrix-vector equation with non-constant parameters.

4.1.1 General Solution of the Telegrapher Equations

The transmission-line equations in the general case can be written as

$$\frac{\partial \bar{\mathbf{X}}(\xi)}{\partial \xi} = \bar{\mathbf{P}}^X(\xi)\bar{\mathbf{X}}(\xi) + \bar{\mathbf{X}}^{(s)}(\xi) \cdot \qquad (118)$$

The super-matrix function $\bar{\mathbf{P}}^X(\xi)$ contains the per-unit-length parameters, while $\bar{\mathbf{X}}$ represents the propagating quantities, which, of course, depend on the particular representation used. For instance, for the voltage-current formulation, $\bar{\mathbf{X}}$ becomes

$$\bar{\mathbf{X}} = \begin{bmatrix} \mathbf{v} \\ \mathbf{i} \end{bmatrix}, \qquad (119)$$

and the parameter matrix is given by

$$\bar{\mathbf{P}}^X(\xi) = \bar{\mathbf{P}}^{vi}(\xi) = -j\omega \begin{bmatrix} 0 & \mathbf{L}' + \dfrac{\mathbf{R}'}{j\omega} \\ \mathbf{C}' + \dfrac{\mathbf{G}'}{j\omega} & 0 \end{bmatrix} \cdot \qquad (120)$$

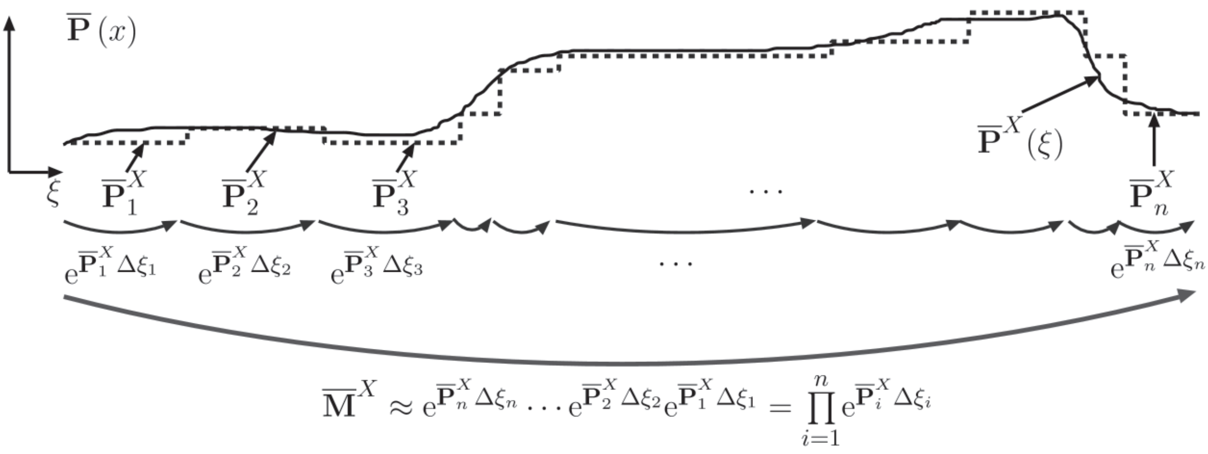

Figure 12. The piecewise-constant approximation of the parameters of a transmission line.

If the TLST is under investigation, of course, the voltage, $\mathbf{v}$, must be replaced by the average potential, ψ. Also, the corresponding parameter matrix must be used. However, the general structure of the equation remains the same.

The general analytic solution of Equation (118) is then given by

$$\bar{\mathbf{X}}(\xi) = \mathcal{M}_{\xi_0}^{\xi}\left\{\bar{\mathbf{P}}^X\right\}\bar{\mathbf{X}}(\xi_0) + \int_{\xi_0}^{\xi}\mathcal{M}_{\eta}^{\xi}\left\{\bar{\mathbf{P}}^X\right\}\bar{\mathbf{X}}'^{(s)}(\eta)\,d\eta \qquad (121)$$

with the product integral or matrizant [48, 51]

$$\mathcal{M}_{\xi_0}^{\xi}\left\{\bar{\mathbf{P}}^X\right\} := \bar{\mathbf{1}} + \int_{\xi_0}^{\xi}\bar{\mathbf{P}}^X(\eta)\,d\eta$$

$$+ \int_{\xi_0}^{\xi}\bar{\mathbf{P}}^X(\eta)\int_{\xi_0}^{\eta}\bar{\mathbf{P}}^X(\tau)\,d\tau\,d\eta + \cdots \qquad (122)$$

$$= \prod_{\xi_0}^{\xi} e^{\bar{\mathbf{P}}^X(\eta)\,d\eta}. \qquad (123)$$

Equation (122) is called *Picard's* iteration, and is obtained by integrating Equation (118) and thereby transforming it into an integral equation. One then gets the final expression by successive substitution of the solution $\bar{\mathbf{X}}(\xi)$. This matrix series possesses properties very similar to those of the matrix exponential.

We write shortly for the end response of the whole transmission line of length $L = \xi_l - \xi_0$

$$\bar{\mathbf{X}}(L) = \bar{\mathbf{M}}^X\bar{\mathbf{X}}(0) + \bar{\mathbf{X}}^{(s)}(L) \qquad (124)$$

with

$$\bar{\mathbf{M}}^X := \mathcal{M}_0^L\left\{\bar{\mathbf{P}}^X\right\} \qquad (125)$$

and

$$\bar{\mathbf{X}}^{(s)}(L) := \int_0^L \mathcal{M}_{\eta}^{L}\left\{\bar{\mathbf{P}}^X\right\}\bar{\mathbf{X}}'^{(s)}(\eta)\,d\eta\,. \qquad (126)$$

Here, we have performed a coordinate transformation from $[\xi_0, \xi_l]$ to $[0, L]$. The super-matrix $\bar{\mathbf{M}}^X$ is called the propagator. It describes the propagation of the quantities $\bar{\mathbf{X}}$ from the beginning to the end of the line.

4.1.2 Solution Techniques

Even if the general solution is given by Equation (121), its numerical computation is a non-trivial task. Various numerical and (semi-) analytical methods are available to calculate the solution numerically, e.g.,

- iteration methods, like Picard's iteration
- methods based on general matrix calculus, e.g., piecewise-constant approximation
- methods based on diagonalization or *Jordan* decomposition
- numerical integration techniques, like the *Runge-Kutta* method.

Since Picard's iteration is not well suited for a numerical computation of the matrizant, the piecewise-constant approximation is often used. This approximation is motivated by the infinitesimal calculus of *Volterra*, which reads

$$\mathcal{M}_{\xi_0}^{\xi}\left\{\bar{\mathbf{P}}^X\right\} = \lim_{\Delta\xi_k \to 0}\prod_{k=1}^{n} e^{\bar{\mathbf{P}}_k^X \Delta\xi_k}. \qquad (127)$$

Integration Method	Matrizant Formula for a Segment
explicit Euler	$\bar{\mathbf{E}}+\bar{\mathbf{P}}^X(\xi_0)\Delta\xi$
implicit Euler	$\left\{\bar{\mathbf{E}}-\bar{\mathbf{P}}^X(\xi_0+\Delta\xi)\Delta\xi\right\}^{-1}$
trapezoid rule	$\left\{\bar{\mathbf{E}}-\frac{\Delta\xi}{2}\bar{\mathbf{P}}^X(\xi_0+\Delta\xi)\right\}^{-1}\left\{\bar{\mathbf{E}}+\frac{\Delta\xi}{2}\bar{\mathbf{P}}^X(\xi_0)\right\}$
Runge-Kutta 4th order	$\bar{\mathbf{E}}+\bar{\mathbf{P}}^{X(1)}\Delta\xi+\bar{\mathbf{P}}^{X(2)}\frac{\Delta\xi^2}{2}+\cdots$ $\cdots+\bar{\mathbf{P}}^{X(3)}\frac{\Delta\xi^3}{6}+\bar{\mathbf{P}}^{X(4)}\frac{\Delta\xi^4}{24}$

Table 1: Formulae to calculate the matrizant

$$\bar{\mathbf{P}}^{X(1)}=\frac{1}{6}\left\{\bar{\mathbf{P}}^X(\xi_0+\Delta\xi)+4\bar{\mathbf{P}}^X(\xi_0+\Delta\xi/2)+\bar{\mathbf{P}}^X(\xi_0)\right\}$$

$$\bar{\mathbf{P}}^{X(2)}=\frac{1}{3}\left\{\bar{\mathbf{P}}^X(\xi_0+\Delta\xi)\bar{\mathbf{P}}^X(\xi_0+\Delta\xi/2)+\bar{\mathbf{P}}^{X^2}(\xi_0+\Delta\xi/2)+\bar{\mathbf{P}}^X(\xi_0+\Delta\xi/2)\bar{\mathbf{P}}^X(\xi_0)\right\}$$

$$\bar{\mathbf{P}}^{X(3)}=\frac{1}{2}\left\{\bar{\mathbf{P}}^X(\xi_0+\Delta\xi)\bar{\mathbf{P}}^{X^2}(\xi_0+\Delta\xi/2)+\bar{\mathbf{P}}^{X^2}(\xi_0+\Delta\xi/2)\bar{\mathbf{P}}^X(\xi_0)\right\}$$

$$\bar{\mathbf{P}}^{X(4)}=\bar{\mathbf{P}}^X(\xi_0+\Delta\xi)\bar{\mathbf{P}}^{X^2}(\xi_0+\Delta\xi/2)\bar{\mathbf{P}}^X(\xi_0)$$

For a numerical computation, the interval $[\xi_0,\xi]$ is divided into a finite number of segments. The interval does not have to be divided into equidistant segments, but rather the grid should match the slope of the matrix function in some norm sense. Within each segment, the matrix function $\bar{\mathbf{P}}^X(\xi)$ is assumed to be constant, and then the matrizant of each such segment is given explicitly by the matrix exponential

$$\mathcal{M}_{\xi}^{\xi+\Delta\xi_i}\left\{\bar{\mathbf{P}}^X\right\}=e^{\bar{\mathbf{P}}_i^X\Delta\xi_i}\,. \qquad (128)$$

The overall matrizant in the interval $[\xi_0,\xi]$ is the sorted product of the matrizants of the individual segments (see Figure 12). The approximation of the exact matrizant becomes better with an increasing number of segments.

A disadvantage of the piecewise-constant approximation is the artificial concentration of the otherwise continuous reflections at the segment boundaries, due to the step discontinuities. This can be avoided by using an interpolation technique, as described in [52], or by the application of higher-order numerical integration schemes, like the Runge-Kutta method.

Numerical-integration formulae can be obtained by applying the integration algorithm to the matrix equation. Table 1 shows the expressions for the computation of the matrizant $\mathcal{M}_{\xi_0}^{\xi_0+\Delta\xi}\left\{\bar{\mathbf{P}}^X\right\}$ for different, often-used methods.

4.2 Networks of Nonuniform and Uniform Transmission Lines

Today's complex systems usually consist of a variety of components and subsystems, which are connected by transmission lines and cables. To model such systems effectively, it is essential to incorporate the TL(S)T into some kind of network description.

4.2.1 Nodal Analysis

One possible way to do this is to apply nodal analysis to the transmission-line network. For that, we have to transform the matrizant solution of the transmission line into an equivalent admittance matrix, $\bar{\mathbf{Y}}_{eq}$,

$$\bar{\mathbf{Y}}_{eq}=\begin{bmatrix}\mathbf{M}_{12}^{vi\,-1}\mathbf{M}_{11}^{vi} & -\mathbf{M}_{12}^{vi\,-1}\\ \mathbf{M}_{21}^{vi}-\mathbf{M}_{22}^{vi}\mathbf{M}_{12}^{vi\,-1}\mathbf{M}_{11}^{vi} & \mathbf{M}_{22}^{vi}\mathbf{M}_{12}^{vi\,-1}\end{bmatrix} \qquad (129)$$

and the source terms into equivalent current sources, $\bar{\mathbf{i}}_{eq}^{(s)}$,

$$\bar{\mathbf{i}}_{eq}^{(s)}=\begin{bmatrix}\mathbf{M}_{12}^{vi\,-1}\mathbf{v}^{(s)}(L)\\ \mathbf{i}^{(s)}(L)-\mathbf{M}_{22}^{vi}\mathbf{M}_{12}^{vi\,-1}\mathbf{v}^{(s)}(L)\end{bmatrix}. \qquad (130)$$

The matrices $\mathbf{M}_{ik}^{vi}$ are $n\times n$ block matrices of the $2n\times 2n$ propagator super-matrix $\bar{\mathbf{M}}^{vi}$, which corresponds to the telegrapher equations in voltage-current representation. Figure 13 shows the equivalent multi-port of a single transmission line. The circuit of the full network can be built with the aid of these equivalent multi-ports. This circuit describes how the lines are connected and terminated, and is solved using conventional nodal analysis or modified nodal analysis, which lead to a sparse admittance matrix of the network. The unknown voltages can be determined by inversion of this admittance matrix.

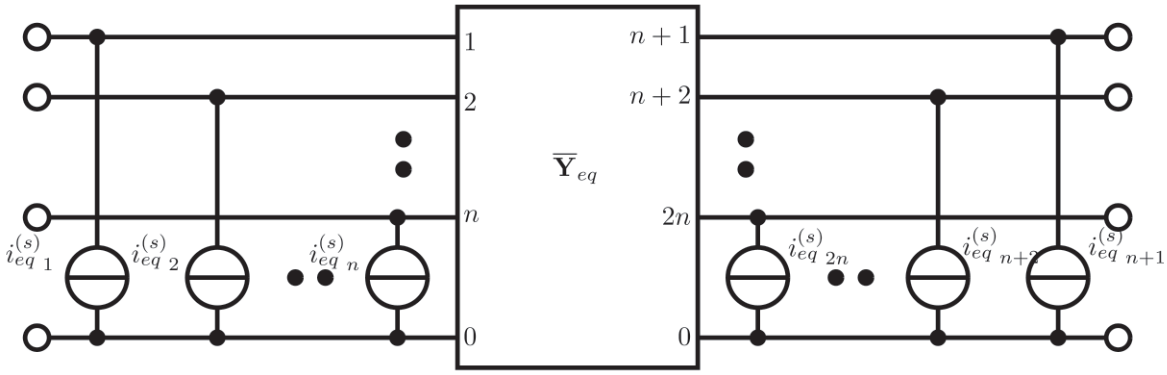

Figure 13. A multi-port representation of a transmission line.

4.2.2 BLT Equation

Another possibility is to apply the BLT equation, which arises from EM topology [53, 54]. Like all network formulations, this theory relies on the decomposition of a complex system into smaller subsystems. These subsystems are described in terms of scattering junctions. Each junction is connected with other junctions by so-called tubes. A tube describes the propagation along a particular path (cable, transmission line). Junctions can represent elementary devices, like simple circuits, but can also represent complex subsystems. A junction is characterized by its scattering matrix, $\underline{\mathbf{S}}$, while a tube is described by the propagation matrix, $\overline{\mathbf{\Gamma}}$. The scattering matrix relates incoming and outgoing waves:

$$\mathbf{b} = \mathbf{S}\,\mathbf{a} \tag{131}$$

A tube, which connects two junctions, supports the propagation of waves between the beginning and the far end of the tube. Assuming a propagation direction as sketched in Figure 14, we obtain the propagation equation of a tube as

$$\overline{\mathbf{w}}(L) = \overline{\mathbf{\Gamma}}\,\overline{\mathbf{w}}(0) + \overline{\mathbf{w}}^{(s)}(L) \tag{132}$$

Collecting all individual propagation equations into a super-matrix equation, we get the propagation equation of the topological network:

$$\overline{\overline{w}}(L) = \overline{\overline{\mathbf{\Gamma}}}\,\overline{\overline{w}}(0) + \overline{\overline{w}}^{(s)}(L) \tag{133}$$

The same procedure is applied to the scattering matrices, but the resulting super-matrix has to be rearranged. This rearrangement has to ensure the equalities

$$b_{i,j} = w_{k,n}(0) \tag{134a}$$

and

$$a_{i,j} = w_{k,n}(L), \tag{134b}$$

i.e., the port j at junction i is connected with port n at tube k. The scattering equation of the topological network then reads

$$\overline{\overline{w}}(0) = \overline{\overline{S}}\,\overline{\overline{w}}(L) \tag{135}$$

Eventually, by combining Equations (133) and (135), we get the BLT equation:

$$\left[\overline{\overline{\mathbf{1}}} - \overline{\overline{S}}\,\overline{\overline{\mathbf{\Gamma}}}\right]\overline{\overline{w}}(0) = \overline{\overline{S}}\,\overline{\overline{w}}^{(s)}(L)\cdot \tag{136}$$

The unknown wave super-vector, $\overline{\overline{w}}(0)$, can be calculated by inversion of the system matrix $\left[\overline{\overline{\mathbf{1}}} - \overline{\overline{S}}\,\overline{\overline{\mathbf{\Gamma}}}\right]$.

To use EM topology for the computation of a transmission-line network, we have to represent all transmission lines by tubes and all terminations and connections of lines by junctions. As mentioned before, the

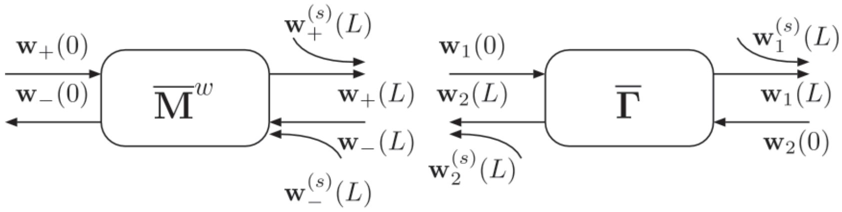

Figure 14. The relation between the propagator and the propagation matrix.

unknown quantities in the topological network are waves, so the solution of the transmission-line equations must be transformed into a wave representation, and afterwards into a propagation matrix.

We have to perform the following operation to do that for the matrizant in the voltage-current representation:

$$\overline{\mathbf{M}}^{w} = \begin{bmatrix} \mathbf{1} & \mathbf{Z}_c(L) \\ \mathbf{1} & -\mathbf{Z}_c(L) \end{bmatrix} \overline{\mathbf{M}}^{vi} \begin{bmatrix} \mathbf{1} & \mathbf{Z}_c(0) \\ \mathbf{1} & -\mathbf{Z}_c(0) \end{bmatrix}^{-1}. \quad (137)$$

Now, the transmission line is described by forward $(+)$ and backward $(-)$ running waves:

$$\begin{bmatrix} \mathbf{w}_+(L) \\ \mathbf{w}_-(L) \end{bmatrix} = \begin{bmatrix} \mathbf{M}_{11}^{w} & \mathbf{M}_{12}^{w} \\ \mathbf{M}_{21}^{w} & \mathbf{M}_{22}^{w} \end{bmatrix} \begin{bmatrix} \mathbf{w}_+(0) \\ \mathbf{w}_-(0) \end{bmatrix} + \begin{bmatrix} \mathbf{w}_+^{(s)}(L) \\ \mathbf{w}_-^{(s)}(L) \end{bmatrix}. \quad (138)$$

The propagation matrix of the corresponding tube is then computed by equating Equation (132) with Equation (138):

$$\overline{\mathbf{\Gamma}} = \begin{bmatrix} \mathbf{M}_{11}^{w} - \mathbf{M}_{12}^{w}\mathbf{M}_{22}^{w\,-1}\mathbf{M}_{21}^{w} & \mathbf{M}_{12}^{w}\mathbf{M}_{22}^{w\,-1} \\ -\mathbf{M}_{22}^{w\,-1}\mathbf{M}_{21}^{w} & \mathbf{M}_{22}^{w\,-1} \end{bmatrix}, \quad (139)$$

and the source terms are given by

$$\begin{bmatrix} \mathbf{w}_1^{(s)}(L) \\ \mathbf{w}_2^{(s)}(L) \end{bmatrix} = \begin{bmatrix} \mathbf{w}_+^{(s)}(L) - \mathbf{M}_{12}^{w}\mathbf{M}_{22}^{w\,-1}\mathbf{w}_-^{(s)}(L) \\ -\mathbf{M}_{22}^{w\,-1}\mathbf{w}_-^{(s)}(L) \end{bmatrix}. \quad (140)$$

The following steps have to be performed to solve an EM coupling problem in a complex system:

- Decomposition of the network into tubes and junctions,
- Calculation of the TLST-parameters,
- Computation of the product integral (matrizant), transformation to the propagation matrix and determination of the source terms for each tube, and
- Solution of the whole network using the BLT equation.

5. Application Examples

5.1 Exact Telegrapher Equations for a Uniform Infinitely Long Line with Field Coupling

The classical transmission-line theory exactly describes the propagation of a TEM-mode wave along an infinitely long, ideally conducting, uniform transmission line for *all* frequencies. The extensions [55] for the coupling of an external field are only "low" frequency approximations with the exception of an incoming wave with grazing incidence [56]. However, there exists an exact solution for this kind of problem [50]. We will now use the transmission-line super theory to find the extended telegrapher equations for a uniform transmission line with field coupling. The results will be compared with the known exact solution.

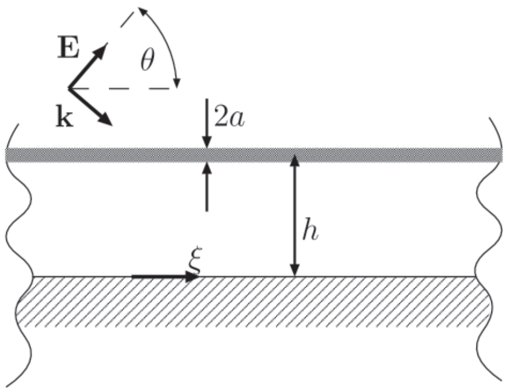

Figure 15. The setup of the uniform infinitely long transmission line.

Figure 15 illustrates the setup of our transmission line. The conductor, which is considered to be a thin wire of radius *a*, is located at a height *h* over the ideal ground plane. With the aid of the image theory, we can easily find the Green's function for the problem:

$$G(\mathbf{x},\mathbf{x}') = g(\xi,\xi')$$

$$= \frac{1}{4\pi}\left[\frac{e^{-jk\sqrt{(\xi-\xi')^2+a^2}}}{\sqrt{(\xi-\xi')^2+a^2}} - \frac{e^{-jk\sqrt{(\xi-\xi')^2+4h^2}}}{\sqrt{(\xi-\xi')^2+4h^2}}\right]. \quad (141)$$

The integral kernels, which in this case are 1×1 matrices, i.e., scalars, become

$$k_l(\xi,\xi') = \mu g(\xi,\xi'), \quad (142)$$

$$k_c(\xi,\xi') = \frac{1}{\varepsilon} g(\xi,\xi'). \quad (143)$$

With that, we can immediately find solutions for the zeroth-order parameters:

$$\overline{\mathbf{P}}^{(0)} = \begin{bmatrix} 0 & l^{(0)} \\ c^{(0)} & 0 \end{bmatrix}, \quad (144)$$

with

$$l^{(0)} = \mu\int_{-\infty}^{\infty} g(\xi,\xi')\,d\xi'\bigg|_{\omega\to0} = \frac{\mu}{2\pi}\ln\frac{2h}{a} \quad (145)$$

and

$$c^{(0)} = \varepsilon\left[\int_{-\infty}^{\infty} g(\xi,\xi')\,d\xi'\bigg|_{\omega\to 0}\right]^{-1} = \frac{2\pi\varepsilon}{\ln\frac{2h}{a}}. \quad (146)$$

These two parameters ($l^{(0)}$ and $c^{(0)}$) coincide with the per-unit-length parameters of the classical transmission-line theory. The matrix $-j\omega\bar{\mathbf{P}}_0^{\star}$ then becomes

$$-j\omega\bar{\mathbf{P}}_0^{\star} = \begin{bmatrix} 0 & -k^2 \\ 1 & 0 \end{bmatrix}, \quad (147)$$

where $k = \omega/v_0$ is the wavenumber, and $v_0 = 1/\sqrt{l^{(0)}c^{(0)}}$ is the speed of light. Then, the product integral for this expression turns out to be

$$\mathcal{M}_{\xi}^{\xi'}\left\{-j\omega\bar{\mathbf{P}}^{\star}\right\} = \begin{bmatrix} \cos k(\xi'-\xi) & -k\sin k(\xi'-\xi) \\ \frac{1}{k}\sin k(\xi'-\xi) & \cos k(\xi'-\xi) \end{bmatrix}. \quad (148)$$

We can solve Equation (111) to get $\bar{\mathbf{I}}^{(1)}$, which then can be used to calculate the new parameters using Equation (90), which become

$$\bar{\mathbf{P}}^{(1)} = \begin{bmatrix} 0 & l^{(1)} \\ c^{(1)} & 0 \end{bmatrix}, \quad (149)$$

where

$$l^{(1)} = \frac{\mu}{2\pi}\ln\frac{2h}{a}, \quad (150)$$

$$c^{(1)} = \frac{2\pi\varepsilon}{\ln\frac{2h}{a}}. \quad (151)$$

These are the same parameters as the starting values for the iteration. For every new iteration we will get the same set of frequency-independent parameters. This means we already started our iteration with the correct parameters, which are not only valid for low frequencies, but for *all* frequencies, and coincide with the per-unit-length parameters of the classical transmission-line theory.

This cannot be said for the sources. As we will see, the classical TLT solution is only a low-frequency approximation. The electric-field strength along the wire for an incident plane-wave field as in Figure 15 is given by

$$v_{\text{inc}}(\xi) = E_0 e^{-jk\xi\cos\theta}, \quad (152)$$

where E_0 is the amplitude that also takes into account the reflections from the ground plane. We have to calculate f_0 in order to compute the source terms. Normally, an iterative procedure is used to determine the sources. However, a closed-from solution can be given for this special case. The dependence of the electric field on the spatial coordinate ξ implies the same dependence of the source terms. Thus, these terms can be expressed as

$$\psi_s(\xi) = E_s e^{-jk\xi\cos\theta}, \quad (153)$$

$$i_s(\xi) = H_s e^{-jk\xi\cos\theta}. \quad (154)$$

The quantities E_s and H_s can be computed by applying the procedure described in Section 3.3.2. After some lengthy mathematics, one obtains

$$E_s = v_{\text{inc}}\frac{F_1 - F_2\cos^2\theta}{F_1\sin^2\theta}, \quad (155)$$

$$H_s = -v_{\text{inc}}\frac{4\pi(F_1 - F_2)\cos\theta}{\sqrt{\frac{\mu}{\varepsilon}}F_1F_2\sin^2\theta}, \quad (156)$$

where

$$F_1 = 4\pi\int_{-\infty}^{\infty} g(\xi,\xi')\cos\left[k(\xi'-\xi)\right]d\xi' \quad (157)$$

$$= 2\ln\frac{2h}{a}, \quad (158)$$

$$F_2 = 4\pi\int_{-\infty}^{\infty} g(\xi,\xi')\cos\left[k(\xi'-\xi)\cos\theta\right]d\xi' \quad (159)$$

$$= -j\pi\left[H_0^{(2)}(ak\sin\theta) - H_0^{(2)}(2hk\sin\theta)\right] \quad (160)$$

Then, the *exact extended telegrapher equations* for a uniform, infinitely long, and perfectly conducting transmission line, with plane-wave-field excitation, are

$$\frac{\partial\psi}{\partial\xi} = -j\omega l\,i + v_{\text{inc}}\frac{F_1 - F_2\cos^2\theta}{F_1\sin^2\theta}, \quad (161)$$

$$\frac{\partial i}{\partial\xi} = -j\omega c\,\psi - v_{\text{inc}}\frac{4\pi(F_1 - F_2)\cos\theta}{\sqrt{\frac{\mu}{\varepsilon}}F_1F_2\sin^2\theta}. \quad (162)$$

These equations are identical with the results obtained in [50] with the aid of a spatial Fourier transformation.

5.2 Semi-Infinite Transmission Line with Vertical Termination

The next configuration is a semi-infinite wire, supplemented with a vertical element as the termination. Thus, the transmission line is shorted to the ground plane. Figure 16 shows the considered wire setup. The integral kernels for this configuration become

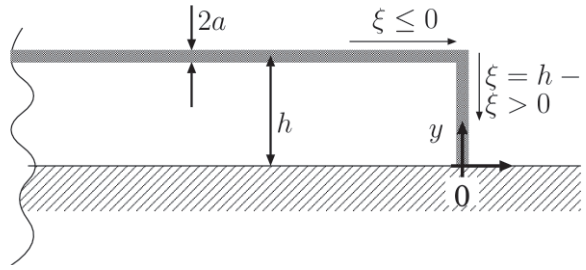

Figure 16. The setup of the semi-infinite line with a vertical termination.

$$k_l = \begin{cases} \frac{\mu}{4\pi}\left(\frac{e^{-jkR_1}}{R_1} - \frac{e^{-jkR_2}}{R_2}\right) & \xi' \le 0, \xi \le 0 \\ \frac{\mu}{4\pi}\left(\frac{e^{-jkR_1}}{R_1} + \frac{e^{-jkR_2}}{R_2}\right) & \xi' > 0, \xi > 0 \\ 0 & \text{otherwise} \end{cases}, \quad (163)$$

$$k_c = \frac{1}{4\pi\varepsilon}\left(\frac{e^{-jkR_1}}{R_1} - \frac{e^{-jkR_2}}{R_2}\right), \quad (164)$$

with

$$R_1(\xi,\xi') = \begin{cases} \sqrt{(\xi'-\xi)^2 + a^2} & \xi'\xi \ge 0 \\ \sqrt{\xi^2 + \xi'^2} & \text{otherwise} \end{cases}, \quad (165)$$

$$R_2(\xi,\xi') = \begin{cases} \sqrt{(\xi'-\xi)^2 + 4h^2} & \xi' \le 0, \xi \le 0 \\ \sqrt{\xi^2 + (2h-\xi')^2} & \xi' > 0, \xi \le 0 \\ \sqrt{\xi'^2 + (2h-\xi)^2} & \xi' \le 0, \xi > 0 \\ \sqrt{(2h-\xi'-\xi)^2 + a^2} & \xi' > 0, \xi > 0 \end{cases}. \quad (166)$$

The zeroth-order parameters can be given explicitly. If $\xi \le 0$, one gets

$$l^{(0)} = \frac{\mu}{4\pi}\left[2\ln\frac{2h}{a} - \ln\frac{R_2(\xi,0)-\xi}{R_1(\xi,0)-\xi}\right], \quad (167)$$

$$c^{(0)} = 4\pi\varepsilon\left\{2\ln\frac{2h}{a} - \ln\frac{R_2(\xi,0)-\xi}{R_1(\xi,0)-\xi}\frac{[R_1(\xi,h)+h][R_2(\xi,a)+a-2h]}{[R_2(\xi,h)-h][R_1(\xi,a)+a]}\right\}^{-1} \quad (168)$$

and for $\xi > 0$, the parameters are

$$l^{(0)} = \frac{\mu}{4\pi}\left\{\ln\frac{[R_1(\xi,h)-h+\xi][R_2(\xi,h)-h-\xi]}{[R_1(\xi,a)+a-\xi][R_2(\xi,a)-2h+a+\xi]}\right\} \quad (169)$$

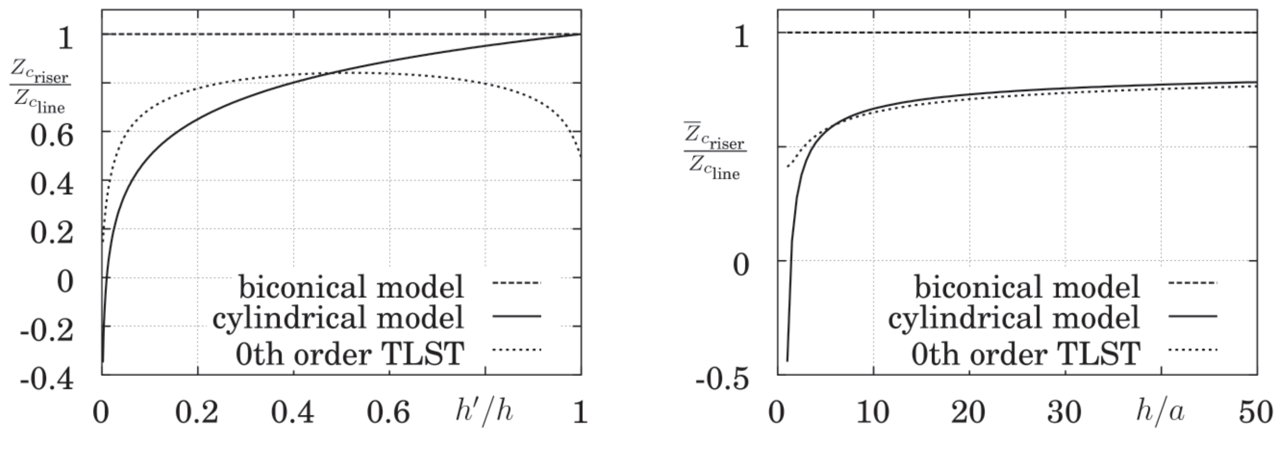

Figure 17. The ratio of the riser characteristic impedance to the characteristic impedance of the horizontal transmission line: (left) along one riser with $a = 1$ mm, $h = 50$ mm, $h' = 0 \ldots h$; (right) the ratio of the average impedances for different ratios of h/a.

$$c^{(0)} = 4\pi\varepsilon \left\{ \ln \frac{R_1(\xi,h)-h+\xi}{R_1(\xi,a)+a-\xi} \right.$$

$$\left. \frac{\left[R_2(\xi,a)-2h+a+\xi\right](2h-\xi)}{\left[R_2(\xi,h)-h-\xi\right]\xi} \right\}^{-1} \qquad (170)$$

We can compare these results with the models presented in Section 2.1. Figure 17 (left) shows the ratio of the riser characteristic impedance to the characteristic impedance of the transmission line as a function of the height, h'. The riser has a radius of $a = 1$ mm and a height of $h = 50$ mm. Of course, for the biconical case, the impedance is constant. The cylindrical approximation shows some non-physical behavior when getting close to the ground plane: the characteristic impedance becomes negative. The zeroth-order TLST parameters do not exhibit this behavior.

For low frequencies, one can represent the riser element as a short transmission line of corresponding length with an average characteristic impedance. Figure 17 (right) depicts these average impedances for the different models as a function of the ratio h/a. Surprisingly, the cylindrical model agrees quite well with the solution from the TLST, except for very short risers. The biconical model leads to significantly larger values. We have to keep in mind that this model is only valid for $\lambda \gg h$, and does not include higher-order modes or radiation.

In order to calculate solutions for higher frequencies, the zeroth-order parameters of the TLST are used to calculate the functions f_1 and f_2, which are then used to obtain the frequency-dependent parameters, as described in Section 3. Figure 18 shows the parameters $l^{(1)}$ and $c^{(1)}$ with their real and imaginary parts, which where calculated numerically.

The per-unit-length inductance on the semi-infinite wire decreases when getting closer to the termination. The per-unit-length capacitance stays almost constant. On the termination wire, both the capacitance and the inductance per unit length increase as one moves closer to the ground plane. The inductance per unit length approaches a fixed value, while the capacitance per unit length tends to infinity. However, the capacitance itself stays finite. There are imaginary parts that are especially large on the termination wire. This indicates that most of the radiation occurs there.

Some comparative computations where performed using the MoM to verify the results. Figure 19 shows the radiated energy from the transmission line, and one can see that both methods deliver the same results. The same is true for the magnitude of the reflection coefficient of the end, which is also presented in this figure. If these values were calculated with the methods presented in Section 2.1, the reflection coefficient would always be one, and there would not be any radiated energy.

5.3 Single Wire above a Ground Plane

In the next example, a single wire was placed over a perfectly conducting ground plane (see Figure 20). The wire was either driven by a voltage source, or illuminated by

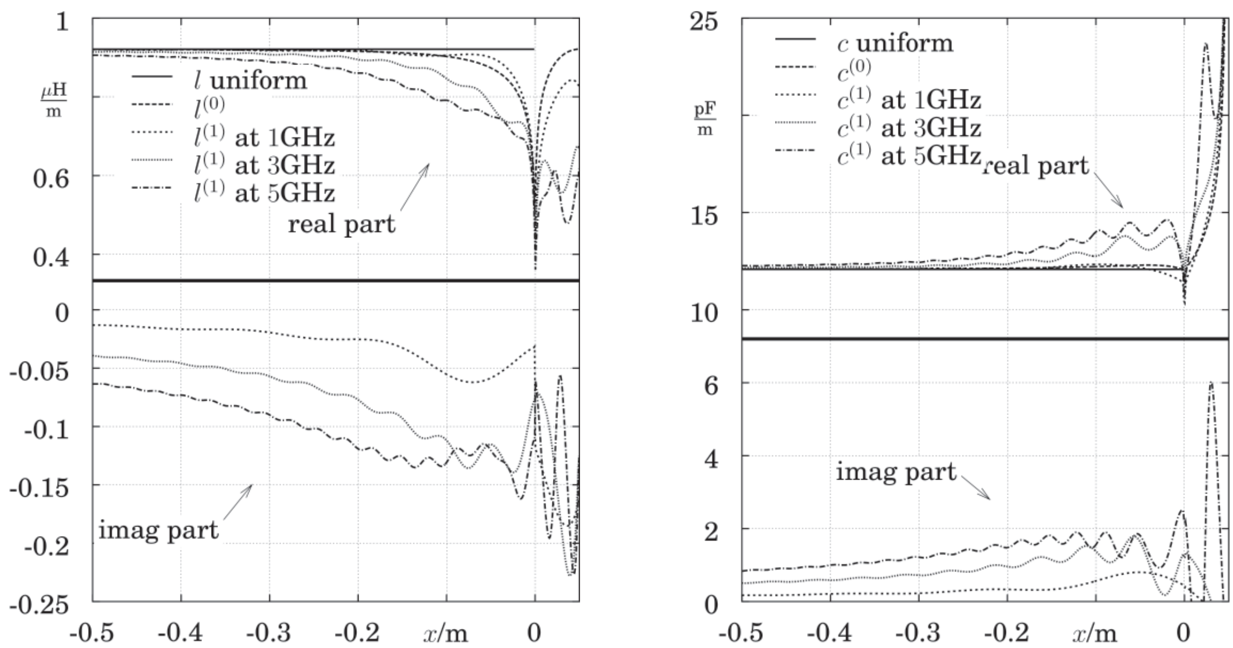

Figure 18. The parameters $l^{(1)}$ (left) and $c^{(1)}$ (right) along the semi-infinite line with a vertical termination for different frequencies ($a = 1$ mm, $h = 50$ mm).

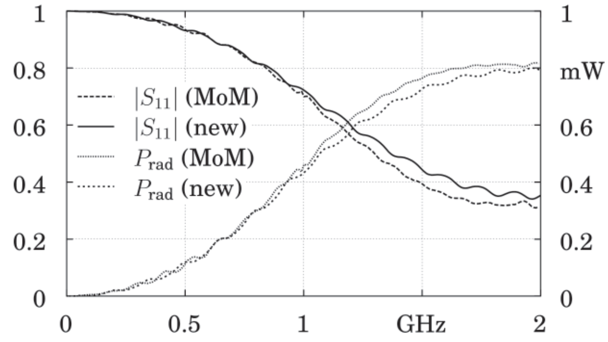

Figure 19. The magnitude of the reflection coefficient and radiated power of the semi-infinite transmission line with a vertical termination, when driven with a 1V source at infinity.

a plane-wave field, and was not terminated (open far end). The angle, α, between the wire and the ground plane was chosen such that classical transmission-line theory was no longer applicable. Since the wire is some kind of an antenna, it will radiate, and antenna theory or a full-wave method must be used to determine the current through the driving source and the current distribution along the wire. Nonetheless, using classical transmission-line theory and approximating the wire by piecewise-uniform line segments, yielded the result for the input current shown in Figure 21a. The measured data and the results computed using the transmission-line super theory, but with only the zeroth-order parameters (zeroth iteration), are also shown. As can be seen, there is a significant difference between the piecewise-uniform transmission line and the measurement, even for low frequencies.

The resonance frequencies of the transmission-line solution were shifted to higher frequencies, which means that the wire appeared electrically shorter than it actually was. Furthermore, the amplitudes at the resonance frequencies were much higher than in the experiment. This was due to the lack of radiation in the transmission-line solution. The solution with TLST (static parameters) showed some improvement of the results. For low frequencies, there was very good agreement of the resonance frequencies, which means that the electrical length of the wire was correctly taken into account. However, there was still a large deviation of the amplitudes in the resonance regions for higher frequencies, since radiation was not considered.

Figure 21b shows the results of the transmission-line super theory with the parameters after the first iteration. From a practical standpoint, there was no difference between the TLST results and the measured data. This is supported by the results shown in Figure 21c. Here, the current distributions determined with the MoM and TLST along the wire are plotted. The real and imaginary parts of the TLST were identical to those from the MoM.

The wire can also be excited by an external electromagnetic field, as shown in Figure 20. For this case, the voltage source at the input terminal is set to zero. Again, the current flowing into the ground plane was considered. Figure 21d shows the results for the TLST, the MoM, and the TLT (piecewise-uniform segments approximation) solutions. The TLST and MoM solutions were also identical here, while the TLT solution showed a significant deviation.

5.4 Network of Nonuniform Lines

In this example, we applied the network formulation based on EM topology to calculate the currents at the terminals of a nonuniform cable harness. This harness could be a part of a car or an aircraft's wiring, for example. The network was made up of three tubes. The first tube contained a three-wire cable, where the two outer wires were twisted around the center wire. The second tube was made of a single, bent wire, with an angle of 45°. The last tube was a corrugated line with two wires. The length of the tubes were 1 m, 2.82 m, and 3 m. The structure was placed above an ideal ground plane, and all wires were terminated with 50Ω resistors. The connection of the tubes in the center of the structure was modeled by an ideal junction S_4, which connected wire 1 and 2 of tube 1 with wires 1 and 2 of tube 3, and wire 3 of tube 1 with wire 1 of tube 2. The harness was excited by a 1V source at the beginning of wire 1 of tube 1. The structure is depicted in Figure 22.

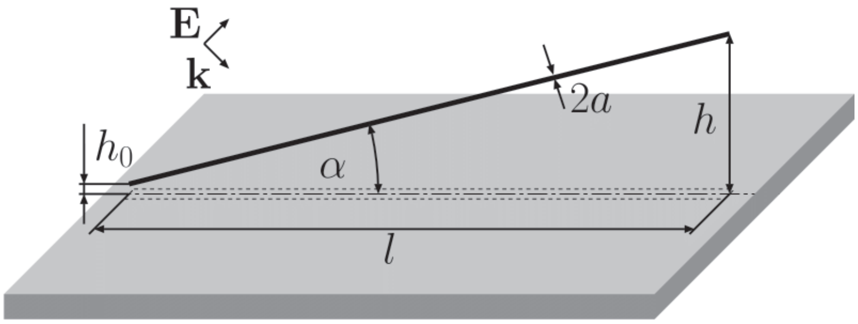

Figure 20. A wire above a perfectly conducting ground plane: $h_0 =$ mm, $h = 200$ mm, $l = 500$ mm, $a = 0.2$ mm, $\alpha = 21.7°$, $|\mathbf{E}| = 1$ V/m.

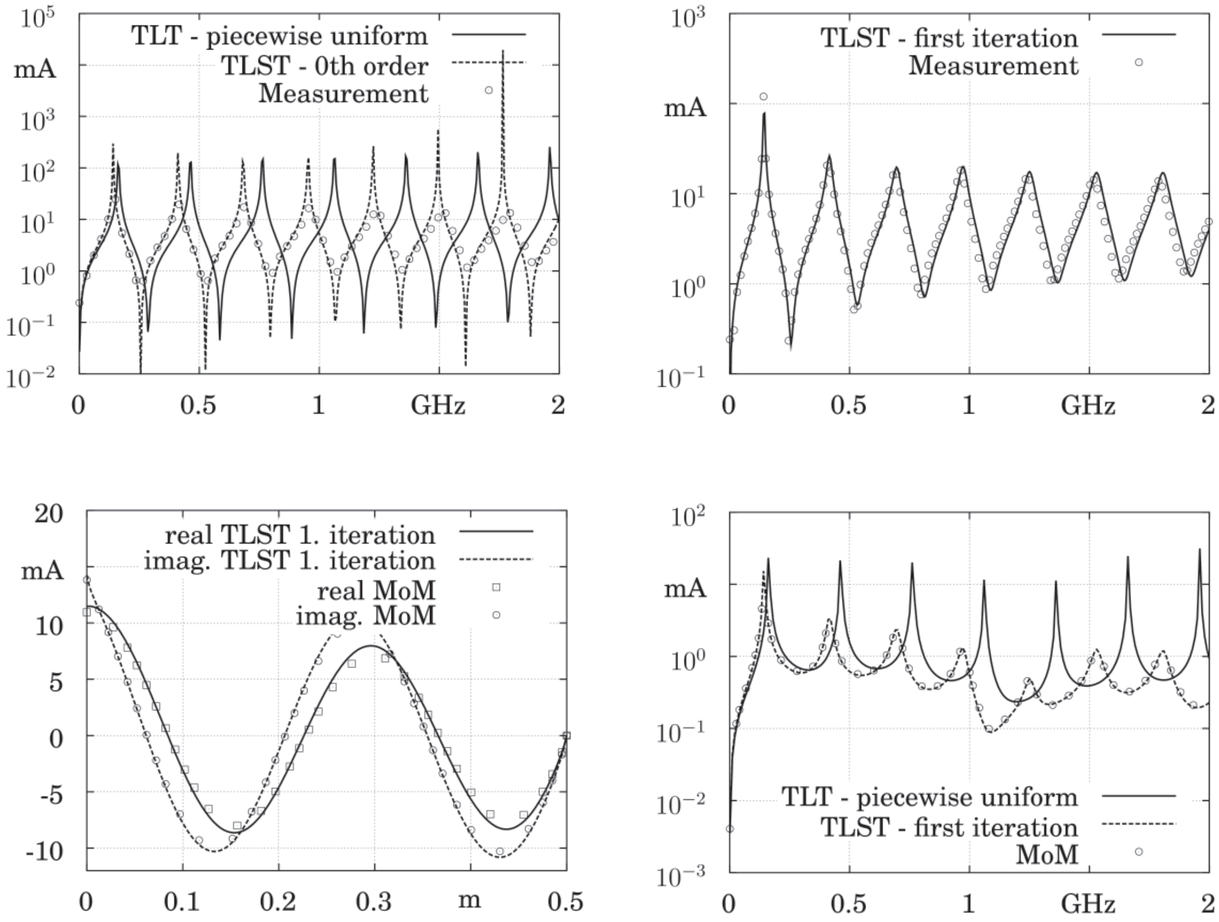

Figure 21. The results for the wire above a perfectly conducting ground plane: (a) The magnitude of the input current of the wire excited by a 1V voltage source; (b) The TLST solutions and measurement; (c) The current distribution along the wire at the resonance frequency of 974 MHz; (d) The magnitude of the input current of the wire excited by a 1 V/m plane wave.

One of the results of the calculation is presented in Figure 23. Here, the magnitude of the crosstalk current at the right end of the harness is shown. The results were calculated using either a piecewise-uniform approximation for the transmission lines or for the TLST. For validation, a MoM solution is also shown. One can see that there is quite good agreement between the TLST/BLT solution and the MoM results, whereas the uniform/BLT method gives wrong results.

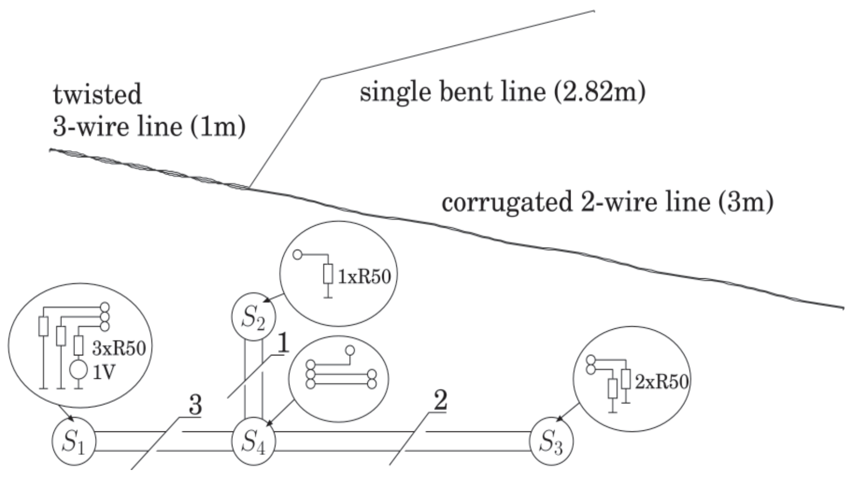

Figure 22. A nonuniform harness and the corresponding topological network.

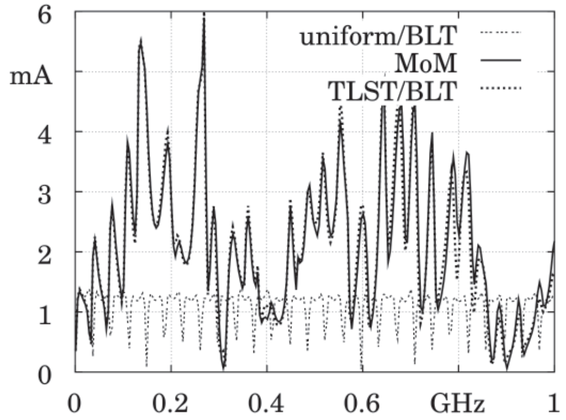

Figure 23. The magnitude of the right-end cross-coupled current.

6. Conclusion

This article has discussed the need for the extension of the well-known usual transmission-line theory. Various aspects were discussed, starting from simple models for discontinuities in the conduction of lines to a completely new, extended theory, valid for arbitrary field modes and high frequencies. We provided a set of approaches for dealing with "real world" interconnections, such as cables, wires, printed-circuit-board traces, microstrips, slit lines, and busses for digital data in modern electronic circuits.

The new theory, which is called the "Transmission-Line Super Theory" (TLST), is a full-wave theory cast into the form of telegrapher equations, with a new set of generalized line parameters. It contains the classical Transmission-Line Theory (TLT) as a special case. The new parameters become position dependent because of the non-uniformity of the transmission line. They also become complex valued and frequency dependent, due to the different field modes at different frequencies and radiation losses. Undoubtedly, one of the benefits of this transmission-line super theory is the fast solution – even for complex wiring – of the corresponding telegrapher equations. They are solved with the aid of the product integral. This solution can be transformed into equivalent n-port parameters, e.g., admittance or scattering parameters. They can thereafter be introduced into network representations like the (modified) nodal analysis or the EM topology approach with the BLT equation. Since the solution contains radiation losses as well as non-TEM coupling at higher frequencies, the results obtained by our method are in very good agreement with full-wave methods like the MoM. Our theory is well suited for parameter-variation studies, because the line parameters are independent of exciting sources and terminations. Only the network response must be recalculated, which can be done very quickly.

The examples demonstrated the successful application of our new theory, even for cases where antenna theory might be the appropriate tool. Convergence occurred after one iteration for the parameter matrices, which showed that the starting values where chosen very adequately. Thus, the zeroth-order parameters, which are frequency independent, represented a very good approximation of the actual parameters, and facilitate the transformation into the time domain without convolution integrals, where nonlinear terminations can be treated.

Further work to improve the theory includes the treatment of thick conductors, i.e., the prediction of the current and charge distribution inside the conductors, in order to model the skin and proximity effects. More advanced techniques to accelerate the calculation of the parameter matrix and the solution of the telegrapher equations are also under investigation. Some work on the description of a transmission line in resonating enclosures and on the investigation of signal integrity on nonuniform lines is also in progress.

7. Acknowledgement

This work was supported by the SUMMA Foundation and the FAF Research Institute for Protective Technologies and NBC Protection (WIS) Munster.

8. References

1. W. Kelvin, "On the Theory of the Electric Telegraph," *Proc. Roy Soc.*, **1855**, pp. 382-399.

2. G. Kirchhoff, "On the Motion of Electricity in Wires," *Phil. Mag. XIII*, **1857**, p. 393.

3. O. Heaviside, *Electromagnetic Theory*, London, E. & F. N. SPON Ltd., 1951.

4. G. Mie, "Elektrische Wellen an zwei parallelen Drähten [Electrical Waves Along Two Parallel Wires]," *Annalen der Physik*, **6**, 1900, p. 201.

5. A. Sommerfeld, *Electrodynamics*, New York, Academic Press, 1964.

6. S. Schelkunoff, "Conversion of Maxwell's Equations into Generalised Telegraphists's Equations," *Bell System Technical Journal*, 1955, pp. 995-1043.

7. A. Djordjevic, T. Sarkar, and R. Harrington, "Time Domain Response of Multiconductor Transmission Lines," *Proceedings IEEE*, **6**, 1987, pp. 743-764.

8. R. Collin, *Foundations of Microwave Engineering*, New York, McGraw-Hill, 1992.

9. C. Paul, *Analysis of Multiconductor Transmission Lines*, New York, John Wiley & Sons, 1994.

10. G. Franceschetti, *Electromagnetics*, New York, Plenum Press, 1997.

11. R. P. King, *Transmission Line Theory*, McGraw-Hill Book Company, 1955.

12.F. Tesche, M. V. Ianoz, and T. Karlsson, *EMC Analysis Methods and Computational Models*, New York, John Wiley & Sons, Inc., 1997.

13.C. Taylor, R. Satterwhite, and C. Harrison, "The Response of a Terminated Two-Wire Transmission Line Excited by a Nonuniform Electromagnetic Field," *IEEE Transactions on Antennas and Propagation*, 1965, pp. 987-989.

14.A. Agrawal, K. H. Price, and S. J. Gurbaxani, "Transient Response of Multiconductor Transmission Line Excited by a Nonuniform Electromagnetic Field," *IEEE Transactions on Electromagnetic Compatibility*, May 1980, pp. 119-129.

15.F. Rachidi, "Formulation of the Field-to-Transmission Line Coupling Equations in Terms of Magnetic Excitation Field," *IEEE Transactions on Electromagnetic Compatibility*, August 1993, pp. 404-407.

16.C. Paul, "Solution of the Transmission-Line Equations Under the Weak-Coupling Assumption," *IEEE Transactions on Electromagnetic Compatibility*, August 2002, pp. 413-423.

17.S. Schelkunoff, *Electromagnetic Waves*, Princeton, NJ, D. Van Nostrand Company, Inc., 1945.

18.S. Schelkunoff and H. Friis, *Antennas, Theory and Practice*, New York, John Wiley & Sons, Inc., 1966.

19.E. Vance, *Coupling to Shielded Cables*, New York, John Wiley and Sons, 1978.

20.P. Degauque and A. Zeddam, "Remarks on the Transmission-Line Approach to Determining the Current Induced on Above-Ground Cables," *IEEE Transactions on Electromagnetic Compatibility*, February 1988, p. 77.

21.O. Gebele, *EMV-Analyse beliebiger Leitungen über oberflächendiskretisierten metallischen Strukturen*, PhD thesis, TU Hamburg-Harburg, July 2002.

22.F. Tesche and B. Brändli, "Observations on the Adequacy of Transmission-Line Coupling Models for Long Overhead Cables," in *International Symposium on EMC*, (Rome, Italy), September 1994, p. 374.

23.W. Liu and Y. Kami, "Vertical Riser Effects of a Finite-Length Transmission Line," in *International Symposium on EMC, Tokyo*, 1999.

24.W. Getsinger, "End-Effects in Quasi-TEM Transmission Lines," *IEEE Transactions on Microwave Theory and Techniques*, April 1993, p. 666.

25.H. Green and J. Cashman, "End Effect in Open-Circuited Two-Wire Transmission Lines," *IEEE Transactions on Microwave Theory and Techniques*, January 1986, p. 180.

26.T. Wu, "Theory of the Dipole Antenna and the Two-Wire Transmission Line," *Journal of Mathematical Physics*, **4**, 1961, p. 550.

27.L. Weinstein, *The Theory of Diffraction and the Factorization Method (Generalized Wiener-Hopf Technique)*, Boulder, Colorado, Golem Press, 1969.

28.R. Olsen and D. Chang, "Analysis of Semi-Infinite and Finite Thin-Wire Antennas above a Dissipative Earth," *Radio Science*, **11**, 1976, p. 867.

29.J. Lam, "Equivalent Lumped Parameter far a Bend in a Two-Wire Transmission Line: Part I. Inductance." *Interaction Note 303*, December 1976 (http://iget104.et.uni-magdeburg.de).

30.J. Lam, "Equivalent Lumped Parameter Far a Bend in a Two-Wire Transmission Line: Part II. Capacitance," *Interaction Note 304*, January 1977 (http://iget104.et.uni-magdeburg.de).

31.T. Nakamura, N. Hayashi, H. Fukuda, and S. Yokokawa, "Radiation from the Transmission Line with an Acute Bend," *IEEE Transactions on Electromagnetic Compatibility*, **EMC-3**, 1995, pp. 317-325.

32.V. Daniele, M. Gilli, and S. Pignari, "EMC Prediction Model of a Single Wire Transmission Line Crossing a Circular Aperture in a Planar Screen," *IEEE Transactions on Electromagnetic Compatibility*, May 1996, p. 117.

33.R. Harrington, *Field Computation by Moment Methods*, New York, MacMillan, 1968.

34.D. Wilton and S. Govind, "Incorporation of Edge Conditions in Moment Method Solutions," *IEEE Transactions on Antennas and Propagation*, **AP-6**, 1977, p. 845.

35.C. Butler, "The Equivalent Radius of a Narrow Conducting Strip," *IEEE Transactions on Antennas and Propagation*, **AP-4**, 1982, p. 755.

36.H. Booker, "Slot Aerials and Their Relation to Complementary Wire Aerials," *JIEE*, 1946, p. 620.

37.K. Lee and F. Yang, "A Wire Passing by a Circular Aperture in an Infinite Ground Plane," *Interaction Note 317*, February 1977 (http://iget104.et.uni-magdeburg.de).

38.K. Umashankar and C. Baum, "On the Further Considerations of Infinitely Long Cable and Aperture Coupled Regions," *Interaction Note 399*, May 1980 (http://iget104.et.uni-magdeburg.de).

39.M. Omid, M. Kami, and Y. Hayakawa, "Field Coupling to Nonuniform and Uniform Transmission Lines," *IEEE Transactions on Electromagnetic Compatibility*, August 1997, pp. 201-211.

40.S. Grivet-Talocia and F. Canavero, "Accuracy of Propagation Modeling on Transmission Lines," in *IEEE International Symposium on EMC*, Seattle, Washington, August 1999, pp. 474-479.

41.H. Haase and J. Nitsch, "Full-Wave Transmission Line Theory (FWTLT) for the Analysis of Three-Dimensional Wire-Like Structures," in *The International Zurich Symposium and Technical Exhibition on Electromagnetic Compatibility*, February 2001, pp. 235-240.

42.H. Haase, T. Steinmetz, and J. Nitsch, "Effects of Nonuniform Cables on the Propagation and Coupling Processes at High Frequencies," in *Proceedings of the International Conference on Electromagnetics in Advanced Applications*, Torino, Italy, September 2001.

43.H. Haase and J. Nitsch, "Generalized Transmission-Line Theory for the Treatment of Nonuniform Multiconductor Transmission Lines," *Journal of Applied Electromagnetics and Mechanics*, **1-3**, 2003, pp. 149-156.

44.H. Haase and J. Nitsch, "Investigation of Nonuniform Transmission Line Structures by a Generalized Transmission-Line

Theory," in *The International Zurich Symposium and Technical Exhibition on Electromagnetic Compatibility*, February 2003, pp. 597-602.

45.S. Tkatchenko, F. Rachidi, and M. Ianoz, "Electromagnetic Field Coupling to a Line of Finite Length: Theory and Fast Iterative Solutions in Frequency and Time Domains," *IEEE Transactions on Electromagnetic Compatibility*, **EMC-4**, 1995.

46.R. Sturm, "On the Theory of Nonuniform Multiconductor Transmission Lines: An Approach to Irregular Wire Configurations," *Interaction Note 541*, June 1998 (http://iget104.et.uni-magdeburg.de).

47.B. O'Neill, *Elementary Differential Geometry*, New York, Academic Press Inc., 1966.

48.F. Gantmacher, *The Theory of Matrices*, New York, Chelsea Publishing Company, 1984.

49.J. Nitsch and F. Gronwald, "Analytical Solutions in Multiconductor Transmission Line Theory," *IEEE Transactions on Electromagnetic Compatibility*, November 1999, pp. 469-479.

50.J. Nitsch and S. Tkachenko, "Complex-Valued Transmission-Line Parameters and Their Relation to the Radiation-Resistance," *Interaction Notes 573*, September 2002.

51.J. Dollard and C. Friedman, *Product Integration with Application to Differential Equations*, Reading, MA, Addison-Wesley Publishing Company, 1979.

52.C. E. Baum and T. Steinmetz, "An Interpolation Technique for Analyzing Sections of Nonuniform Multiconductor Transmission Lines," in *The International Zurich Symposium and Technical Exhibition on Electromagnetic Compatibility*, February 18-20, 2003, pp. 593-596.

53.C. Baum, T. Liu, and F. Tesche, "On the Analysis of General Multiconductor Transmission-Line Networks," *Interaction Note 350*, November 1978 (http://iget104.et.uni-magdeburg.de).

54.J. Parmantier, "Application of EM Topology on Complex Wiring Systems," in *International Symposium on Electromagnetic Compatibility*, (Magdeburg), October 1999, pp. 1-8 (ISBN 3-929757-25-7).

55.F. Tesche, "Principles and Application of EM Field Coupling to Transmission Lines," in *International Zurich Symposium and Technical Exhibition on EMC*, March 1995.

56.J. Nitsch and S. Tkachenko, "Source Dependent Transmission Line Parameters: Plane Wave vs TEM Excitation," *Interaction Notes 577*, November 2002.

URSI Homepage

Dear Radioscientist,

Although we try to update the information on the URSI homepage as often as possible, it was time to work on the layout and the presentation of its contents. On 10 November the URSI website received a facelift...

We invite you to go and have a look :

http://www.ursi.org

URSI visibility in Geneva

There will never be a right time to write a report like this so long as the SCT is developing rapidly. Starting a new era is taking a long time, but progress is good. Readers will recall that visibility of URSI is a concern, and was the subject of a current questionnaire – see the June, 2003, edition of this journal (*Radio Science Bulletin*, No. 305, p. 45), and that is very relevant to this report.

On October 6-9, the Working Parties of ITU-R Study Group 7 met in Geneva, and there was a meeting of the SCT's URSI/ITU-R Network alongside them. There were also several important meetings with influential individuals, and it seems timely to report on these now, although things are moving forward as this is written. The meetings in Geneva were both with those who attended the Network sessions and with officials in the bureaux (BR, TSB, and BDT) of ITU-R, ITU-T, and ITU-D, the three Sectors of the ITU: Radiocommunications, Telecommunications Standardisation and Telecommunications Development (in developing countries).

Much of the current status of the SCT is recorded in the article in the June, 2003, edition of this journal (*Radio Science Bulletin*, No. 305, pp. 38-44), but the meetings in Geneva in October will make a significant difference. There now seem to be three ways of improving the position of URSI in relation to the ITU:

1. Pursuing topics for research reports, following those in the style of "Appendix 1" of the June article and the SCT Web site;

2. Extending the use of URSI meetings in association with ITU meetings, following the style of meetings of "Climpara," and

3. Having URSI-related lecturers give state-of-the-art science presentations to ITU-related audiences.

None of these needs to be exclusive to URSI relations with ITU, and developing relations with WHO is already an Activity of the SCT. Further activities of this kind are to be encouraged.

On the first of these three areas, significant developments have been achieved and potential developments explored, and more ideas will be very welcome before progress is recorded on the SCT website (http://www.ursi.org/SCT.htm). Proposed new topics are on ultra-wideband technology, metrology, and space platforms. IMT 2000 and systems beyond may be another. But the important stages must soon begin to find who from within the URSI community is currently active in researching the subjects of the selected topics, possibly encouraging research to move that way, and of course making use of recent knowledge held by only a few individuals. After that, it's a matter of reporting the relevant results appropriately. "But why should we?" is the obvious question! Well, until a few years ago, it seemed to be in a sponsor's interests to have others see the value of what was being done in the sponsor's name, and there were kudos in putting material to ITU-R (or whomever): it was a demonstration of merit. Now, the sponsors seem only really concerned to see the results of what is being done with their money. So, perhaps we look to the research scientists themselves. They need to see their results published in order to be recognized by other research scientists, but perhaps there is also the need to say "look what I can do for you – it will be worth your while (and money) to give me a contract!" There also may be the possibility of doing something for the good name of URSI at a time when visibility of URSI is being considered.

There will then be the need for formally reporting the work in a manner that ITU-R (or whomever) can apply. For ITU-R, this generally means the author (indeed, the researcher) having a good idea of what is needed to improve or develop an existing Recommendation text, or to develop a new one that is needed. It is probably best done by those active in National Administrations of the body concerned (e.g., ITU-R). This has proven successful in reporting results from European COST projects (being projects covering specific cooperation in science and technology).

On the second area listed above, meetings of Climpara (on the use of climatic parameters in the prediction of radio-wave propagation) were held immediately before those of ITU-R Working Parties most likely to be able to use the results from papers presented at the URSI meetings. They were very specific, and had a direct consequence to the subsequent development of the research as well as to the application to ITU-R texts. They were attended mainly by experts active both in URSI and in ITU-R, but they also encouraged those active only in URSI or in ITU-R to participate also in the companion meeting. Another in this series has recently added effects of diffraction (by buildings, terrain features, etc.); ClimDiff met in Brazil on November 17-19, 2003. These meetings were generally small and intensive meetings, but there might be scope for other URSI-sponsored meetings to interact in a similar way. This is currently being explored in the ITU context, but all are very welcome to offer suggestions.

The third area possibly may be closest to the work of ITU-D, but it is not yet clear what should be sought! Perhaps it could be in the form of a directory of subjects people are prepared to lecture on ("offers" = author, address, title of proposed lecture, and synopsis), for a fee and travel/ accommodation expenses, as well as "requirements" (with information as above, but "organization and contact" replacing "author"). Agreement might then be met between the two parties. Early offers would be welcome in addition to the two I have.

The meetings of the URSI/ITU-R Network were held at the time of ITU-R Study Group 7 Working Party meetings. Sixteen people attended the Network meetings and a specific report is available to SCT Participants. This marks a step evolution in the SCT, and further comments are requested from those active in URSI.

Martin Hall
SCT Chair
Martin.Hall@rl.ac.UK

An Announcement and Questionnaire from the URSI Working Group on the Leap Second

The URSI Secretariat has received a letter from the Special Rapporteur Group of the International Telecommunication Union (ITU). The charter of this group is to study and make recommendations on the redefinition of Coordinated Universal Time (UTC), which differs from International Atomic Time (TAI) by the insertion of leap seconds to account for the variable rotation of the Earth. The letter invites URSI participation in their study. This has since been narrowed to consideration of whether the current practice of inserting leap seconds so as to keep |UT1-UTC| < 0.9 seconds should be replaced by a policy of inserting no leap seconds, so that UTC-TAI will remain at a fixed value indefinitely. This would affect systems that depend upon UT1 being close enough to UTC that the difference can be ignored, or that the format for specifying the difference can have a fixed size. An analysis of the motivation for a change was recently published in *Metrologia*, **38**, 2001, pp. 509-529.

Previous to the formation of the ITU Special Rapporteur Group, an URSI Commission J Working Group was formed at the 1999 URSI General Assembly in Toronto, Canada. Subsequently, the 2002 URSI General Assembly in Maastricht, The Netherlands, formed an URSI Working Group (WG) to study the effects of such a change upon systems relevant to URSI radio scientists, and to propose a response to the ITU. The members of the WG are Demetrios Matsakis (Chair), Wim Brouw, Sigfrido Leschiutta, and Inoue Makoto. An informal listserv on the technical, scientific, and political aspects of this matter can be accessed via http://rom.usno.navy.mil/archives/leapsecs.html, and a broader summary is being maintained by Markus Kuhn at http://www.cl.cam.ac.uk/~mgk25/time/leap/. Both of these sites provide an excellent summary by Markus Kuhn of discussions and presentations at an ITU-sponsored symposium on this subject, held in May, 2003, at Torino, Italy.

In order to fulfill our charter, we have composed a questionnaire that we have asked all URSI Commission Chairs to distribute to their official numbers. This questionnaire will help us better understand their needs. While we do ask that the form of the questionnaire be followed, the responders should feel free to use as much space to answer the questions as required.

Please send the completed questionnaire to Matsakis.Demetrios@usno.navy.mil by **March 15, 2004.**

Dr. Demetrios Matsakis

Chair, URSI Working Group on the Leap Second

Questionnaire on UTC Definition

Please respond to
Matsakis.Demetrios@usno.navy.mil
by March 15, 2004

Name and Position:

Contact information:

URSI Commissions of specific interest to you:

Note that one current plan under consideration would halt new leap seconds after 2021. If it were decided to change the definition of UTC so that no leap seconds would be inserted after 2021, please provide the approximate cost to your systems, and your systems' users, of incorporating the next leap second or any possible deletion of a second. If you feel the questions do not correctly parameterize your system or its users systems, please indicate a better formulation. Please ignore inflation and assume exchange rates remain constant.

1. Name of System:
2. Brief Description of System:
3. Hours of labor:
4. Equipment purchase:
5. Costs in terms of final product or system performance if the leap second or second-deletion is not correctly included:
6. Costs in terms of final product or system performance to incorporate a leap second or second-deletion:
7. Has your system or its users ever applied the leap second incorrectly, and if so what percentage of the time?
8. If it were decided to halt new leap seconds after a specified date other than 2021, is there an implementation date that would significantly affect the costs indicated in your response to questions 5 and 6? If so, please provide the associated costs in today's dollars, ignoring inflation.
9. Please use this space to make any comments or provide any information you feel appropriate.
10. It is possible that we would like to publicly identify your system(s) or your response as relevant to the decision. In that case, do we have your permission to fully quote your reply?

Conferences

CONFERENCE REPORTS

Atmospheric Remote Sensing using Satellite Navigation Systems

Matera, Italy, 13-15 October 2003

A special symposium of the URSI FG joint working group 'Atmospheric Remote Sensing using Satellite Navigation Systems' was held from 13-15 October 2003. The symposium was held at the at ASI Centro di Geodesia Spaziale "Giuseppe Colombo" close to the ancient town of Matera. The Italian Space Agency (ASI) kindly provided venue and local arrangements. The local organising committee was headed by Francesco Vespe and additional organisational assistance was also received from the ASI centre in Rome through Vittorio de Cosmo.

The joint working group "FG" aims to bring together researchers working in the fields of the URSI Commissions 'F' (Wave Propagation and Remote Sensing) and 'G' (Ionospheric Radio and Propagation) in order to exchange knowledge and ideas relating to the use of satellite navigation systems for atmospheric and ionospheric remote sensing.

The symposium had four themes, each of which contained both 'F' and 'G' commission participants.

- Atmospheric/ionospheric measurements using ground-based GNSS sensors
- GNSS radio occultation and novel radio occultation techniques
- Scintillation - ionospheric and tropospheric effects
- *Imaging and data assimilation techniques*

In all some seventy presentations from sixteen different countries were divided across invited and contributed talks and posters. A special feature of this symposium was a session of four invited talks by young scientists, one from each topic area.

The initial session consisted of invited papers to introduce the concepts of atmospheric and ionospheric measurements using GNSS. The techniques for extracting information about atmospheric water vapour from GPS observations were described. Studies on the shell-approach to surface mapping the ionospheric total electron content (TEC) used in Satellite-Based Augmentation Systems (such as WAAS and EGNOS) were then presented. The related poster session addressed the measurement issues such as receiver inter-frequency biases and the physical phenomena seen to affect the measurement techniques.

The young scientist session covered each of the four topics. A case study comparison between GPS slant wet delay and collocated radiometer observations attempted to quantify the accuracy of a GPS technique in the troposphere and raised questions about the requirement for a better approach. The successful CHAMP mission was then viewed from the perspective of the ionospheric radio-occultation results over the last two years. The recent interest in GPS scintillation was highlighted in a new collaboration between two young scientists to join together experimental and theoretical studies relating to the auroral ionosphere. Finally, the theoretical and experimental progression from local-scale ionospheric tomography to global GPS imaging was explained.

The radio-occultation sessions included results from CHAMP, GPS/MET SAC-C and Oersted. Approaches that extend beyond the established Abel transform were shown to offer a real improvement and the assimilation of data into a physical model was demonstrated with data from a number of established LEO satellite missions. Proposed missions ACE+ and COSMIC are now on the horizon and the technical challenges in implementing the LEO-LEO links in ACE+ were outlined. The plans for a number of future missions showed this to be an increasingly important area of research.

In the scintillation sessions the important work on the theoretical understanding of ionospheric scintillation by the late Prof. K.C. Yeh was acknowledged. Recent studies of both phase and amplitude GPS scintillations in northern Europe were shown and related to geomagnetic activity. The new five-frequency ground-to-satellite and satellite-to-satellite CITRIS receiver was announced. The likely impact of tropospheric amplitude scintillations on the Cross-Atmosphere LEO-LEO Sounder at 10, 17 and 23 GHz was discussed. Scintillation models and simulations of ionospheric scintillation were discussed and new experimental results showing scintillation on GPS signals from the northerly settlement of Svalbard were shown.

In the imaging sessions the possibility of imaging the troposphere with an array of GPS receivers and a radiometer was outlined. The assimilation of satellite-to-ground TEC data into a three-dimensional physical or empirical model was explained and the potential for auroral/polar ionosphere studies was clearly identified. Example results from the EISCAT radar in Norway were shown. Finally, the possibility was demonstrated of successfully joining together both ground-based and LEO-based GPS observations to make electron density images.

Sponsorship for the meeting was generously provided by URSI (Young scientists), Saab-Ericsson, Laben, ASI and ESA. Both Saab-Ericsson and Laben speakers gave talks about their state-of-the-art activities in radio-occultation research.

In summary there were several positive outcomes to the meeting. Firstly it achieved its aim in bringing together researchers in traditionally different areas and allowed them to gain an understanding of the other's work. A number of ideas for new international collaborative projects were formed. Links were strengthened between the European COST communities and the URSI commissions. A new connection between the International Union of Geophysics and Geodesy (IUGG) sub-commission (4.3) for atmospheric remote sensing using GNSS and the URSI working group was formed and will be strengthened by members of the symposium technical committee.

Proceedings of the symposium will be produced on cd. Further copies of the cd will be available by email request to C.N.Mitchell@bath.ac.uk.

Bertram Arbesser-Rastburg, European Space Agency
and Cathryn Mitchell, University of Bath,UK

CONFERENCE ANNOUNCEMENT

2004 International Symposium on Signals, Systems and Electronics (ISSSE'04)

Linz, Austria, 10 - 13 August 2004

ISSSE'04 will be held at the University of Linz, Austria, on August 10-13, 2004. Linz is the capital of Upper Austria, located right in-between Vienna and Salzburg. This symposium is organized and sponsored by the International Union of Radio Science (URSI), Commissions C and D, and is co-sponsored by the IEEE COM/MTT Joint Chapter Austria, and the ÖVE (Austrian Electrotechnical Association).

Topics

The Symposium will be focused on (but not limited to) the following topics:

- Electronics for Communications, Sensing and Control
- Circuits & Systems
- Networks & Signals
- Digital Signal Processing
- Applications in Communications & Information Engineering
- Automotive Applications
- Applications in Control Engineering and Mechatronics
- Wireless, Optical, and Cable-Based Systems
- Devices and Techniques for RF and Baseband Circuits
- Devices and Techniques for Photonics
- Radar Techniques and Devices
- System and Circuit Simulation
- Hardware-oriented Signal Processing
- Numerical and CAD Techniques
- Software Defined Radio
- Coding, Modulation, Equalization, and Detection Strategies
- Smart Antennas / MIMO Techniques
- Hardware/Software Cooperation in Electronics
- Electronic System Partitioning & Interfaces
- Others

Steering Committee

- Kurt Schlacher, University of Linz, Austria, General Co-Chair

- Robert Weigel, University of Erlangen-Nuremberg, Germany, General Co-Chair
- Gernot Kubin, TU Graz, Austria, TPC-Co-Chair
- Andreas Springer, University of Linz, Austria, TPC-Co-Chair

Deadlines

Extended abstracts: January 15, 2004
Notification of acceptance: March 15, 2004
Final manuscript: May 1, 2004

Special Features

- ISSSE'04 Award: During ISSSE'04, the ISSSE'04 Award will be donated to the authors of the papers selected from those accepted for presentation at ISSSE'04, as outstanding contributions to the URSI Commissions C and D fields.
- Young scientist support: Limited support is available. Candidates must be up to 35 years of age on August 1, 2004, and have a Ph.D. or equivalent degree.
- Workshops and Tutorials
- Exhibition
- Conference Tours

Contact

Professor Dr. Andreas Springer
Technical Program Committee Co-Chair
ISSSE'04
c/o ISSSE'04 Secretariat,
Institute for Communications &
Information Engineering.
Johannes Kepler University of Linz
Altenbergerstrasse 69, A-4040 Linz, Austria
E-mail: issse04@icie.jku.at

Website: http://www.icie.jku.at/issse04

Bianisotropics 2004
10th Conference on Complex Media and Metamaterials

Ghent, Belgium, 22 - 24 September 2004

Scope

Bianisotropics 2004 – "10th Conference on Complex Media and Metamaterials" focuses on the electromagnetics of complex media and metamaterials in a general sense. The characterisation, modeling and applications for novel devices and components from the microwave to the optical regime will be addressed. Media ranging from anisotropic media, chiral media, bianisotropic media, artificial media, temporally agile media, nonlocal media, nonlinear media, random media, backward wave media (also called as double-negative media, negative-index media, or left-handed media), frequency selective surfaces, sculptured thin films, multifunctional materials, functional gradient materials, piezoelectric, ferro-electric thin films to periodic media and in particular photonic bandgap materials are considered. The conference will provide a critical and up-to-date review of the field and aims to identify future directions of research, development and applications.

The conference will comprise 5-6 half-day sessions. The program will include special talks by the key speakers, oral and poster sessions with contributed papers and discussions on hot topics. There also will be a panel discussion conducted by the committee members to scrutinise most recent research.

Topics

- Electromagnetic theory in such media
- Radiation and propagation of electromagnetic waves in such media
- Waveguides and printed structures using such media
- Scattering by bodies in such media
- Inverse scattering techniques for such media
- New microwave and optical devices using such media
- Modeling and applications of such media
- Experimental research on such media

Deadlines

March 1, 2004: Deadline for paper submission
April 15, 2004: Notification of acceptance
June 15, 2004: Deadline for early registration

Invited Speakers

- **Prof. John Arnold**, Department of Electronics and Electrical Engineering, University of Glasgow, UK.
- **Dr. Giorgio Bertotti**, Istituto Elettrotecnico Nazionale 'Galileo Ferraris', Torino, Italy.

- **Prof. Nader Engheta**, The Moore School of Electrical Engineering, University of Pennsylvania, USA.
- **Prof. Isabelle Huynen**, **Prof. Jean-Pierre Raskin** and **Prof. Christophe Craeye**, Université Catholique de Louvain, Belgium.
- **Prof. Gerhard Kristensson**, Department of Electroscience, Lund Institute of Technology, Sweden.
- **Prof. Ismo Lindell**, Electromagnetics Laboratory, Helsinki University of Technology, Finland.
- **Prof. Sergei Tretyakov** and **S. Maslovski**, Radio Laboratory, Helsinki University of Technology, Finland.
- **Prof. Keith Whites**, Department of Electrical and Computer Engineering, South Dakota School of Mines and Technology, USA.
- **Prof. Richard W. Ziolkowski**, Department of Electrical and Computer Engineering, University of Arizona, USA.

Conference Contacts

Chairs Local Organising Committee

Prof. Frank Olyslager : frank.olyslager@intec.ugent.be
Prof. Ann Franchois : ann.franchois@intec.ugent.be

Chair Technical Programme Committee

Prof. Ari Sihvola : ari.sihvola@hut.fi

Secretary

Mrs. Isabelle Van der Elstraeten
isabelle.vanderelstraeten@intec.ugent.be
Tel: +32-(0)92643321, Fax: +32-(0)92643593

For more information, please contact our Conference Website at http://www.intec.ugent.be/bian04.

JINA 2004

13th International Symposium on Antennas

Nice, France, 8 - 10 November 2004

The thirteenth edition of the biennial "Journées Internationales de Nice sur les Antennes" will be held at "Palais des Congrès Acropolis" in Nice, France, from 8 to 10 November 2004. As in previous editions, presentations will include invited conferences and convivial posters selected among submitted proposals.

Suggested topics

- Theorical electromagnetism
- Analytic and numerical techniques
- Synthesis and optimization
- Detection, inverse scattering, microwave imaging
- Radar cross section
- Integration, coupling and interaction, EMC
- Biological interactions
- New materials, metamaterials
- Electromagnetic bandgap structures (EBG)
- Frequency selective surfaces
- Industrial and medical applications
- Measurements and instrumentation
- Power handling, PIMP
- Feeds, reflector antennas and lenses
- Radiating elements and associated circuits
- Multifrequency and/or wideband antennas
- Millimetre and sub-millimetre wave antennas
- Array antennas, array reflectors
- Digital beamforming
- Adaptive and signal processing antennas (MIMO, …)
- Active and integrated antennas (MEMS, …)
- Small antennas
- Conformal antennas
- Antennas for mobile communications (UWB, WLAN, WIFI, …)
- Antennas for space applications (telecommunications, navigation, …)
- Onboard antennas (aircrafts, UAV, UCAV, ships, …)

Deadlines

May 10, 2004: Deadline for submission of complete papers
July 1, 2004: Notification of accepted papers

Contact

Scientific Secretariat JINA
France Télécom R&D
Fort de la Tête de Chien
06320 La Turbie, FRANCE
Fax : +33 4 92 10 65 19
E-mail : jina.2004@wanadoo.fr

Web site : www.jina2004.com

URSI CONFERENCE CALENDAR

An up-to-date version of this Conference Calendar, with links to the various conference web sites can be found at www.ursi.org : Calendar of supported meetings.

If you wish to announce your meeting in this calendar, you will find more information at www.ursi.org.

URSI cannot be held responsible for any errors contained in this list of meetings.

February 2004

WARS04 (Workshop on Applications of Radio Science)
Hobart, Australia, 18-20 February 2004
Contact : Dr. Phil WILKINSON, Dept. of Industry, Tourism and Resources, IPS Radio and Space Services, P.O. Box 1386, Haymarket, NSW 1240, AUSTRALIA, Fax : +61 2-9213 8060, E-mail : phil@ips.gov.au, www.ips.gov.au/IPSHosted/NCRS/wars/wars2004/index.html

March 2004

Métrologie et capteurs en électromagnetisme
(Journees scientifiques du CNFRS)
Meudon, France, 29-30 mars 2004
Contact : http://cnfrs.get-telecom.fr

May 2004

International NIR Workshop & Symposium
Seville, Spain, 20-22 May 2004
Contact : Dr. Bernard VEYRET, Labo PIOM/ENSCPB , Université de Bordeaux, BP 108, F-33402 TALENCE CEDEX, FRANCE, Phone : +33 5 56 84 66 29, Fax : +33 5 56 84 66 31, E-mail :b.veyret@piom.u-bordeaux.fr, b.veyret@enscpb.fr , http://www.icnirp.de/NIRProg.htm

EMTS'04 - 2004 International Symposium on Electromagnetic Theory
Pisa, Italy, 23-27 May 2004
cf. announcement in RSB September 2003, p.61-62
Contact persons : Prof. Makoto Ando, Commission B Chair, Dept. of Electrical and Electronic Engineering, Tokyo Institute of Technology, J2-12-1, Oookayama, Meguro, Tokyo 152-8552, Japan, E-mail: mando@antenna.ee.titech.ac.jp
and
Prof. Lotfollah Shafai, Commission B Vice-Chair, Dept. of Electrical & Computer Eng., University of Manitoba, 15 Gillson Street, Winnipeg, MB R3T 5V6, Canada, E-mail: shafai@ee.umanitoba.ca

June 2004

EMC'04 Sendai - 2004 International Symposium on Electromagnetic Compatibilty/Sendai
Sendai, Japan, 1-4 June 2004
Contact :Prof. R. Koga, Dept. of Communications Network Engineering, Okayama University, Japan, koga@cne.okayama-u.ac.jp, www.dev.cne.okayama-u.ac.jp

MSMW'04 - 5th International Kharkov Symposium on Physics and Engineering of Microwaves
Kharkov, Ukraine, 21-26 June 2004
cf. announcement in RSB September 2003, p.62-63
Contact : MSMW'04, IRE NASU 12, Ac. Proskura St., Kharkov 61085, Ukraine, Phone/Fax : +380 572-441105, E-mail: msmw04@ire.kharkov.ua, E-mail : www.ire.kharkov.ua/MSMW2004/

July 2004

35th COSPAR Scientific Assembly an Associate Events
Paris, France, 18-25 July 2004
cf. announcement in RSB September 2003, p.63-64
Contact :COSPAR Secretariat, 51, bd. de Montmorency, F-75016 Paris, France, Tel: 0033-1-45250679, Fax: 0033-1-40509827, E-mail: COSPAR@COSPARHQ.org , http://www.copernicus.org/COSPAR/paris2004/useful.htm

August 2004

ISSSE'04 - 2004 Int. Symp. on Signals, Systems and Electronics
Linz, Austria, 10-13 August 2004
Contact : Prof. Dr. Andreas Springer, Technical Program Committee Co-Chair, ISSSE'04, c/o ISSSE'04 Secretariat, Institute for Communications and Information Engineering, Johannes Kepler University of Linz, Altenbergerstrasse 69, A-4040 Linz, Austria, E-mail: issse04@icie.jku.at, http://www.icie.jku.at/issse04/

ISAP'04 - 2004 Int. Symp. on Antennas and Propagation
Sendai, Japan, 17-21 August 2004
Contact : ISAP'04, Attn. Dr. Tokio Taga, NTT DoCoMo, Inc., 3-5, Hikarino-oka, Yokosuka, 239-8536 Japan, E-mail : isap-2004@mail.ieice.org , http://www.ieice.org/cs/isap/2004

AP-RASC 2004 - 2nd Asia-Pacific Radio Science Conference
Qing, China, 24-27 August 2004
Contact : Prof. Zong Sha, China Research Institute , of

Radio Propagation, P.O. Box 134-70, 100040 Beijing, China (CIE), Phone : +86 10-6821-2267, Fax : +86 10-6821-6857, E-mail : z.sha@ieee.org, www.cie-china.org/AP-RASC/

September 2004

Bianisotropics 2004
Ghent, Belgium, 22-24 September 2004
Contact : Mrs. Isabelle Van Der Elstraeten, INTEC, Sint-Pietersnieuwstraat 41, B-9000 Ghent, Belgium, Tel. +32-(0)9-2643321, Fax +32-(0)9-2643593, E-mail: isabelle.vanderelstraeten@intec.ugent.be, www.intec.ugent.be/bian04/

November 2004

JINA 2004 - 13 èmes Journées Internationales de Nice sur les Antennes
Nice, France, 8-10 November 2004
Contact : Secretariat JINA, France Telecom R&D, Fort de La Tête de Chien, F-06320 La Turbie, France, Fax : +33 4 92 10 65 19, E-mail : jina.2004@wanadoo.fr, www.jina2004.com

August 2005

ISMOT 2005 - 10th International Symposium on Microwave and Optical Technology
Fukuoka, Japan, 22-25 August 2005
Contact : Prof. Kiyotoshi YASUMOTO, Dpt. Comp. Sci. & Comm. Eng., Kyushu University, 6-10-1 Hakozaki, Higashi-ku, Fukuoka 812-8581, Japan, Phone: +81-92-642-4045, Fax: +81-92-632-5204, E-mail: yasumoto@csce.kyushu-u.ac.jp, http://ismot2005.fit.ac.jp

October 2005

XXVIIIth URSI General Assembly
New Delhi, India, 23-29 October 2005
Contact : URSI Secretariat, c/o INTEC, Sint-Pietersnieuwstraat 41, B-9000 Ghent, Belgium, Phone : +32 (0)9 264 3320, Fax +32 (0)9 264 4288, E-mail: ursi@intec.rug.ac.be, www.ursi.org

News from the URSI Community

NEWS FROM THE MEMBER COMMITTEES

EGYPT

THE 21ST NATIONAL RADIO SCIENCE CONFERENCE (NRSC'04)

Cairo, Egypt, 16-18 March 2004

The 21st National Radio Science Conference NRSC 2004, will be held in Cairo Egypt. The National Telecommunication Institute (NTI) will host the conference during the period from 16-18 March 2004. The conference program will consist of invited sessions on selected topics and contributed sessions.

Program

The submitted papers must describe original work and cover the activities of the URSI commissions A-K, namely
A) Electromagnetic metrology
B) Fields and waves
C) Signals and systems
D) Electronics and photonics
E) Electromagnetic noise and interference
F) Wave propagation and remote sensing
G) Lonospheric radio and propagation
H) Waves in plasma
I) Radio astronomy
K) Electromagnetic in biology and medicine

Conference Deadlines

Submission of papers:November 15th 2003
Notification of acceptance:December 30th 2003
Camera-ready manuscript: January 30th 2004

Sponsors

Ministry of Communications and Information Technology, IEEE Egypt's section) / EDS chapter, Telecom Egypt and the Egyptian Radio and TV union (ERTU).

Conference Chairmen

- Chairman: Prof. Ibrahim A. Salem, Chairman of the Egyptian NRSC, National Academy of Science and Technology,E - mail : iasalem@ieee.org, Tel : 202-2580256, Fax : 202-7921270
- Vice-Chairman: Prof. Ahmed El-Shirbini, Director of the National Telecommunication Institute, Professor at Cairo University.

Contact

Prof. Said E. El-Khamy
Chairman of Electrical Engineering Department
Faculty of Engineering, Alexandria University
E-mail: elkhamy@ieee.org
Tel: (203) 5464998, Fax: (202) 5921853

Website at http://www.nrsc2004.sci.eg.

FRANCE

Metrologie et capteurs en Electromagnetisme

Meudon, France, 29 et 30 mars 2004

Sous le Haut Patronage de l'Académie des Sciences, le Comité National Français de Radioélectricité Scientifique (CNFRS), section française de l'Union Radio Scientifique Internationale (URSI), organise les Journées Scientifiques du CNFRS (http://cnfrs.get-telecom.fr).

Les Journées Scientifiques sont organisées autour de sessions animées par des spécialistes reconnus du domaine. Elles seront introduites par des conférences invitées présentant soit l'état de l'art, soit de nouveaux développements intéressant l'ensemble de la communauté, suivies de communications orales et/ou affichées.

Elles auront lieu à l'Observatoire de Meudon, 5 place Jules Janssen, 92195 Meudon, France et elles débuteront le lundi 29 mars à 10h30, et finiront le mardi 30 mars par l'Assemblée Générale du CNFRS.

Les insciptions sont à adresser avant le 15 mars 2004 à eric.tanguy@univ-nantes.fr.

Les Communications seront sélectionnées par le comité scientifique. La sélection sera faite sur des critères scientifiques en prenant en compte l'équilibre des sujets présentés dans chaque session.

Sauf exception, la langue de travail est le français.

Thèmes

1) Etalons de mesure en électromagnétisme :
   Fréquences, temps, longueur, électricité…
   Exemples : atomes froids, fontaines atomiques, effet Hall quantique,…
2) Techniques de mesure et Capteurs en nanosciences, en biologie, en médecine, en radioastronomie, en CEM…
   mesures de champs faibles,…
   télélocalisation, télédétection,…
3) Traitements du signal et des données adaptés à la métrologie.

Comité d'Organisation

- Christian Boisrobert (président du Comité Scientifique)
- Gérard Beaudin (CNFRS)
- Pierre Bauer (CNFRS)
- Maurice Bellanger (CNFRS)
- Pierre-Noël Favennec (CNFRS)
- Joël Hamelin (CNFRS)
- Maurice Pyée (CNFRS)
- Eric Tanguy (Université de Nantes)
- Bernard Veyret (CNFRS)

Comité Scientifique

- Christian Boisrobert (Président)
- Gérard Beaudin (Observatoire de Paris)
- Maurice Bellanger (Académie des Technologies)
- Thierry Bosch (INPT Toulouse)
- Maguelonne Chambon (BNM Paris)
- Pierre-Noël Favennec (CNFRS)
- Frédérique de Fornel (CNRS/LPUB Dijon)
- Jean Kovalevsky (Académie des Sciences)
- Bernard Picinbono (Académie des Sciences)
- Dominique Placko (SEE)
- Maurice Pyée (CNRS Orléans)
- Smaïl Tedjini (INPG Valence)
- Joe Wiart (France Télécom R&D)

Conférences Invitées

- Constantes fondamentales et systèmes d'unités par Marc Himbert
- Pulsars et applications à la métrologie par Ismaël Cognard
- La balance du Watt par Gérard Genevès
- Gyro-accéléromètre à atomes froids par Arnaud Landragin
- Nanosciences et capteurs en MicroOptoElectro-Mécaniques par Daniel Courjon

- Métrologie et interaction des ondes radioélectriques avec les tissus vivants par Joe Wiart
- Techniques de champ proche pour la caractérisation des systèmes rayonnants par Jean-Charles Bolomey

Publications - Editions

Les textes des communications seront consultables en ligne sur le site du CNFRS (http://cnfrs.get-telecom.fr). Après avis du Comité Scientifique, certains auteurs seront invités à remettre leur contribution pour publication dans le Bulletin du BNM, revue à comité de lecture.

Responsable des publications est Pierre-Noël Favennec.

Dates à Rétenir

- 10/12/2003 : clôture de réception des propositions de communication. Ces propositions seront soumises sous la forme d'un résumé clair et concis permettant une bonne évaluation scientifique. D'une à deux pages, rédigé en pdf selon le format joint, il est à envoyer à pierre-noel.favennec@get-telecom.fr et christian.boisrobert@univ-nantes.fr,
- 30/01/04 : réponse du Comité Scientifique aux proposants
- 15/03/04 : date limite de dépôt en ligne des textes des communications date limite d'inscription, à adresser à eric.tanguy@univ-nantes.fr , au-delà de cette date, les inscriptions seront sujettes à acceptation par le comité d'organisation.
- 29 et 30/03/04 : journées scientifiques
- 30/03/04 : liste des textes sélectionnés pour publication dans revue à comité de lecture.
- 30/03/04 : Assemblée Générale du CNFRS et clôture

Informations

Vous pourrez trouver toutes informations sur le site web du CNFRS : http://cnfrs.get-telecom.fr

LETTER FROM AN URSI RADIOSCIENTIST

Thank You !
The URSI GA 2002!

I am a recipient of Young Scientist Award at the URSI GA 2002, though the General Assembly was held one year ago, however, its impression on me is so deep that I cannot feel easy until I write something to express my sincere thankfulness to her.

It is taken for granted that the competition is the major driving force for the development of modern science and technology. However, the URSI GA 2002 gives me such an impression that if a person has been bathed in the warmth brought by friendship and understanding, his or her heart will be like a racket being charged with everlasting fuel to be ready for anywhere where it is needed.

Usually, our researchers have to collect scientific information through literature and books or Internet, what we read are dull words, numbers and formulas; what we think is just what kind of new conclusion have been reached and by what way; and what the problems are that still need to resolve. Thus, this kind of learning or collecting information will quite often agitate a sense of competition and pressure in the heart. Thanks for the URSI GA 2002, we young scientists have got an opportunity to experience something much different from this. During the assembly, all the young scientists have been accommodated at same place, thus it gave us a chance to know each other. When we talked face to face, what directly attracted us were not the research work we were doing but the vivid character, thoughts, and concerns each one had, which has been deeply imprinted by the colorful local culture and also common problems of the world. Thus, we astonishingly found that beside the research works, in order to live a more meaningful life, and in order to make the world have a more beautiful future, there are still so many other ideas for us to exchange and also so many common perplex, such as the philosophy of life, the pollutions, and the protection of environment, the conflictions between Palestine and Israel, etc., for us to go on exploring together. It naturally leads to such a realization that we, all the young scientists and all the youth and all the people living in different countries, are equally the same children of the world who are just working in different parts of the Earth village for a common goal — to make the world, our home become more and more beautiful. A more beautiful Ukraine, Germany, Romania, India, Pakistan, Algeria, etc., will mean a more beautiful world, any other one's dream is just part of one's own. With such an understanding, what kind of feeling could be aroused in the heart but expecting the best for each other, and supporting and cooperating with each other once possible and needed in the future?

So, in this sense, at least in the eyes of the young scientists, the URSI GA 2002 is not only a place for us to exchange academic ideas but also a window leading us to see the world as a whole, and a warm hand sowing the seeds of mutual understanding, respect, and love in the hearts. It is for such an unusual and wonderful experience we have got, which will be cherished as an ever shining light in our hearts lightening the path of our future life, I would like to be on behalf of all my friends I met there to say:

"Thank you, the URSI GA 2002!"

With equal sincerity, we would like also, through the secretary agency of URSI, to thank for all the sponsors for their kind supports.

May the URSI General Assembly, the window, which leads people to see our world with a broad and integrate view, to be opened wider and wider; may more and more excellent young scientists can enjoy warmth of her embrace; May more and more people come to give their supports to the URSI General Assembly, and may their future will be benefited from their today's contribution. Through the ceaseless efforts of the pounding hearts that are agitated by the universal love, may our world becomes more and more harmonic and beautiful!

Being eager to make more and more the potential young scientists be able to share the sweetness of the wonderful experience I have got from the URSI GA 2002 and even more, I also wonder whether the future URSI General Assembly could give her consideration to the following suggestions:

At first, thinking of the limitation of experience of the young scholars and also their strong desire to make progress in their research work, could the General Assembly arrange some special academic reports for the young scientists concerning some new developing techniques and their corresponding applications, and some difficult problems being encountered in some area? Could the URSI specially invite some famous experts in the EM area to make an introduction on their research experience or to have some free talks directly with the young scholars?

Secondly, in order to make the General Assembly become more helpful to the young scholars, and also to make the URSI General Assembly become more influential, I wonder whether the URSI could make and keep a record of some important information of all the young scientists, such as the research area of their interests, specialty and main contribution, their research plan and their wishes for their research condition, etc., and set up special organ for communicating the young scientists so that their problems can be noticed in time and the possible help can be offered when it is needed. And thereby, gradually, the URSI makes it a warm home of all the young scientists of all over the world even at the breaks of the General Assembly.

Qingyi Zhang
Department of Electrical Engineering
China University of Mining and Technology at Beijing
Beijing, 100083, China
zhang_qingyi@hotmail.com

International Geophysical Calendar 2004

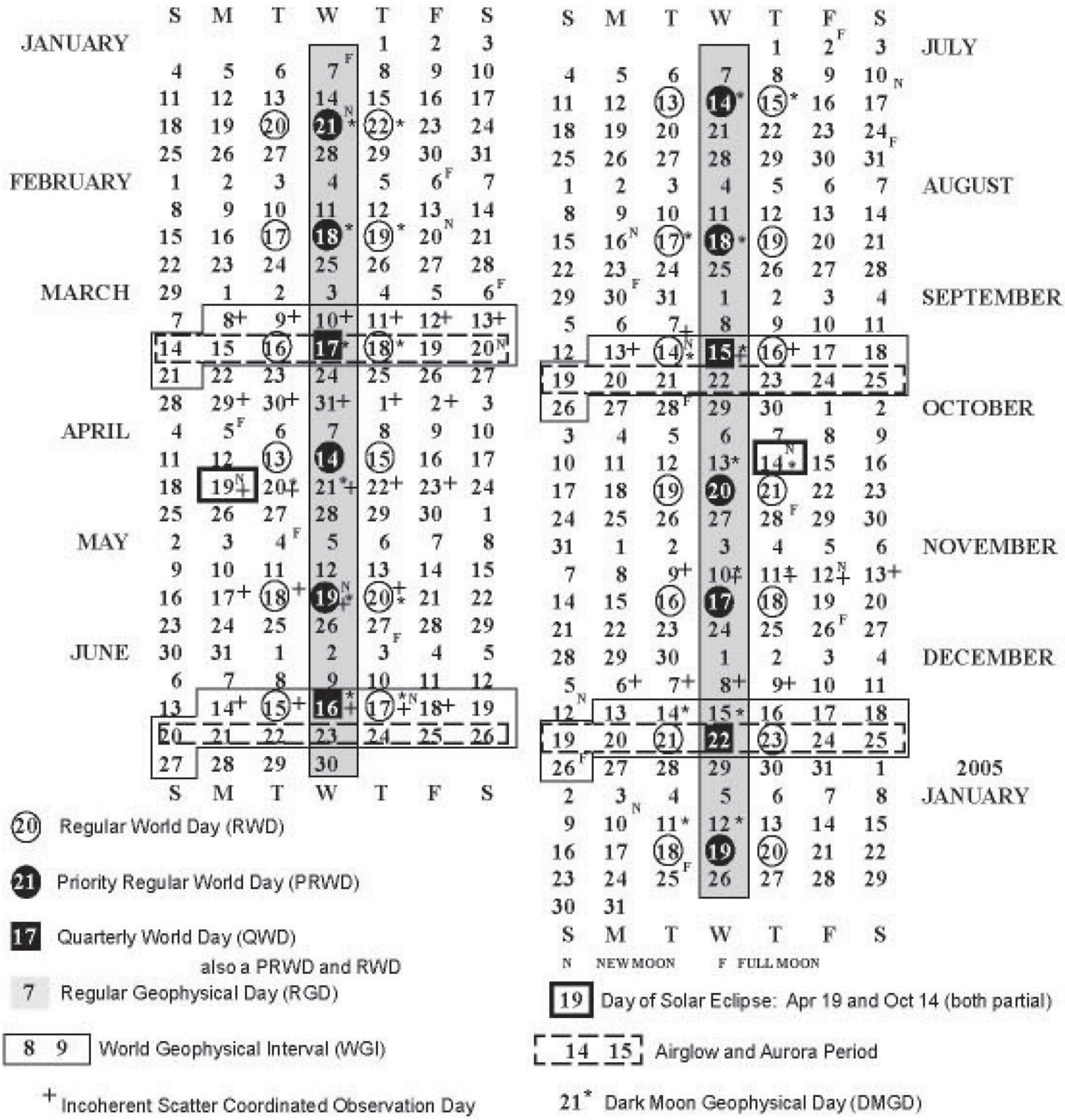

This Calendar continues the series begun for the IGY years 1957-58, and is issued annually to recommend dates for solar and geophysical observations, which cannot be carried out continuously. Thus, the amount of observational data in existence tends to be larger on Calendar days. The recommendations on data reduction and especially the flow of data to World Data Centers (WDCs) in many instances emphasize Calendar days. The Calendar is prepared by the *International Space Environment Service (ISES*) with the advice of spokesmen for the various scientific disciplines.

The **Solar Eclipses** are:

Unusually, 2004 has no total or annular eclipses of the Sun.

- **19 April 2004 (partial) eclipse** will be visible from the southern part of Africa and from the coast of Antarctica facing it. The peak coverage of 75% will occur in the ocean off Antarctica. Cape Town, South Africa, will have a 60% eclipse, and the partiality will diminish to zero at a line going across the northern coast of Angola and the northeastern tip of Madagascar
- **14 October 2004 (partial) eclipse** visible in northeast Asia and northern Pacific Ocean, also in western Alaska (point of greatest partiality, 93% coverage, occurs in Alaska at the terminator). The limit of 0% coverage slices across Asia from northern Siberia to the southwest through mid-Mongolia, and passes southern tips of Korea and Japan. Tokyo has ~20% coverage and Seoul ~10% coverage. The limit of 0% coverage extends as far south as the equator near the International Dateline. The top of Kamchatka Peninsula will see ~80% coverage.

Observers should note the transit of Venus across the Sun on June 8, 2004, the first transit of Venus visible from Earth since 1882.

Description by Dr. Jay Pasachoff, Williams College, Chair of IAU WG on Solar Eclipses, jmp@williams.edu, based on maps from Fred Espenak, NASA GSFC. See http://sunearth.gsfc.nasa.gov/eclipse/SEcat/SEdecade2001.html and http://www.williams.edu/Astronomy/IAU_eclipses. See also International Astronomical Union Program Group on Public Education at the Times of Eclipses: http://www.eclipses.info.

Meteor Showers (selected by R. Hawkes, Mount Allison Univ., Canada, rhawkes@mta.ca) include important visual showers and also unusual showers observable mainly by radio and radar techniques. The dates are given in Note 1 under the Calendar.

Definitions:

Time = Universal Time (**UT**);
Regular Geophysical Days (**RGD**) = each Wednesday;
Regular World Days (**RWD**) = Tuesday, Wednesday and Thursday near the middle of the month (see calendar);
Priority Regular World Days (**PRWD**) = the Wednesday **RWD**;
Quarterly World Days (**QWD**) = **PRWD** in the **WGI**;
World Geophysical Intervals (**WGI**) = 14 consecutive days each season (See calendar);
ALERTS = occurrence of unusual solar or geophysical conditions, broadcast once daily soon after 0400 UT;
STRATWARM = stratospheric warmings
Retrospective World Intervals (**RWI**) = MONSEE study intervals.

For more detailed explanations of the definitions, please see one of the following or contact H. Coffey (address below): ISES Synoptic Codes for Solar and Geophysical Data; URSI Information Bulletin; COSPAR Information Bulletin; IAGA News; IUGG Chronicle; WMO Bulletin; IAU Information Bulletin; and the Journal of Atmospheric and Terrestrial Physics (UK). WWW homepage **http://www.ises-spaceweather.org.**

Priority recommended programs for measurements not made continuously — (in addition to unusual ALERT periods):

Aurora and Airglow — Observation periods are New Moon periods, especially the 7 day intervals on the calendar;

Atmospheric Electricity — Observation periods are the RGD each Wednesday, beginning on 7 January 2004 at 0000 UT, 14 January at 0600 UT, 21 January at 1200 UT, 28 January at 1800 UT, etc. Minimum program is PRWDs.

Geomagnetic Phenomena — At minimum, need observation periods and data reduction on RWDs and during MAGSTORM Alerts.

Ionospheric Phenomena — Quarter-hourly ionograms; more frequently on RWDs, particularly at high latitude sites; ionogram scaled parameters to WDCs; continuous observations for solar eclipse in the eclipse zone. See **Airglow and Aurora**.

Incoherent Scatter — Observations on Incoherent Scatter Coordinated Days; also intensive series on **WGIs** or **Airglow and Aurora** periods.

Special programs: Dr. Wes Swartz, 316 Rhodes Hall, School of Electrical and Computer Engineering, Cornell University, Ithaca, NY 14853 ,Tel. 607-255-7120, Fax 607-255-6236, e-mail wes@ece.cornell.edu, URSI Working Group G.5. See http://people.ece.cornell.edu/wes/URSI_ISWG/.

Ionospheric Drifts — During weeks with RWDs.

Traveling Ionosphere Disturbances — special periods, probably PRWD or RWDs.

Ionospheric Absorption — Half-hourly on RWDs; continuous on solar eclipse days for stations in eclipse zone and conjugate area. Daily measurements during Absorption Winter Anomaly at temperate latitude stations (Oct-Mar Northern Hemisphere; Apr-Sep Southern Hemisphere).

Backscatter and Forward Scatter — RWDs at least.

Mesospheric D region electron densities — RGD around noon.

ELF Noise Measurements of earth-ionosphere cavity resonances — WGIs.

All Programs — Appropriate intensive observations during unusual meteor activity.

Meteorology — Especially on RGDs. On WGIs and STRATWARM Alert Intervals, please monitor on Mondays and Fridays as well as Wednesdays.

GAW (Global Atmosphere Watch) — WMO program to integrate monitoring of atmospheric composition. Early warning system of changes in atmospheric concentrations of greenhouse gases, ozone, and pollutants (acid rain and dust particles). WMO, 7 via avenue de la Paix, P.O. Box 2300, 1211 Geneva, Switzerland.

Solar Phenomena — Solar eclipse days, RWDs, and during PROTON/FLARE ALERTS.

CAWSES (Climate and Weather of the Sun-Earth System) — Program within the SCOSTEP (Scientific Committee on Solar-Terrestrial Physics): 2004-2008. Its focus is to mobilize the community to fully utilize past, present, and future data; and to produce improvements in space weather forecasting, the design of space- and Earth-based technological systems, and understanding the role of solar-terrestrial influences on Global Change. Contact is Su. Basu (sbasu@bu.edu), Chair of CAWSES Science Steering Group. Program "theme" areas are: Solar Influence on Climate – M. Lockwood (UK); Space Weather: Science and Applications – J. Kozyra (USA) and K. Shibata (Japan); Atmospheric Coupling Processes – F. Luebken (Germany); Space Climatology – C. Frolich (Switzerland) and J. Sojka (USA); and Capacity Building and Education, M.A. Geller (USA). In 2004, CAWSES is encouraging worldwide observations during the Coupling Processes in the Equatorial Atmosphere (CPEA) campaign. See http://www.ngdc.noaa.gov/stp/SCOSTEP/CAWSESDraft.html

Space Research, Interplanetary Phenomena, Cosmic Rays, Aeronomy — QWDs, RWD, and Airglow and Aurora periods.

The **International Space Environment Service (ISES)** is a permanent scientific service of the International Union of Radio Science (URSI), with the participation of the International Astronomical Union and the International Union Geodesy and Geophysics. ISES adheres to the Federation of Astronomical and Geophysical Data Analysis Services (FAGS) of the International Council for Science (ICSU). The ISES coordinates the international aspects of the world days program and rapid data interchange.

This Calendar for 2004 has been drawn up by H.E. Coffey, of the ISES Steering Committee, in association with spokesmen for the various scientific disciplines in SCOSTEP, IAGA and URSI. Similar Calendars have been issued annually beginning with the IGY, 1957-58, and have been published in various widely available scientific publications. PDF versions are available online (ftp://ftp.ngdc.noaa.gov/STP/SOLAR_DATA/IGC_CALENDAR).

Published for the International Council for Science and with financial assistance of UNESCO.

Additional copies are available upon request to ISES Chairman, Dr. David Boteler, Geological Survey of Canada National Geomagnetism Program, #7 Observatory Crescent, Ottawa, Ontario, Canada, K1A 0Y3 FAX (613) 824-9803, e-mail Boteler@geolab.NRCan.gc.ca, or ISES Secretary for World Days, Ms. H.E. Coffey, WDC-A for Solar-Terrestrial Physics, NOAA, E/GC2, 325 Broadway, Boulder, Colorado 80305, USA, FAX (303)497-6513, e-mail Helen.E.Coffey@noaa.gov.

The calendar is available on-line at **http://www.ises-spaceweather.org.**

NOTES on other dates and programs of interest:

1. Days with **significant meteor shower activity** are: Northern Hemisphere 4 Jan; 21-23 Apr; 4-5 May; 6-11, 27-29 Jun; 11-13 Aug; 21-22 Oct; 13-15, 21-23 Dec 2004; Southern Hemisphere 4-5 May; 6-11, 27-29 Jun; 27 Jul - 2 Aug; 21-22 Oct; 13-15 Dec 2004. These can be studied for their own geophysical effects or may be "geophysical noise" to other experiments.
2. **Global Atmosphere Watch (GAW)** — early warning system for changes in greenhouse gases, ozone layer, and long range transport of pollutants. (See Explanations.)
3. **Climate and Weather of the Sun-Earth System (CAWSES) -** SCOSTEP Program 2004-2008. Theme Areas: Solar Influence on Climate; Space Weather; Science and Applications; Atmospheric Coupling Processes; Space Climatology; and Capacity Building and Education. (See Explanations)
4. **+ Incoherent Scatter Coordinated Observations Days** (see Explanations) starting at 1300 UT on the first day of the intervals indicated, and ending at 1600 UT on the last day of the intervals: 8-13 Mar or 29 Mar - 2 Apr or 19-23 Apr M-I Coupling: Storm Effects, CPEA; 17-20 May Synoptic (wide F-region coverage with topside and temperatures); 14-18 Jun LTCS, MST; 13-16 Sep Synoptic (wide F-region coverage with some topside or E-region); 9-13 Nov LTCS, C/NOFS; 6-9 Dec Synoptic (wide F-region coverage with some topside or E-region) see http://people.ece.cornell.edu/wes/URSI_ISWG/2004WDschedule.htm**,** where

   C/NOFS = Communications/Navigation Outage Forecasting System (O. delaBeaujardiere - Odile.delaBeaujardiere@hanscom.af.mil);

   CPEA = Coupling Processes in the Equatorial Atmosphere (S. Kukao - fukao@kurasc.kyoto-u.ac.jp);

   LTCS = Lower Thermosphere Coupling Study (L. Goncharenko - lpg@haystack.mit.edu);

   M-I Coupling = Magnetosphere-Ionosphere Coupling Storm/Substorm Effects Mid & Low Latitude Iono. (C. Huang -cshuang@haystack.mit.edu)

   MST = Coordinated D- and E-region Campaigns in high resolution MST mode (J. Chao - chau@jro.igp.gob.pe)

   Synoptic = Wide coverage of the F-region augmented with topside or E-region measurements (W. Swartz - wes@ece.cornell.edu)

URSI Publications

Modern Radio Science 1999

Editor: Maria Stuchly
ISBN 0-7803-6002-8
List Price : USD 49.95 Member Price : USD 45.00
IEEE Product No. PC5837

Published by Oxford University Press
in cooperation with URSI and IEEE Press
Order 24 hours a day, 7 days a week :
1-732-981 0060 (Worldwide)
1-800-678 4333 (USA & Canada)
Fax 1-732 981 9667
E-mail : customer-service@ieee.org

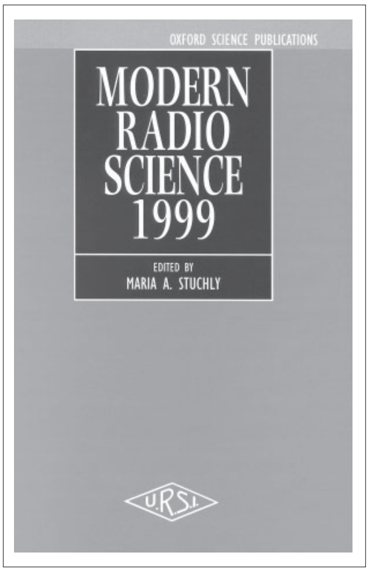

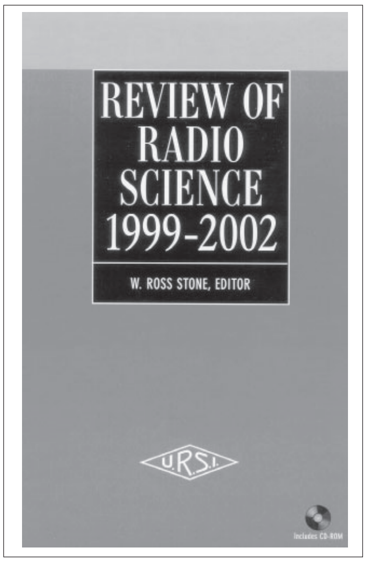

Review of Radio Science 1999-2002

Editor: W. Ross Stone
July 2002/Hardcover/977 pp
ISBN 0-471-26866-6
List Price : USD 125.00 Member Price : USD 106.25
IEEE Product No. #18493

Published by Wiley-Interscience
in cooperation with URSI and IEEE Press
Order can be sent to John Wiley & Sons, Inc.
from 8.30 a.m. to 5.30 p.m. :
1-732-469-4400 (Worldwide)
1-800-225-5945 (USA & Canada)
Fax 1-732 302-2370
E-mail : customer@wiley.com

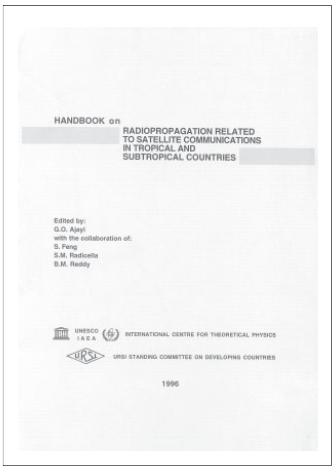

Handbook on Radiopropagation Related to Satellite Communications in Tropical and Subtropical Countries

Editor: G.O. Ajayi
with the collaboration of :
S. Feng, S.M. Radicella, B.M. Reddy

Available from the URSI Secretariat
c/o Ghent University (INTEC)
Sint-Pietersnieuwstraat 41
B-9000 Gent, Belgium
tel. +32 9-264-33-20
fax +32 9-264-42-88
e-mail : ursi@intec.rug.ac.be

The Journal of Atmospheric and Solar-Terrestrial Physics

SPECIAL OFFER TO URSI CORRESPONDENTS

AIMS AND SCOPE

The *Journal of Atmospheric and Terrestrial Physics* (JASTP) first appeared in print in 1951, at the very start of what is termed the "Space Age". The first papers grappled with such novel subjects as the Earth's ionosphere and photographic studies of the aurora. Since that early, seminal work, the Journal has continuously evolved and expanded its scope in concert with - and in support of - the exciting evolution of a dynamic, rapidly growing field of scientific endeavour: the Earth and Space Sciences. At its Golden Anniversary, the now re-named *Journal of Atmospheric and Solar-Terrestrial Physics* (JASTP) continues its development as the premier international journal dedicated to the physics of the Earth's atmospheric and space environment, especially the highly varied and highly variable physical phenomena that occur in this natural laboratory and the processes that couple them. The *Journal of Atmospheric and Solar-Terrestrial Physics* is an international journal concerned with the inter-disciplinary science of the Sun-Earth connection, defined very broadly. The journal referees and publishes original research papers, using rigorous standards of review, and focusing on the following: The results of experiments and their interpretations, and results of theoretical or modelling studies; Papers dealing with remote sensing carried out from the ground or space and with in situ studies made from rockets or from satellites orbiting the Earth; and, Plans for future research, often carried out within programs of international scope. The Journal also encourages papers involving: large scale collaborations, especially those with an international perspective; rapid communications; papers dealing with novel techniques or methodologies; commissioned review papers on topical subjects; and, special issues arising from chosen scientific symposia or workshops. The journal covers the physical processes operating in the troposphere, stratosphere, mesosphere, thermosphere, ionosphere, magnetosphere, the Sun, interplanetary medium, and heliosphere. Phenomena occurring in other "spheres", solar influences on climate, and supporting laboratory measurements are also considered. The journal deals especially with the coupling between the different regions. Solar flares, coronal mass ejections, and other energetic events on the Sun create interesting and important perturbations in the near-Earth space environment. The physics of this subject, now termed "space weather", is central to the Journal of Atmospheric and Solar-Terrestrial Physics and the journal welcomes papers that lead in the direction of a predictive understanding of the coupled system. Regarding the upper atmosphere, the subjects of aeronomy, geomagnetism and geoelectricity, auroral phenomena, radio wave propagation, and plasma instabilities, are examples within the broad field of solar-terrestrial physics which emphasise the energy exchange between the solar wind, the magnetospheric and ionosphericplasmas, and the neutral gas. In the lower atmosphere, topics covered range from mesoscale to global scale dynamics, to atmospheric electricity, lightning and its effects, and to anthropogenic changes. Helpful, novel schematic diagrams are encouraged. Short animations and ancillary data sets can also be accommodated. Prospective authors should review the *Instructions to Authors* at the back of each issue.

Complimentary Information about this journal:
http://www.elsevier.com/locate/JASTP?
http://earth.elsevier.com/geophysics

Audience:
Atmospheric physicists, geophysicists and astrophysicists.

Abstracted/indexed in:
- CAM SCI Abstr
- Curr Cont SCISEARCH Data
- Curr Cont Sci Cit Ind
- Curr Cont/Phys Chem & Sci
- INSPEC Data
- Meteoro & Geoastrophys Abstr
- Res Alert

Editor-in-Chief:
T.L. Killeen, National Centre for Atmospheric Research, Boulder, Colorado, 80307 USA

Editorial Office:
P.O. Box 1930, 1000 BX Amsterdam, The Netherlands

Special Rate for URSI Radioscientists 2003:
Euro 149.00 (US$ 149.00)
Subscription Information
2002: Volume 65 (18 issues)
Subscription price: Euro 2659 (US$ 2975)
ISSN: 1364-6826

CONTENTS DIRECT:
The table of contents for this journal is now available pre-publication, via e-mail, as part of the free ContentsDirect service from Elsevier Science. Please send an e-mail message to cdhelp@elsevier.co.uk for further information about this service.

For ordering information please contact Elsevier Regional Sales Offices:

Asia & Australasia/ e-mail: asiainfo@elsevier.com
Europe, Middle East & Africa: e-mail: nlinfo-f@elsevier.com
Japan: Email: info@elsevier.co.jp
Latin America : e-mail: rsola.info@elsevier.com.br
United States & Canada : e-mail: usinfo-f@elsevier.com